



UNIVERSIDAD NACIONAL AUTÓNOMA DE MÉXICO

DOCTORADO EN CIENCIAS BIOMÉDICAS

INSTITUTO DE ECOLOGÍA

Regulación de la proliferación y diferenciación celular de órganos complejos: genética molecular y análisis celular
cuantitativo en la raíz de *Arabidopsis thaliana*

TESIS

QUE PARA OPTAR POR EL GRADO DE:

DOCTOR EN CIENCIAS

PRESENTA:

MARIO ALBERTO PACHECO ESCOBEDO

DIRECTOR DE TESIS

DRA. ADRIANA GARAY ARROYO

INSTITUTO DE ECOLOGÍA

COMITÉ TUTOR

DRA. MARÍA ELENA ÁLVAREZ-BUYLLA ROCES

INSTITUTO DE ECOLOGÍA

DR. JESÚS ÁGUILA LINARES

INSTITUTO DE FISIOLOGÍA CELULAR

CIUDAD DE MÉXICO ABRIL DE 2017



UNAM – Dirección General de Bibliotecas

Tesis Digitales
Restricciones de uso

DERECHOS RESERVADOS ©
PROHIBIDA SU REPRODUCCIÓN TOTAL O PARCIAL

Todo el material contenido en esta tesis está protegido por la Ley Federal del Derecho de Autor (LFDA) de los Estados Unidos Mexicanos (Méjico).

El uso de imágenes, fragmentos de videos, y demás material que sea objeto de protección de los derechos de autor, será exclusivamente para fines educativos e informativos y deberá citar la fuente donde la obtuvo mencionando el autor o autores. Cualquier uso distinto como el lucro, reproducción, edición o modificación, será perseguido y sancionado por el respectivo titular de los Derechos de Autor.

¿En perseguirme, mundo, qué interesa?

¿En qué te ofendo, cuando sólo intento
poner bellezas en mi entendimiento
y no mi entendimiento en las bellezas?

Yo no estimo tesoros ni riquezas,
y así, siempre me causa más contento
poner riquezas en mi entendimiento
que no mi entendimiento en las riquezas.

Y no estimo hermosura que vencida
es despojo civil de las edades
ni riqueza me agrada fementida,

teniendo por mejor en mis verdades
consumir vanidades de la vida
que consumir la vida en vanidades.

Sor Juana Inés de la Cruz

Para mis papás,
para mi hermano Carlos,
para Mariana,
para mis familiares y amigos, los presentes y los ausentes.

Agradecimientos

La presente tesis doctoral se realizó en el Laboratorio de Genética Molecular, Desarrollo y Evolución de Plantas del Instituto de Ecología, de la Universidad Nacional Autónoma de México bajo la dirección de la Dra. Adriana Garay Arroyo. Además se contó con la coordinación académico-científica de las Dras. María Elena Álvarez-Buylla Roces, Berenice García Ponce de León y Ma. de la Paz Sánchez Jiménez, la coordinación administrativa y logística de Diana Romo; así como el apoyo de Laura Rodríguez y la Dra. Teresa Romero, en la preparación de soluciones, medios y materiales diversos importantes para la realización de esta tesis.

La investigación realizada fue financiada por los proyectos UNAM-DGAPA-PAPIIT: IN211516, IN208517, IN205517, IN204217 y de CONACyT: 240180 y 180380 a cargo de las Doctoras Berenice García Ponce de León, Elena Álvarez-Buylla, María de la Paz Sánchez y Adriana Garay Arroyo a quienes les agradecemos su apoyo.

Este proyecto de doctorado fue realizado en el Instituto de Ecología de la Universidad Nacional Autónoma de México dentro del Programa de Posgrado en Ciencias Biomédicas y fue financiado por una beca de doctorado otorgada por CONACyT (2007-2012).

Quiero agradecer a todos los coautores de los artículos en los que tuve la suerte de participar, sin cuyas ideas y aportaciones no habría sido posible realizar el presente trabajo: Adriana Garay Arroyo, María Elena Álvarez-Buylla Roces, Joseph Dubrovsky, Víctor B. Ivanov, Germán Arriaga-Mejía, Hibels Ávila, Iván Ránsom Rodríguez, Enrique Ortiz Moreno, María de la Paz Sánchez, Angus S Morphy, Berenice García Ponce, Nayelli Marsch-Martínez, Stefan de Folter, Adriana Corvera Poiré, Fabiola Jaimes Miranda, Soraya Pelaz, Karla García Cruz, Yamel Ugartechea Chirino, Bénédicte Desvoyes, Rosalinda Tapia López, Crisanto Gutierrez, Arturo Pimentel, Gabriel Corkidi, Ilya A. Baklanov y Peter Doerner.

A la Dra. Adriana Garay Arroyo por su apoyo durante todo este tiempo. Al final, logramos terminar un largo proceso de manera exitosa.

A la Dra. Elena Álvarez-Buylla por su apoyo para que pudiera concluir con el doctorado en general y en particular con el trabajo sobre el análisis estadístico del patrón longitudinal de la raíz. Agradezco la oportunidad que me dio de poder trabajar en su grupo y la retroalimentación que he tenido todo este tiempo.

A los doctores Joseph G. Dubrovsky y Victor B. Ivanov, que me dieron un gran apoyo y sin quienes el trabajo del patrón longitudinal de la raíz no hubiera sido posible. De ellos adquirí mucho de mi forma de ver y analizar el crecimiento de las raíces. Mi más sincero reconocimiento a ellos como científicos, pero más como personas.

A Iván Ránsom Rodríguez, su tenacidad y compromiso en su trabajo de tesis de licenciatura, que realizó con una calidad admirable, hizo posible tener los perfiles de longitudes celulares que se analizaron con los modelos de múltiple cambio estructural. Gracias por creer que un trabajo tan árido como medir células al microscopio puede hacer aportaciones importantes a la biología.

A Germán Arriaga Mejía e Hibels Ávila Ortega, colaboradores y amigos. De numerosos proyectos que hemos iniciado, interesantes discusiones en ESFM-IPN y hasta pláticas sobre modelación en Hooters surgió la idea de aplicar modelos de múltiple cambio estructural en la raíz. Estoy seguro que seguiremos desarrollando proyectos interesantes.

Al Dr. Jesús Aguirre Linares, miembro de mi comité tutorial en el Doctorado en Ciencias Biomédicas.

A la Dra. Fabiola Jaimes Miranda, por su asistencia técnica en la elaboración de esta tesis.

A mis sinodales: Dr. Jorge Manuel Vásquez Ramos, Dra. Alejandra Alicia Covarrubias Robles, Dra. Tzvetanka Dimitrova Dinkova, Dra. María del Rocío Cruz Ortega y Dra. María Elena Álvarez-Buylla Roces por sus comentarios y sugerencias durante la revisión de este tesis.

A mis amigos: Fabiola Jaimes, Aurora Gamez, Andrea Sanjuan y Julio Flores Sánchez.

A todos los compañeros de Aikido -UNAM, en especial a sensei Paris Alvarez Yslas.

Estoy en deuda con la comunidad informática por proporcionar acceso libre a software tan poderoso y confiable como el sistema operativo GNU/Linux; el paquete de análisis estadístico R; los lenguajes de programación Python, PHP, javascript y HTML5; el procesador de documentos L^AT_EX y LyX; el programa para manejo de referencias Mendeley. Además mi reconocimiento y agradecimiento a todas las instituciones que preocupadas con compartir y difundir el conocimiento desarrollaron y mantienen la plataforma edx.org.

Índice general

Resumen	1
Introducción	3
El patrón de regionalización longitudinal de la raíz	4
Anatomía de la raíz de <i>Arabidopsis</i> y su relación con el crecimiento	4
Problemas y conflictos en el análisis del patrón de regionalización longitudinal de la raíz	6
El gen <i>XANTAL1</i> y su papel en la regulación del crecimiento de la raíz	10
Hipótesis	15
Objetivos	16
Resultados	17
El patrón de regionalización longitudinal de la raíz	18
Modelos de múltiple cambio estructural aplicados a perfiles de longitudes celulares	18
Cálculo del número de transiciones o puntos de rompimiento	23
Discusión	39
XAL1 y XAL2 participan en la regulación del balance proliferación/diferenciación celular en la raíz de <i>Arabidopsis</i>	39
La zona de crecimiento de la raíz de <i>Arabidopsis</i> está compuesta de tres regiones discretas	42
Conclusiones	46
Apéndice 1. El factor transcripcional MADS XAL2/AGL14 modula el transporte de auxinas a través de la regulación transcripcional de los transportadores PIN	47

Apéndice 2. El factor transcripcional XAANTAL1 participa en la regulación de la proliferación y la transición a la diferenciación	60
Apéndice 3. Análisis de perfiles de longitudes celulares en lenguaje R	71
Apéndice 4. Análisis de perfiles de longitudes celulares en lenguaje PHP	75
Apéndice 5. Análisis cuantitativo de raíces <i>Arabidopsis</i>, ecotipo C24	85
Bibliografía	86

Resumen

La raíz de *Arabidopsis thaliana* (*Arabidopsis*) es un modelo experimental de gran importancia en biología vegetal y del desarrollo. Entre sus principales características está la posibilidad de analizar los distintos procesos involucrados en el crecimiento a lo largo de su eje longitudinal. Para poder aprovechar esta característica es necesario describir cuantitativa y cualitativamente las diferentes regiones longitudinales, las cuales se diferencian por la relación entre proliferación, alargamiento y diferenciación celular. Actualmente no existe consenso acerca de cuántas regiones existen en la zona de crecimiento de la raíz, ni en cómo delimitar estas regiones. En el presente trabajo se propone que modelos de múltiple cambio estructural (MCE) de los perfiles de las longitudes celulares solucionan ambos problemas.

Los modelos MCE de las filas de las células de córtex de raíces tipo silvestre (wt) de 7 y 9 días posteriores a la siembra (dps) aportan evidencias a favor de la existencia de tres regiones discretas en la zona de crecimiento de la raíz de *Arabidopsis*: el dominio de proliferación (DP), el dominio de transición (DT) —estas dos regiones pertenecen al meristemo apical (RAM por sus siglas en inglés)— y la zona de alargamiento (ZA). Además, se muestra la correspondencia entre la posición del límite DP/DT determinada por los modelos MCE con el patrón de expresión de las líneas reporteras de la transición G2/M de ciclo celular (*CycB1;1DB:GFP*) y endorreduplicación (*pCCS52A1:GUS*). Lo anterior, junto con el análisis de las pendientes de las rectas que corresponden a cada región en los modelos MCE, muestra que la transición DP/DT representa un cambio en la proliferación celular, mientras que la transición RAM/ZA se relaciona con un cambio en la velocidad del alargamiento celular. Los modelos MCE también pueden calcular los tamaños críticos de división celular (L_{CritD}) y de transición a la ZA (L_{CritA}).

Adicionalmente se encontró que el gen MADS-box *XAANTAL1* (*XAL1*) es necesario para el crecimiento del DP durante las primeras dos semanas de crecimiento. Esto se relaciona con el crecimiento prácticamente constante de raíces de pérdida de función (*xal1*), en comparación con el crecimiento acelerado de raíces wt. Además raíces *xal1* presentan alteraciones en los tamaños críticos L_{CritD} y L_{CritA} .

Los modelos MCE son una herramienta objetiva en la descripción de diferentes fondos genéticos, condiciones experimentales o cambios a lo largo del tiempo en la zona de crecimiento de la raíz. Es necesario investigar si el

el mismo patrón longitudinal que se observa en *Arabidopsis* se encuentra en otras especies. Con el objetivo de facilitar la aplicación de modelos MCE en el estudio de raíces se proporciona el sitio: www.ibiologia.com.mx/MSC_analysis.

Introducción

El lograr comprender cómo se regula el balance entre la proliferación y diferenciación celular, de tal manera que durante el desarrollo se producen estructuras complejas, es central en el estudio de la morfogénesis y sus alteraciones o patologías. En los últimos años se han identificado parte de los componentes de las redes reguladoras que gobiernan, tanto en plantas como en animales, el balance entre proliferación y diferenciación celular. En estas redes participan una plétora de factores transcripcionales, ARNs no codificantes, hormonas, mecanismos epigenéticos, señales ambientales y restricciones mecánicas, entre otros muchos factores, que interactúan de modo combinatorio y dinámico.

Si bien es cierto que en modelos animales hay avances muy importantes, realizar investigaciones integradoras *in vivo* de los mecanismos y procesos involucrados en el balance entre proliferación y diferenciación celular que abarquen diferentes niveles de complejidad, desde las redes reguladoras hasta tejidos y órganos, implica altos costos operativos. En cambio, estos mecanismos y procesos se pueden estudiar «*in vivo*» en sistemas vegetales que son más accesibles desde el punto de vista económico y técnico.

En general, el meristemo apical de las raíces de las angiospermas y en particular el de la raíz de *Arabidopsis thaliana* (de aquí en adelante *Arabidopsis*) presenta características que la hacen un modelo adecuado para estudios cuantitativos acerca de la regulación del balance entre proliferación y diferenciación celular (Webster y MacLeod, 1980; Ivanov, 1981, 1994; van der Weele *et al.*, 2003; Iwamoto *et al.*, 2006). Entre estas características podemos mencionar una organización estructural relativamente simple, que consta de pocos tipos celulares con una disposición concéntrica; un patrón longitudinal que permite analizar el comportamiento celular en una sola dimensión; un tamaño reducido, por lo que resulta sencillo cuantificar el número de células proliferativas; y el hecho de que se tienen las etapas de diferenciación en regiones relativamente bien delimitadas (Ivanov, 1981, 1994; Dolan *et al.*, 1993; Ivanov y Dubrovsky, 2013). Además, las raíces han servido como sistemas para probar el efecto de diversos químicos cancerígenos y radiación sobre la proliferación celular, el crecimiento y la diferenciación celular (Ivanov, 1981, 1994, entre otros).

Gracias a las características de la raíz de *Arabidopsis* se tienen identificados numerosos componentes de las redes que regulan el balance entre proliferación y diferenciación celular en ella. Entre los numerosos genes que

participan en esta regulación se encuentran miembros de la familia MADS-box (los cuales codifican reguladores transcripcionales) como: *ARABIDOPSIS NITRATE REGULATED 1 (ANR1)* (Zhang y Forde, 1998; Gan *et al.*, 2005), *XANTAL1 (XAL1)* (Tapia-López *et al.*, 2008) y *XAL2* (Garay-Arroyo *et al.*, 2013). Sin embargo, es relativamente poco lo que se conoce de la función que tienen los genes MADS-box en la regulación del desarrollo de la raíz, a pesar de que diversos miembros de esta familia se expresan en este órgano (Alvarez-Buylla *et al.*, 2000; Burgeff *et al.*, 2002; Nawy *et al.*, 2005) y de la gran cantidad de información que se tiene acerca de la importancia de éstos y los factores transcripcionales que codifican en la determinación de la identidad de los verticilos florales o la regulación del inicio de la floración (Coen y Meyerowitz, 1991; Egea-Cortines *et al.*, 1999; Honma y Goto, 2001; Pelaz *et al.*, 2001; Theissen y Saedler, 2001; Theissen, 2001). Esta falta de conocimiento de la función de las proteínas de dominio MADS en la regulación del desarrollo de la raíz se puede deber, entre otras cosas, a la redundancia funcional que pueden presentar los miembros de esta familia y a que el principal interés de los grupos de investigación se ha concentrado en su función en la parte aérea de la planta. Además, los efectos en el fenotipo de la ganancia o pérdida de función de genes MADS-box no siempre son tan evidentes y necesitan de análisis cuantitativos detallados para detectarlos.

El presente trabajo consistió en el estudio del balance entre proliferación y diferenciación celular en la raíz de *Arabidopsis* a través del análisis de la distribución de longitudes celulares mediante modelos estadísticos. Estos modelos estadísticos permitieron establecer la regionalización longitudinal de la raíz y proporcionaron un método cuantitativo a través del cual se pueden analizar los efectos de diferentes condiciones experimentales en el balance proliferación/diferenciación celular. Estos modelos estadísticos se usaron para profundizar en la caracterización fenotípica de la función del gen MADS-box *XAL1* en el desarrollo de la raíz.

El patrón de regionalización longitudinal de la raíz

Anatomía de la raíz de *Arabidopsis* y su relación con el crecimiento

El crecimiento de la raíz se regula por la actividad combinada de dos procesos fuertemente relacionados entre sí: la división y el alargamiento celular. Gracias a su organización longitudinal y a que estos procesos ocurren de manera diferencial en distintas regiones de la zona de crecimiento (revisado en: Ivanov y Dubrovsky 2013), la raíz de *Arabidopsis* en lo particular, es un modelo adecuado para realizar estudios cuantitativos de la relación entre estos dos procesos.

La raíz de *Arabidopsis* tiene una organización relativamente simple. Transversalmente tiene una organización concéntrica que consiste de un cilindro vascular en la posición central, formado por xilema, floema, parénquima vascular y periciclo; alrededor del cilindro vascular se encuentran la endodermis y el córtex; y finalmente la epidermis,

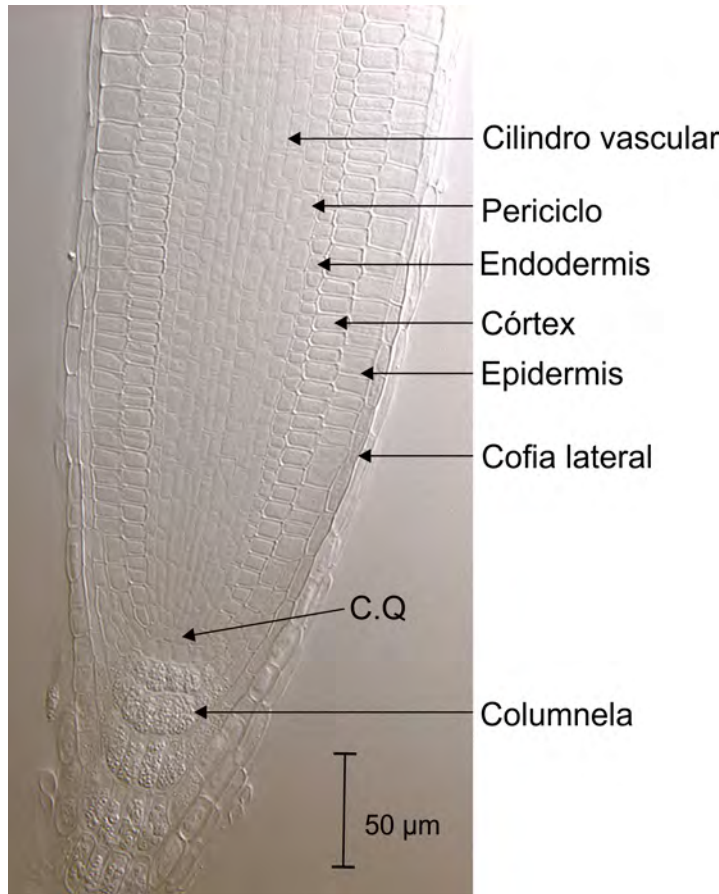


Figura 1: Micrografía Nomarsky del meristemo apical de una raíz de *Arabidopsis* de siete días posteriores a la siembra (dps). Fotografía del autor.

el anillo más externo (Figura 1). La epidermis está formada por dos tipos celulares, tricoblastos (desarrollan pelos radiculares) y atricoblastos (no desarrollan pelos radiculares), cuya identidad depende de su posición relativa a las células de córtex con las que están en contacto. Las células de epidermis que están en contacto con las paredes anteciliares que se encuentran entre dos células de córtex (o que se encuentran en contacto con dos células corticales) se diferenciarán en tricoblastos, mientras que las células de epidermis que se encuentran en contacto con una sola célula de córtex se diferencian en atricoblastos. En el extremo apical de la raíz se encuentran las células de la columnela central y las células de la cofia lateral (ver: Dolan *et al.* 1993).

Longitudinalmente la raíz está conformada, de manera general, por la zona de crecimiento (la región más distal) y la zona de diferenciación (ZD). La zona de crecimiento se conforma del meristemo apical o RAM (por sus siglas en inglés Root Apical Meristem) y la zona de alargamiento (ZA) (Figura 2A). Estas dos regiones se distinguen principalmente por los procesos celulares que predominan en cada una de ellas. En el RAM las células tienen una alta probabilidad de dividirse. La ZA es la región donde las células se alargan a tasas de crecimiento

considerablemente altas, a una velocidad por lo menos seis veces mayor de lo que lo hacen en el RAM (van der Weele *et al.*, 2003), y además donde ya no son capaces de dividirse.

El RAM está constituido por dos dominios: el dominio de proliferación (DP), donde las células tienen una alta probabilidad de dividirse; y el dominio de transición (DT), donde las células aún son capaces de dividirse, pero con una probabilidad cercana a cero, y continúan alargándose a la misma velocidad que las células del DP (Ivanov y Dubrovsky, 2013). El hecho de que las células en el DT prácticamente sean incapaces de dividirse provoca que las células en este dominio sean más largas con respecto a las del DP (Ivanov y Dubrovsky, 2013) (Figura 2B). En la región distal del DP se encuentra el centro quiescente (CQ) (Figura 1), nicho de células troncales conformado por cuatro células con muy poca actividad mitótica, rodeando a las células del CQ se encuentran las células troncales iniciales (Clowes, 1956; Dolan *et al.*, 1993; Sabatini *et al.*, 2003). Las cuatro células troncales (o iniciales) dan lugar a todos los tipos celulares de la raíz de la siguiente manera: las iniciales de tejido vascular, las de columnela, cofia lateral y epidermis y las de córtex y endodermis. Mediante experimentos de ablación celular por láser y datos genéticos se determinó que el CQ inhibe la diferenciación de las células iniciales que lo rodean (Berg *et al.*, 1997). Esta inhibición de la diferenciación celular se da en el rango de una sola célula, por lo que se da una división asimétrica, donde después de cada división de las células iniciales, una de las células hijas continúa con identidad de célula inicial, y la que ya no está en contacto con CQ queda libre de la inhibición y puede diferenciarse (Berg *et al.*, 1997).

Problemas y conflictos en el análisis del patrón de regionalización longitudinal de la raíz

Una adecuada descripción y delimitación de las diferentes zonas y dominios longitudinales de la raíz que se describen arriba es de gran importancia para poder evaluar y entender los efectos que distintas alteraciones genéticas, químicas y físicas pueden tener sobre la proliferación celular, el crecimiento y la diferenciación en el desarrollo radicular. Por ejemplo, es común que cuando se comparan distintas condiciones experimentales, el tamaño y/o el número de células proliferativas, normalmente medidos en una fila de córtex, sean parámetros reportados (Casamitjana-Martínez *et al.*, 2003; Dello Ioio *et al.*, 2007; Tapia-López *et al.*, 2008; Tsukagoshi *et al.*, 2010; Zhou *et al.*, 2011; Garay-Arroyo *et al.*, 2013). Sin embargo, aún no existe un consenso acerca de cuántas regiones componen longitudinalmente a la raíz o la nomenclatura que se usa para referirse a éstas (Ivanov y Dubrovsky, 2013).

Tampoco existe un consenso en la forma en la que se determinan los límites o fronteras entre estas regiones, y en muchas ocasiones se utilizan métodos subjetivos. Lo anterior tiene consecuencias importantes porque se vuelve

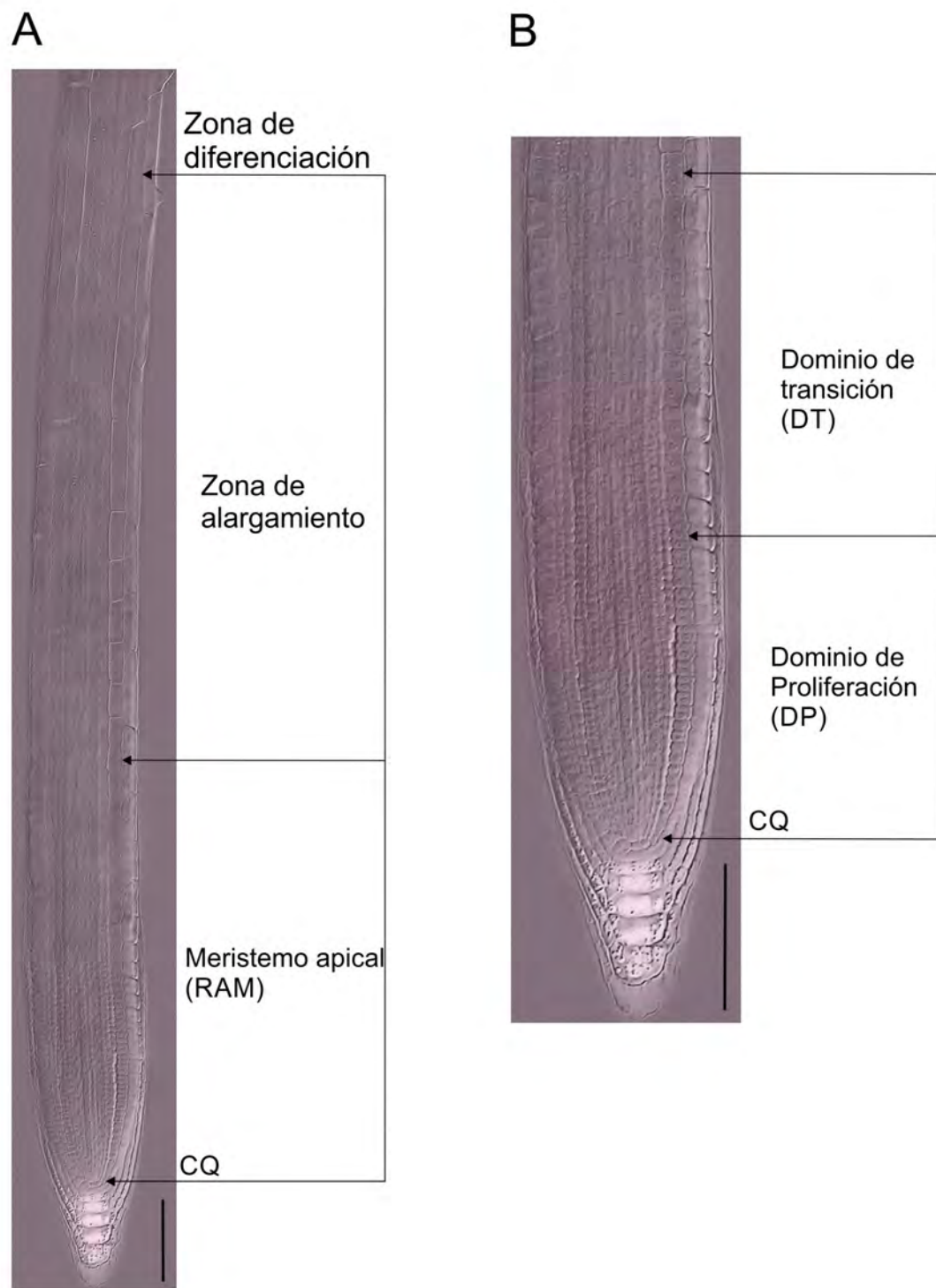


Figura 2: Patrón de regionalización longitudinal de la zona de crecimiento de una raíz de *Arabidopsis*. (A) El meristemo apical (RAM) de la raíz y la zona de alargamiento (ZA) de una raíz tipo silvestre (wt) Col-0 de siete días posteriores a la siembra; imagen compuesta de una preparación fija aclarada. (B) RAM de la raíz mostrada en (A). Escala = 100 μ m. Fotografía cortesía del biólogo Iván Ransom Rodríguez; composición de la imagen diseñador gráfico Francisco José Guijarro Higuera.

difícil comparar los resultados reportados por distintos laboratorios que usan diferentes terminologías y criterios (Ivanov y Dubrovsky, 2013)¹.

Respecto a las fronteras entre los dominios y zonas longitudinales de la raíz, se siguen distintas metodologías y criterios para su determinación. Por ejemplo, Casamitjana-Martínez y colaboradores (2003), definen la transición RAM/ZA como el punto donde las células comienzan a alargarse rápidamente. El incremento en la velocidad de alargamiento se toma como único criterio en numerosas publicaciones para distinguir entre las dos regiones (el RAM y la ZA). Este criterio se realiza «a simple vista», sin haber medido las longitudes de las células, por lo que la identificación del punto donde hay un aumento drástico en la velocidad de alargamiento es muy variable entre investigadores, producto de un alto grado de subjetividad. Un método más objetivo para determinar esta frontera consiste en encontrar la posición en la cual la longitud de una célula en una fila es mayor que el doble de la célula anterior (tomando al CQ como origen) (González-García *et al.*, 2011). Sin embargo, este método puede dar resultados sesgados porque es posible que antes de que haya un aumento en la velocidad de alargamiento, una célula de más del doble de largo que la anterior se encuentre antes de una más corta (lo cual puede suceder con relativa frecuencia en el DT), lo que indica que este criterio no siempre es suficiente para establecer la transición RAM/ZA. Recientemente se propuso un método geométrico para detectar la transición RAM/ZA (French *et al.*, 2012). Este método consiste en trazar una línea recta entre el primer y último punto en una gráfica de la longitud celular en función del número de células, y define el punto con la mayor distancia perpendicular a esta línea como la transición RAM/ZA (que los autores denominan como zona de transición) (French *et al.*, 2012). Dicha propuesta geométrica es relativamente fácil de implementar y proporciona resultados similares a aquellos obtenidos por expertos en el estudio de la raíz que utilizan otros criterios (French *et al.*, 2012).

En numerosos estudios se establece la transición RAM/ZA mediante alguno de los criterios o métodos mencionados (Dello Ioio *et al.*, 2007; Tsukagoshi *et al.*, 2010; Moubayidin *et al.*, 2010; French *et al.*, 2012), pero la gran mayoría de las publicaciones no determinan la posición de la transición DP/DT. Esto se debe a que la existencia y características del DT es motivo de debate actualmente. Algunas escuelas de pensamiento establecen que en una fila de células la transición de la zona de proliferación celular a la ZA es puntual y no consiste en una región celular (Dello Ioio *et al.*, 2007; Moubayidin *et al.*, 2010), y dado que esta transición ocurre en diferentes posiciones en distintas filas de células, la zona de transición es simplemente la región donde se encuentran las fronteras RAM/ZA de todas las filas de células de una raíz (Dello Ioio *et al.*, 2007). Esta definición tiene un error conceptual importante relacionado con el crecimiento simplástico,² el cual condiciona que todas las filas de células se alarguen aproximadamente a la misma velocidad a la misma distancia del CQ. En algunas ocasiones el término

¹En esta tesis adopto la terminología propuesta por Ivanov y Dubrovsky (2013).

²La presencia de una pared celular rígida cementada entre células adyacentes, implica que en el crecimiento de los órganos vegetales no se observen desplazamientos entre células adyacentes, a diferencia de lo que se observa en tejidos animales, por lo que la posición relativa entre células vecinas se mantiene a lo largo del tiempo. A este tipo de crecimiento se le conoce como «crecimiento simplástico» (ver: Sinnott 1939; Ivanov *et al.* 2002; Weizbauer *et al.* 2011; Ivanov y Dubrovsky 2013).

«zona de transición» se usa para referirse a la frontera RAM/ZA en una sola fila de células (French *et al.*, 2012), lo que refleja la falta de consenso o el uso incorrecto de la terminología.

El concepto de dominio de transición en la raíz —definido como la región donde las células realizan todos los cambios fisiológicos necesarios para pasar de la proliferación a la ZA, y donde además poseen características funcionales únicas— es relativamente reciente, sin embargo esta región empezó a ser reconocida en trabajos tan tempranos como «The Power of Movement in Plants» de Charles y Francis Darwin (revisado por Baluška *et al.* 2010). Quizás la evidencia reciente experimental más fuerte en favor de la existencia del DT como región y no como una transición puntual (cuando nos referimos a una fila de células) es la proporcionada por Hayashi y colaboradores (2013), quienes demostraron que las células comienzan a endorreduplicar antes de que la velocidad de alargamiento aumente drásticamente. Este cambio en el comportamiento proliferativo de las células concuerda con lo establecido por Ivanov y Dubrovsky (2013), que definen que la transición del DP al DT implica un decremento considerable del índice mitótico (porcentaje de células capaces de dividirse al menos una vez más) o una disminución significativa de la probabilidad de división celular. Por lo tanto, la transición DP/DT implica esencialmente un cambio en el comportamiento proliferativo de las células, mientras que la transición RAM/ZA está caracterizada principalmente por un aumento drástico en la velocidad de alargamiento. En el presente trabajo se muestran nuevos datos que apoyan la existencia del DT como una región que comprende más de una célula. Por lo tanto, se aportan evidencias de que en el eje longitudinal de la raíz existen tres transiciones en el comportamiento celular: 1) la transición DP/DT, que implica un cambio en el comportamiento proliferativo, sin cambiar la velocidad de alargamiento celular; 2) la transición RAM/ZA, que está asociada a un incremento drástico en la velocidad de alargamiento celular, y 3) la transición ZA/ZD, donde las células terminaron de diferenciarse, y las tasas de proliferación y alargamiento celular son igual a cero (Pacheco-Escobedo *et al.*, 2016).

Si se acepta la existencia de la transición DP/DT es necesario determinar su posición. La posición de la transición DP/DT es más difícil de determinar que la transición RAM/ZA, ya que ésta tiene un carácter oscilatorio, su posición varía a lo largo del tiempo en una sola fila de células, y no necesariamente sucede a la misma distancia del CQ en diferentes filas de células (Ivanov y Dubrovsky, 2013; Baluška y Mancuso, 2013). En cambio, la transición RAM/ZA necesariamente tiene que ocurrir a la misma distancia del CQ en todas las filas, debido a las restricciones que impone el crecimiento simplástico. Al igual que en el caso de la determinación de la transición RAM/ZA, existen diferentes soluciones propuestas al problema de la posición de la transición DP/DT. Esta posición se puede determinar como el punto en el que la longitud celular promedio comienza a incrementarse ligeramente, o cuando la distancia entre los núcleos de células contiguas a lo largo de una fila de células es igual o mayor al diámetro de los núcleos (Rost y Baum, 1988; Dubrovsky *et al.*, 1998a,b; Garay-Arroyo *et al.*, 2013). El inicio del DT también se puede definir como la posición en donde el índice mitótico se reduce aproximadamente un 50 % del valor máximo para el tejido que se está midiendo (Ivanov y Dubrovsky, 2013). Sin embargo, esta última propuesta puede ser difícil de aplicar

y no necesariamente es válida para todas las especies (Joseph Dubrovsky, comunicación personal). Todos estos criterios para determinar la posición de la transición RAM/ZA pueden producir resultados variables o con un grado de subjetividad considerable, o bien pueden exigir un alto grado de experiencia por parte de los investigadores para poder obtener resultados confiables y reproducibles.

Por la importancia que tiene cada una de las regiones longitudinales de la raíz en el desarrollo y particularmente en la regulación del balance entre proliferación y diferenciación celular (Dello Ioio *et al.*, 2007; Moubayidin *et al.*, 2010; Tsukagoshi *et al.*, 2010), establecer correctamente la posición de las transiciones RAM/ZA y DP/DT es esencial para una descripción fenotípica completa de la raíz en diferentes condiciones experimentales. Por lo tanto, este problema requiere el desarrollo de criterios y metodologías cuantitativas que permitan la determinar las posiciones de estas transiciones de manera objetiva y reproducible. En este trabajo se propone que modelos poligonales o de múltiple cambio estructural (MCE) de las longitudes celulares de la zona de crecimiento (los cuales se pueden obtener fácilmente de preparaciones fijas) se pueden usar con dos propósitos: determinar el número de transiciones celulares que suceden en una fila de células de la raíz y aproximar la posición de estas transiciones. Una vez que se tienen los submodelos lineales para cada una de las regiones longitudinales de la raíz, éstos se pueden utilizar para calcular distintos parámetros celulares. De esta manera, los modelos MCE representan una solución a los dos problemas descritos en el patrón de regionalización longitudinal de la raíz: conocer cuántas transiciones existen y las posiciones de éstas.

Además de presentar brevemente el algoritmo utilizado para generar los modelos MCE, se muestra la utilidad y versatilidad de este método al analizar perfiles de longitudes celulares de raíces en distintas condiciones experimentales que abarcan: dos ecotipos (Col-0 y C24); dos fondos genéticos (tipo silvestre y un alelo de pérdida de función de *XANTAL 1*), en dos tiempos distintos (siete y nueve días posteriores a la siembra); y diferentes concentraciones de nitrógeno en el medio de cultivo. También se comparan los resultados obtenidos mediante los modelos MCE, y aquellos por medio de marcadores moleculares.

También, con el objetivo de facilitar el uso de esta metodología, se presenta un código en lenguaje PHP (**Apéndice 4**) que permite obtener modelos MCE de perfiles de longitudes celulares y calcular diversos parámetros útiles. Esta herramienta está a disposición de la comunidad el sitio: www.ibiologia.com.mx/MSC_analysis.

El gen *XANTAL1* y su papel en la regulación del crecimiento de la raíz

Antecedentes directos del presente trabajo muestran que el gen *XANTAL1* (*XAL1*), miembro de la familia MADS-box, participa en la regulación del balance proliferación/diferenciación celular en la raíz (Tapia-López *et al.*, 2008),

esto representa uno de los pocos casos en que se ha logrado describir funcionalmente a un miembro de esta familia en el desarrollo de la raíz. El desconocimiento que se tiene aún de la función que desempeñan los MADS-box en el desarrollo de la raíz, contrasta con el amplio conocimiento que se tiene de ellos en la regulación de la transición a la floración y la determinación de los verticilos florales (ver: Alvarez-Buylla *et al.*, 2010). De hecho, la mayor parte del conocimiento que se tiene acerca de los MADS-box en plantas está relacionado a su función en el meristemo floral.

Estudios genéticos de diversos mutantes homeóticos florales condujeron a la propuesta del modelo ABC para el desarrollo floral. Este modelo propone que mediante la acción combinatoria de tres conjuntos de genes, los genes de función A, B y C, se especifica la identidad de los cuatro órganos florales: sépalos, pétalos, estambres y carpelo (Bowman *et al.*, 1989, 1991; Coen y Meyerowitz, 1991). En *Arabidopsis*, *APETALA1* (*AP1*) y *AP2* son los genes de función A, *PISTILLATA* (*PI*) y *AP3* son los genes de función B, y *AGAMOUS* (*AG*) el gen de función C. Con excepción de *AP2* todos estos genes pertenecen a la familia MADS-box.

Mediante experimentos de sobreexpresión *in vivo*, que lograron la conversión de hojas en pétalos, y análisis de interacción por dos híbridos en levadura se logró determinar que los factores transcripcionales de dominio MADS (codificados por los genes MADS-box), *AP1*, *AP3*, *PI* y *AG*, junto con *SEPALLATA1* (*SEP1*), *SEP2* y *SEP3* (que son también factores transcripcionales de dominio MADS) forman complejos proteicos que son la base combinatoria molecular del modelo ABC (Honma y Goto, 2001; Pelaz *et al.*, 2001). Previamente se demostró mediante ensayos de dos híbridos en levadura que las proteínas *DEFICIENS* (*DEF*), *SQUAMOSA* (*SQUA*) y *GLOBOSA* (*GLO*) de *Antirrhinum majus* son capaces de formar complejos multiméricos, que constan de un heterodímero *DEF-GLO* y un homodímero *SQUA-SQUA* (Egea-Cortines *et al.*, 1999).

Estos descubrimientos dieron como resultado que el modelo ABC, basado en los genes, se transformara en un modelo basado en la combinatoria de factores transcripcionales. En este modelo, combinaciones de dos dímeros MADS interactúan para formar tetrámeros proteicos con mayor complejidad y especificidad en sus funciones reguladoras, por lo que se le denominó modelo de «cuartetos florales» (Theissen y Saedler, 2001; Theissen, 2001).

La capacidad de las proteínas de dominio MADS de formar complejos multiméricos es un mecanismo combinatorio que permite incrementar la diversidad de factores transcripcionales y la especificidad de sus sitios blanco. A partir del análisis de dos híbridos en levadura a gran escala, donde se utilizó el conjunto completo de proteínas MADS en *Arabidopsis*, se logró determinar que al menos 269 dímeros son potencialmente posibles (de Folter *et al.*, 2005). Si además de la capacidad de estos dímeros de combinarse y formar tetrámeros sumamos el hecho de que las proteínas de dominio MADS de plantas son capaces de interactuar con proteínas de otras familias —como se ha determinado para *AP1* y *SEP3* con *SEUSS* (Sridhar *et al.*, 2006); *AGAMOUS-Like 15* (*AGL15*), *SUPPRESSOR OF OVEREXPRESSION OF CO 1* (*SOC1*) y *AGL24* con miembros del complejo *SIN3/HDAC*, en particular con *SAP18* (Hill *et al.*, 2008; Liu *et al.*, 2009); y *SHORT VEGETATIVE PHASE* (*SVP*) también denominado *AGL22*

con TERMINAL FLOWER 2 (TFL2) (Liu *et al.*, 2009)—, tanto la diversidad de complejos proteicos de orden superior y sus funciones, como la especificidad de sus blancos se incrementa enormemente. En este contexto es evidente que para poder tener un conocimiento adecuado de las funciones de los factores transcripcionales MADS es fundamental estudiarlos desde una perspectiva combinatoria.

Aunque aún no se tienen caracterizados complejos multiméricos MADS en la raíz de *Arabidopsis*, tal como los que se han descrito en la parte aérea, no es difícil imaginar que este tipo de complejos existan y realicen funciones importantes en este órgano. Dentro de los primeros pasos dados en la caracterización funcional de complejos MADS en la raíz, está la descripción de los patrones de expresión por hibridación *in situ* de los genes *AGL12*, *AGL17*, *AGL19* y *AGL21* (Alvarez-Buylla *et al.*, 2000; Burgeff *et al.*, 2002). Posteriormente, se determinó que *ARABIDOPSIS NITRATE REGULATED 1* (*ANR1*) es parte de la vía de señalización que regula el crecimiento de las raíces laterales en respuesta a la adición de NO_3^- externo (Zhang y Forde, 1998; Gan *et al.*, 2005).

Nawy y colaboradores (2005) encontraron que *AGL42* tiene una fuerte expresión en las células del CQ, la cual se debilita drásticamente en las células contiguas, por lo que usaron la expresión de este gen como marcador molecular y realizaron un perfil transcripcional de las células del CQ. Además encontraron que *PISTILLATA* (*PI*) también forma parte del conjunto de factores transcripcionales que se expresa en el CQ (Nawy *et al.*, 2005). Como ya mencioné, *PI* es uno de los genes homeóticos del modelo ABC, que junto con *AP3* determina la función B, necesaria para la determinación de pétalos y estambres (Bowman *et al.*, 1989, 1991; Coen y Meyerowitz, 1991). El heterodímero *PI/AP3* activa transcripcionalmente al gen *NAP* (*NAC-LIKE, ACTIVATED BY AP3/PI*) en la flor (Sablowski y Meyerowitz, 1998). Es interesante que tanto *PI* como *NAP* se expresan en el CQ de la raíz de *Arabidopsis*, pero no *AP3* (Nawy *et al.*, 2005). Esto sugiere que el factor transcripcional *PI* puede tener distintos intercambios y genes blanco en la raíz de los que tiene en flor, lo que pone de manifiesto una vez más la riqueza funcional, producto de la combinatoria, que tienen las proteínas MADS.

Un aspecto que es importante resaltar acerca de los factores transcripcionales MADS es la redundancia funcional. Esta característica se manifiesta en la carencia de fenotipos de diversos mutantes sencillos, e incluso dobles, de pérdida de función. Por ejemplo, diversos mutantes sencillos de pérdida de función de genes MADS, entre los que se encuentran *AGL42*, *PI*, *AGL19*, *SOC1*, *AGL71* y *AGL72* no mostraron alteraciones evidentes en el fenotipo de la raíz; incluso dobles mutantes como *agl42-1 agl19-1* y *agl42-1 soc1* carecieron de fenotipos evidentes (Nawy *et al.*, 2005). Esta redundancia funcional es un factor que dificulta el estudio de la función de los complejos MADS en la raíz, en donde su efecto es más evidente que en la flor. Todo lo anterior nos indica que el estudio del papel de los complejos MADS en la raíz no es trivial, que es necesario realizar desde una perspectiva combinatoria que no es fácil de realizar y que puede consumir una gran cantidad de tiempo (principalmente por el gran número de miembros de la familia). Estos estudios genéticos combinatorios se deben guiar con información espacial detallada de la distribución de los factores transcripcionales MADS y de sus intercambios (Nawy *et al.*, 2005).

A pesar de la redundancia funcional de los MADS-box mencionada, en raíces de alelos de pérdida de función de los genes *AGL12* y *AGL14*, que se renombraron como *XAANTAL1* (*XAL1*) y *XAL2* respectivamente (Tapia-López *et al.*, 2008; Garay-Arroyo *et al.*, 2013), se pueden observar alteraciones en el desarrollo de la raíz, particularmente en el balance proliferación/diferenciación celular. En el caso de *XAL1* se encontró que alelos de pérdida de función presentan raíces más cortas en relación a las raíces tipo silvestres (ecotipos Col-0 y Ler), producto de una duración del ciclo celular mayor y un menor número de células proliferativas (Tapia-López *et al.*, 2008). También se observó que el alelo *xal1-2* (ecotipo Col-0) presenta células totalmente diferenciadas más cortas respecto a las raíces silvestres y que la expresión de *XAL1* es regulada positivamente en presencia de auxinas en el floema (Tapia-López *et al.*, 2008). Recientemente *XAL2* se caracterizó funcionalmente como un promotor de la proliferación y del alargamiento celular (Garay-Arroyo *et al.*, 2013). Además, *XAL2* es un regulador transcripcional directo de los transportadores polares de auxinas PIN1 y PIN4 (Garay-Arroyo *et al.*, 2013).

A través de modelos MCE en perfiles de longitudes celulares en raíces tipo silvestre (wt) y *xal1-2* (*xal1*), se encontró que *XAL1* es necesario para el crecimiento del DP durante los primeros días de desarrollo (Pacheco-Escobedo *et al.*, 2016). Las raíces de plántulas *xal1* presentan una velocidad de crecimiento prácticamente constante, en contraposición a la aceleración positiva que se observa en las raíces wt. Esta diferencia en las velocidades de crecimiento se debe a que el número de células proliferativas permanece casi constante en las raíces *xal1*, mientras que en las raíces wt se observa un crecimiento de la población de células proliferativas. Además, la pérdida de función de *XAL1* provoca un aumento tanto en el tamaño crítico de inicio de la división celular (L_{CritD}) como en el tamaño crítico de transición a la ZA (L_{CritA}) (Pacheco-Escobedo *et al.*, 2016). De esta forma se muestra cómo los modelos MCE permiten un mejor aprovechamiento de las características estructurales de la raíz de *Arabidopsis* en particular, y de las angiospermas en general, al realizar una mejor caracterización fenotípica a nivel celular se pueden comprender los cambios en las tasas de crecimiento, la distribución de las divisiones celulares, el ciclo celular y el patrón de regionalización longitudinal. El uso de los modelos MCE en la caracterización funcional de otros genes MADS-box puede ayudar a comprender mejor el papel de los miembros de esta familia en el desarrollo de la raíz, al proporcionar análisis cuantitativos de la zona de crecimiento de la raíz, sin los cuales alteraciones en el desarrollo pueden pasar inadvertidas.

El presente trabajo consiste en la adaptación de modelos MCE en el análisis del patrón de regionalización longitudinal de la zona de crecimiento de la raíz de *Arabidopsis*. Estos modelos estadísticos nos proporcionan una solución a dos problemas particulares: 1) Determinar cuántas regiones longitudinales existen en la zona de crecimiento de la raíz; y 2) Determinar la posición de las fronteras entre estas regiones. Se presenta una breve descripción de los modelos MCE y se discute su aplicación en perfiles de longitudes celulares de raíces de *Arabidopsis* en distintas condiciones experimentales. También se analiza la utilidad de los modelos MCE como una herramienta de fácil implementación en la caracterización fenotípica de la raíz. La mayor parte de estos resultados y detalles

metodológicos se encuentran en la publicación que se incluye en la sección de resultados (Pacheco-Escobedo *et al.*, 2016). Además se incluyen en los **Apéndices 1 y 2** dos publicaciones (Garay-Arroyo *et al.*, 2013; García-Cruz *et al.*, 2016) que se enfocan en el papel de *XAL1* y *XAL2* en la raíz. En estas publicaciones participé en los análisis celulares que se presentan en ellos. Las principales aportaciones de estos trabajos son el descubrimiento de *XAL2* como regulador transcripcional directo de los transportadores de auxinas *PIN1* y *PIN4* (Garay-Arroyo *et al.*, 2013) y que *XAL1* regula positivamente a distintos componentes del ciclo celular como *CYCD3;1*, *CYCA2;3*, *CYCB1;1*, *CDKB1;1* y *CDT1a* (García-Cruz *et al.*, 2016). Los **Apéndices 3 y 4** incluyen códigos R y PHP, respectivamente, para realizar modelos MCE de perfiles de longitudes celulares. Finalmente el **Apéndice 5** muestra los resultados de un análisis cuantitativo por modelos MCE de raíces *Arabidopsis* C24. Estos resultados se incluyeron como material suplementario en el artículo Pacheco-Escobedo *et al.* 2016.

Hipótesis

La zona de crecimiento de la raíz de *Arabidopsis* está compuesta de tres regiones discretas: El DP, DT (que conforman el RAM) y la ZA. Estas tres regiones se pueden identificar y delimitar a través de modelos MCE de la distribución de longitudes celulares en la zona de crecimiento.

Objetivos

1. Aplicar algoritmos de modelos MCE a perfiles de longitudes celulares en la zona de crecimiento de raíces de *Arabidopsis*.
2. Detectar a través de estos modelos la existencia de tres regiones en la zona de crecimiento de la raíz de *Arabidopsis*: El DP, el DT y la ZA.
3. Comparar las transiciones detectadas a través de los modelos MCE con los patrones de expresión de marcadores moleculares de proliferación y endorreduplicación.
4. Determinar el tamaño de cada una de las regiones, principalmente el DP, a través de los modelos MCE generados y comparar los resultados con aquellos obtenidos con otros métodos comúnmente aplicados en la investigación (ver: Rost y Baum 1988; Dubrovsky *et al.* 1998a,b; Garay-Arroyo *et al.* 2013).
5. Utilizar los modelos MCE para caracterizar cuantitativamente la zona de crecimiento de raíces *wt* y *xal-1* en dos edades distintas. Por medio de estos resultados, analizar la función de *XAL1* en la regulación del balance entre proliferación y diferenciación celular.
6. Generar herramientas de cómputo que permitan aplicar de manera sencilla modelos MCE al análisis fenotípico de raíces.

Resultados

El patrón de regionalización longitudinal de la raíz

Es mucho mejor contar con una respuesta aproximada a la pregunta adecuada...

que contar con una respuesta exacta a una pregunta mal planteada

John Tukey

Modelos de múltiple cambio estructural aplicados a perfiles de longitudes celulares

En el caso del patrón de regionalización longitudinal de la raíz podemos decir que existen dos problemas fundamentales que hemos mencionado: 1) determinar el número de dominios o zonas que existen en la zona de crecimiento activo, o dicho de otra forma, el número de transiciones por las que pasan las células en la raíz a lo largo del eje longitudinal; y 2) proponer un método objetivo para establecer la posición longitudinal de dichas transiciones.

A partir de perfiles de velocidad de crecimiento con respecto a la distancia al CQ en *Arabidopsis* (la velocidad con la que se aleja cada punto de la raíz del CQ), van der Weele y colaboradores (2003) establecen que en la raíz se pueden distinguir tres regiones longitudinales: Una región que comienza en el CQ ($x = 0$) donde la velocidad se incrementa, prácticamente desde cero, gradualmente con respecto a la posición; después, aproximadamente a unos 500 μm de distancia del CQ, se da un incremento drástico de la velocidad de crecimiento; y finalmente se alcanza una velocidad constante, lo que indica el fin de la zona de crecimiento activo. Estas regiones corresponden al RAM, la ZA y la ZD, respectivamente.

Dos aspectos importantes de estos perfiles de velocidad de crecimiento son que estas tres regiones están delimitadas por dos transiciones abruptas y que los incrementos de velocidad con respecto a la posición parecen ser lineales en el RAM y la ZA —los autores apoyan esta última conclusión con el análisis de residuales de las ecuaciones lineales obtenidas para raíces individuales y con referencias a trabajos previos hechos en diferentes

especies— (van der Weele *et al.*, 2003). Gracias a estas dos características van der Weele y colaboradores (2003) ajustaron los perfiles de velocidad a un modelo conformado por tres ecuaciones lineales unidas por dos puntos de rompimiento (*breakpoints*) o transiciones abruptas. Para un modelo del perfil de velocidad de la zona de crecimiento activo, la derivada, es decir la aceleración, es una función compuesta por dos fases escalonadas que corresponde a una tasa de alargamiento relativamente constante en el RAM, y una tasa, también constante, pero mucho más alta en la ZA con una rápida transición entre estas dos fases (van der Weele *et al.*, 2003).

Estos resultados apoyan la idea de ajustar los perfiles de longitud celular con respecto a la posición relativa al CQ a modelos poligonales, es decir modelos conformados por ecuaciones lineales para cada una de las regiones separadas por puntos de rompimiento.³ Estos modelos son conocidos como modelos poligonales, modelos segmentados, modelos de línea quebrada, regresiones de multifase o modelos de Múltiple Cambio Estructural (MCE) (Bai y Perron, 2003; Muggeo, 2003). En los modelos MCE, los puntos donde el comportamiento o respuesta de la variable dependiente cambia drásticamente son conocidos como puntos de rompimiento, puntos de cambio o puntos de transición (Muggeo, 2003). Estos cambios drásticos o puntos de rompimientos, los podemos identificar como cambios en la pendiente y/o cambios en la ordenada al origen de las rectas que forman el modelo. En los perfiles de longitud celular (L) donde ésta es función de la posición relativa al CQ (X), los puntos de rompimiento corresponden a las transiciones o fronteras entre dos regiones longitudinales adyacentes de la raíz.

¿Por qué hacer el análisis en perfiles de longitud celular y no en perfiles de velocidad como los realizados por van der Weele y colaboradores? Existen dos razones para elegir ajustar modelos MCE en perfiles de longitud celular en lugar de perfiles de velocidad. En primer lugar, es mucho más sencillo obtener perfiles de longitud celular, los cuales se pueden obtener de preparaciones fijas de raíces. La segunda razón es que los perfiles de velocidad, al menos como son obtenidos por van der Weele y colaboradores (2003), son capaces de distinguir cambios en la tasa de alargamiento celular, pero incapaces de detectar cambios en la tasa de proliferación celular en las distintas regiones longitudinales de la raíz. Debemos recordar que el DP y el DT no difieren en la tasa de alargamiento, sino en la tasa de proliferación, por lo tanto si deseamos comprobar la existencia del DT y determinar la posición de sus límites, los perfiles de velocidad de análisis cinemáticos, que se basan en el seguimiento de puntos en la superficie de la raíz (Beemster y Baskin, 1998; van der Weele *et al.*, 2003), no son los adecuados porque no detectan si dos puntos en la superficie pertenecen a una o a dos células diferentes. Por esta razón la presencia del DT no es detectada por van der Weele *et al.* (2003).

Así, la principal propuesta de este trabajo es que el ajuste de perfiles de longitud celular de raíces individuales a modelos MCE resuelve los dos problemas fundamentales del patrón de regionalización longitudinal de la raíz mencionados. A continuación se explica brevemente los fundamentos de los modelos MCE.

³La idea de aplicar modelos poligonales a los perfiles de longitud celular surgió a partir de la colaboración que tuve con el físico Germán Arriaga y el ingeniero Hibels Ávila, ambos de la Escuela Superior de Física y Matemáticas del IPN.

El análisis de regresión consiste básicamente en ajustar los datos experimentales a un modelo o ecuación matemática relativamente sencilla. De manera general podemos suponer que Y es una variable cuantitativa dependiente y que tenemos p diferentes variables independientes, X_1, X_2, \dots, X_p . En el análisis de regresión se asume que existe una relación entre Y y $X = (X_1, X_2, \dots, X_p)$, la cual se puede escribir de la siguiente forma general:

$$Y = f(X) + \epsilon \quad (1)$$

Donde f es una función determinada pero desconocida de X_1, X_2, \dots, X_p , y ϵ es un término de error aleatorio, el cual es independiente de X y tiene una media igual a cero. En este planteamiento se puede decir que f representa la información «sistemática» que nos proporciona X acerca de nuestra variable dependiente Y . Por lo tanto, el análisis de regresión o ajuste a un modelo matemático consiste en conocer f . Los modelos matemáticos que se obtienen pueden tener, a grandes rasgos, dos propósitos principales: hacer predicciones o realizar inferencias (James *et al.*, 2013).

En los modelos predictivos, el interés principal está en calcular con cierto nivel de precisión el valor de Y , mientras que la naturaleza exacta de f , es decir la relación entre Y y X , no es nuestro principal objetivo. En cambio, en los modelos inferenciales estamos interesados en conocer la forma en la que X afecta el cambio de Y , no en predecir el valor de esta última. Los modelos o funciones pueden cumplir con estos dos propósitos hasta cierto grado, aunque en muchas situaciones es necesario decidir un propósito específico (James *et al.*, 2013). En el caso del presente trabajo, los modelos que deseamos obtener son principalmente de carácter inferencial, ya que es de poco interés predecir la longitud de cada una de las células de las raíces; nuestro interés es conocer cómo cambia la longitud de las células en función de su posición con respecto al CQ y en qué posición cambia el comportamiento de las células. El cálculo de los tamaños críticos es un caso especial donde sí es de interés calcular la longitud de una célula específica, en este caso hablamos de modelos predictivos.

Los métodos estadísticos paramétricos se basan en determinar *a priori* la forma de la función f . Por ejemplo, en el caso de las regiones longitudinales de la raíz, se supone que los datos siguen una función lineal respecto a la posición. Dado que la función que calculamos no es f sino una aproximación a esta que denotamos como \hat{f} tenemos:

$$\hat{f}(X) = \alpha + \beta X \quad (2)$$

Al hacer esta suposición, el problema de calcular \hat{f} se reduce, ya que sólo es necesario calcular los coeficientes α y β (la ordenada al origen y la pendiente respectivamente), es decir deseamos conocer los valores de los parámetros de la función. Dado que $\hat{f}(X) \approx L$ (la longitud celular respecto a la posición) en el caso de los perfiles de longitud celular tenemos:

$$L \approx \alpha + \beta X \quad (3)$$

Refiriéndose a los perfiles de longitud celular α representa la longitud de la célula en la posición cero y β la tasa o velocidad de alargamiento respecto a la posición.⁴

El método más usado, aunque no el único, para calcular el valor de los parámetros de una función es el método de los mínimos cuadrados. La principal desventaja de los métodos paramétricos es que el tipo de función seleccionada no necesariamente es el tipo de función real de los datos, lo que puede ocasionar que el poder predictivo del modelo sea relativamente bajo (James *et al.*, 2013).

En resumen, lo que se pretende obtener para cada una de las regiones longitudinales de la raíz es una ecuación lineal que modele las longitudes celulares que corresponden a cada una de estas regiones. Posteriormente, una vez delimitadas las regiones se analizará si efectivamente se comportan efectivamente de manera lineal.

Los modelos MCE son una secuencia de submodelos lineales unidos entre ellos por puntos llamados de rompimiento, si estos puntos son conocidos, el problema se reduce a ajustar cada uno de los conjuntos de puntos, delimitados por los puntos de rompimiento, a una ecuación o modelo lineal; si los puntos de rompimiento son desconocidos, como en el caso del patrón de regionalización de la raíz, el problema es de mayor dificultad (Bellman y Roth, 1969).

En términos generales, la resolución de este problema consiste en encontrar el conjunto de submodelos o rectas con la mejor bondad de ajuste (pueden ser usados diferentes criterios, por ejemplo el mínimo de la suma del cuadrado de los residuales). A continuación se describe el modelo general para un perfil de longitudes celulares adaptando el planteamiento de Bai y Perron (2003) para la resolución de este problema de manera computacional.

Para el caso de los perfiles de longitudes celulares, se puede escribir el sistema de ecuaciones lineales con m puntos de rompimiento o transiciones ($m + 1$ regiones o zonas y dominios longitudinales) como:

$$l_t = \alpha_j + x'_t \beta_j + u_t \quad t = T_{j-1} + 1, \dots, T_j \quad (4)$$

para $j = 1, \dots, m + 1$. En este modelo, donde cada ecuación del sistema corresponde a una región de la raíz, l_t es la longitud de una célula en la posición t ; x_t ($p \times 1$) es el vector con las posiciones t con respecto al CQ; α_j y β_j son los vectores de los coeficientes correspondientes a la región j , es decir, la ordenada al origen y pendiente de cada región; u_t es el error o desviación en la posición t . Los índices (T_1, \dots, T_m) corresponden a las transiciones o puntos de rompimiento entre regiones longitudinales, los cuales son desconocidos. Se considera por convención

⁴Es importante tener en cuenta que esta tasa o velocidad de alargamiento es respecto a la posición, no respecto al tiempo. El tiempo no está considerado aquí.

que $T_0 = 0$ y $T_{m+1} = T$, lo que nos da todas las posiciones de las células que se incluyen en el perfil considerado. En este contexto, el problema principal consiste en calcular los puntos de rompimiento.

El sistema de ecuaciones lineales (4) se puede expresar en forma de matriz como:

$$L = \bar{Z}\alpha + \bar{Z}\beta X + U \quad (5)$$

donde $L = (l_1, \dots, l_T)'$, $X = (x_1, \dots, x_T)'$, $U = (u_1, \dots, u_T)'$, $\alpha = (\alpha'_1, \alpha'_2, \dots, \alpha'_{m+1})'$, $\beta = (\beta'_1, \beta'_2, \dots, \beta'_{m+1})'$, y \bar{Z} es la matriz que parte diagonalmente a Z en (T_1, \dots, T_m) , es decir $\bar{Z} = \text{diag}(Z_1, \dots, Z_{m+1})$ con $Z_i = (Z_{T_{i-1}+1}, \dots, Z_{T_i})'$. Esta matriz contiene las ecuaciones lineales de todos los segmentos que es posible formar con los puntos de un perfil de longitudes celulares con m transiciones. Lo que se busca es conocer los parámetros «verdaderos» de este sistema. Si los valores «verdaderos» de los parámetros se indican con un superíndice 0, tenemos el sistema:

$$L = \bar{Z}^0\alpha^0 + \bar{Z}^0\beta^0 X + U \quad (6)$$

El cual contiene las ecuaciones lineales o submodelos para el MCE con las transiciones o puntos de rompimiento en las posiciones (T_1^0, \dots, T_m^0) . Nuevamente, el principal problema consiste en determinar (T_1^0, \dots, T_m^0) , una vez hecho esto es fácil conocer el valor de los coeficientes. Para encontrar los parámetros de este sistema, Bai y Perron (2003) utilizan el criterio de mínimos cuadrados de los residuales, para cada partición posible con m transiciones de un perfil de longitudes celulares:

$$(L - \bar{Z}\alpha - \bar{Z}\beta X)' (L - \bar{Z}\alpha - \bar{Z}\beta X) = \sum_{i=1}^{m+1} \sum_{t=T_{i-1}+1}^{T_i} [l_t - z'_t\alpha_i - z'_t x'_t \beta_i]^2 \quad (7)$$

Sean $\hat{\alpha}(\{Z_j\})$ y $\hat{\beta}(\{Z_j\})$ los parámetros calculados para una determinada región longitudinal para un patrón con $m+1$ con regiones longitudinales (Z_1, \dots, Z_{m+1}) , donde cada región se denota con $\{Z_j\}$. Sustituyendo estos parámetros en (7) y denominando la suma de residuales al cuadrado como $S_T(T_1, \dots, T_m)$, las posiciones de las transiciones o puntos de rompimiento calculadas $(\hat{T}_1, \dots, \hat{T}_m)$ serán aquellas que en conjunto minimicen el valor de la función (7). De manera general, podemos decir que la estrategia a seguir es: 1) encontrar todos los segmentos posibles que se puedan formar con el conjunto total de puntos que tiene nuestro perfil de longitudes celulares; 2) calcular las ecuaciones lineales para cada uno de estos segmentos; 3) calcular la suma de residuales para cada modelo correspondiente a cada segmento; y 4) encontrar el conjunto de $m+1$ segmentos (estos segmentos se consideran conjuntos de puntos mutuamente excluyentes y comprenden el total de puntos del perfil de longitudes celulares) que tenga la menor suma global de residuales.

La estrategia anterior se implementó a través de algoritmos basados en programación dinámica por primera vez por Bellman y Roth (1969) y retomado posteriormente por Bai y Perron (2003). El algoritmo desarrollado por Bai y Perron (2003) fue implementado en el paquete *strucchange* del lenguaje estadístico *R* (Zeileis *et al.*, 2002, 2003). Este paquete determina la posición óptima global de m transiciones en un perfil de longitudes celulares (la aplicación de modelos MCE en que estamos interesados), pero además calcula los intervalos de confianza de dichas posiciones a través de la función de distribución dada por Bai (1997). Este paquete puede ser usado de forma libre, por lo que el patrón de regionalización de una raíz se puede realizar usando las funciones de *strucchange*. En el **Apéndice 3** se proporciona un ejemplo de cómo utilizar este paquete para analizar una raíz en el lenguaje *R*.

Con el objetivo de proporcionar una herramienta en línea que pueda ser utilizada de manera sencilla para determinar la posición de las transiciones en un perfil de longitudes celulares, se desarrollo un código *PHP* que se encuentra disponible al público en: http://www.ibiologia.com.mx/MSC_analysis/. Este programa toma una idea similar a la de la programación dinámica desarrollada por Bai y Perron (2003), pero está enfocado exclusivamente a encontrar las transiciones de un perfil de longitudes celulares. El programa permite calcular una o dos transiciones. El código se incluye en el **Apéndice 4**.

Cálculo del número de transiciones o puntos de rompimiento

Diversos autores consideran que en la región de crecimiento activo de la raíz existen dos regiones el RAM y la ZA, es decir no consideran la existencia del DT (véase: Dello Iorio *et al.* 2007; Moubarak et al. 2010). Por lo tanto, un problema a considerar al momento de calcular modelos MCE de los perfiles de longitudes celulares es el número de transiciones o puntos de rompimiento que son considerados. Uno puede determinar *a priori* cuántas transiciones tendrá un modelo MCE y mediante el criterio de mínimo cuadrado de los residuales calcular la posición óptima de estas transiciones. Sin embargo, el número de transiciones de un modelo puede ser un parámetro arbitrario que no tiene relación necesariamente con el número de transiciones que realmente existe. Por lo tanto, es necesario un criterio o método que permita determinar cuál es el número apropiado de transiciones para modelar un conjunto de datos, en este caso un perfil de longitudes celulares.

Existen distintos procedimientos para determinar el número de transiciones, los cuales consideran un criterio de información (Yao, 1988; Liu *et al.*, 1997; Bai, 1997; Bai y Perron, 2003; Kim *et al.*, 2000, 2009). En este trabajo se usa el criterio de información bayesiana (BIC por sus siglas en inglés) o criterio de Schwarz (Yao, 1988), el cual tiene un buen desempeño cuando existe al menos una transición o punto de rompimiento en los datos que se modelan y es capaz de detectar cambios pequeños (Bai y Perron, 2003; Kim *et al.*, 2009).

El BIC hace un ajuste o corrección a la suma de residuales conforme se introducen más transiciones o variables independientes a un modelo. La suma del cuadrado de residuales irá disminuyendo conforme se introduzcan más

variables en un modelo, o en el caso de los modelos MCE si se introducen transiciones o puntos de rompimiento, por lo que la suma de residuales no puede usarse como criterio para elegir dentro de un conjunto de modelos con distintos número de transiciones (James *et al.*, 2013). Para un modelo de suma del cuadrado de residuales (*SCR*) con m transiciones o puntos de rompimiento el BIC está dado por:

$$BIC = \frac{1}{n} \left(SCR + \log(n)m\hat{\sigma}^2 \right) \quad (8)$$

donde n es el número de observaciones o el número de longitudes celulares que se incluyen en el perfil que se modela, $\hat{\sigma}^2$ es la varianza calculada del error U asociada con cada medición en (6). Se puede observar cómo el BIC adiciona una penalización igual a $\log(n)m\hat{\sigma}^2$ a la *SCR* que depende del número de transiciones o puntos de rompimiento (James *et al.*, 2013). Es evidente que la penalización se hace mayor conforme el modelo MCE tiene más transiciones.

De esta forma, para un mismo perfil de longitudes celulares se generan diversos modelos MCE con $0, 1, 2, \dots, n$ puntos de rompimiento. Cada uno de estos modelos se genera como se describió en la sección anterior, es decir, se generan modelos con una, dos, tres o más rectas con la menor *SCR*. Una vez que se tienen estos modelos para un perfil de longitudes celulares determinado se calcula el BIC mediante (8) para cada modelo. El modelo seleccionado será aquel con el menor BIC calculado.

Los modelos MCE y el uso del BIC como criterio para seleccionar el número de puntos de rompimiento que se acaban de describir, son la base de los principales resultados que se obtuvieron durante mis estudios de doctorado. A continuación se presenta el artículo donde se publican estas aportaciones. Debo destacar la labor del biólogo Iván Ránsom que proporcionó la mayor parte de los perfiles de longitudes celulares que se analizaron, sin los cuales mucho de lo presentado no se habría logrado.

PART OF A SPECIAL ISSUE ON ROOT BIOLOGY

Longitudinal zonation pattern in *Arabidopsis* root tip defined by a multiple structural change algorithm

Mario A. Pacheco-Escobedo^{1,†}, Victor B. Ivanov^{2,†}, Iván Ransom-Rodríguez¹, Germán Arriaga-Mejía³, Hibels Ávila³, Ilya A. Baklanov², Arturo Pimentel⁴, Gabriel Corkidi⁴, Peter Doerner⁵, Joseph G. Dubrovsky^{4,*}, Elena R. Álvarez-Buylla^{1,*} and Adriana Garay-Arroyo^{1,*}

¹Laboratorio de Genética Molecular, Desarrollo y Evolución de Plantas, Instituto de Ecología, Universidad Nacional Autónoma de México, 3er Circuito Ext. Junto a J. Botánico, Ciudad Universitaria, UNAM, México DF, Mexico, ²Department of Root Physiology, Timiryazev Institute of Plant Physiology, Russian Academy of Sciences, ul. Botanicheskaya 35, Moscow, 127276 Russia, ³Escuela Superior de Física y Matemáticas, Instituto Politécnico Nacional, U.P. Adolfo López Mateos, México DF, México, ⁴Instituto de Biotecnología, Universidad Nacional Autónoma de México, Apartado Postal 510-3, 62250 Cuernavaca, Morelos, México and ⁵Institute of Molecular Plant Science, School of Biological Sciences, University of Edinburgh, Edinburgh, UK

*For correspondence. E-mail jdubrov@ibt.unam.mx or eabuylla@gmail.com or garay.adriana@gmail.com

†These authors contributed equally to this work.

Received: 11 January 2016 Returned for revision: 8 March 2016 Accepted: 8 April 2016 Published electronically: 29 June 2016

• **Background and Aims** The *Arabidopsis thaliana* root is a key experimental system in developmental biology. Despite its importance, we are still lacking an objective and broadly applicable approach for identification of number and position of developmental domains or zones along the longitudinal axis of the root apex or boundaries between them, which is essential for understanding the mechanisms underlying cell proliferation, elongation and differentiation dynamics during root development.

• **Methods** We used a statistics approach, the multiple structural change algorithm (MSC), for estimating the number and position of developmental transitions in the growing portion of the root apex. Once the positions of the transitions between domains and zones were determined, linear models were used to estimate the critical size of dividing cells (L_{critD}) and other parameters.

• **Key Results** The MSC approach enabled identification of three discrete regions in the growing parts of the root that correspond to the proliferation domain (PD), the transition domain (TD) and the elongation zone (EZ). Simultaneous application of the MSC approach and G2-to-M transition (*CycB1;IDB:GFP*) and endoreduplication (*pCCS52A1:GUS*) molecular markers confirmed the presence and position of the TD. We also found that the MADS-box gene *XANTAL1* (*XAL1*) is required for the wild-type (wt) PD increase in length during the first 2 weeks of growth. Contrary to wt, in the *xal1* loss-of-function mutant the increase and acceleration of root growth were not detected. We also found alterations in L_{critD} in *xal1* compared with wt, which was associated with longer cell cycle duration in the mutant.

• **Conclusions** The MSC approach is a useful, objective and versatile tool for identification of the PD, TD and EZ and boundaries between them in the root apices and can be used for the phenotyping of different genetic backgrounds, experimental treatments or developmental changes within a genotype. The tool is publicly available at www.ibiologia.com.mx/MSC_analysis.

Key words: *Arabidopsis thaliana*, cell differentiation, cell proliferation, proliferation domain, transition domain, elongation zone, root apical meristem, longitudinal zonation pattern, critical size of dividing cells, *XANTAL1*, multiple structural change model, breakpoints.

INTRODUCTION

Plant growth and development are regulated by the combined activity of two processes that are closely linked: cell division and cell elongation. Fully elongated cells undergo terminal differentiation. Reliable and quantitative characterization of both processes in organs is thus essential for understanding their role during development. The *Arabidopsis thaliana* (arabidopsis) root is an important model system for molecular genetics and cellular studies of plant development, including understanding cell cycle regulation and the balance

of proliferation and differentiation in complex organs. The root is an excellent model system because of, among other characteristics, its relatively simple longitudinal organization and the possibility of observing different developmental stages in the same root along its longitudinal axis. Another advantage of the root is that it has few cell types, organized concentrically around the vascular tissues, composed of xylem, phloem, vascular parenchyma and pericycle. Outside of the vascular tissues there are concentric rings of cells of endodermis, cortex and epidermis, covered at the very tip by the lateral root cap and columella cells. The growing part of

the root consists of two zones: the root apical meristem (RAM) and the elongation zone (EZ) (Fig. 1A).

The RAM includes the proliferation domain (PD), where cells have a high probability of dividing, and the transition domain (TD) (Baluška *et al.*, 1996). The most distal portion of the PD contains the quiescent centre (QC), a stem cell niche, surrounded by the initial (stem) cells (Clowes, 1956; Dolan *et al.*, 1993; Sabatini *et al.*, 2003). In the TD domain cells can still divide but at a low probability and continue elongating at the same low rate as in the PD. Hence, cells in this domain are slightly longer than cells in the PD (Fig. 1B) (Ivanov and Dubrovsky, 2013). The EZ is the zone where cells of different tissues simultaneously start rapid elongation at rates much

higher than those in the RAM. The EZ is followed by the differentiation zone (DZ), where elongated cells reach their final length and differentiation state. The rootward border of the DZ corresponds to the position at which cell elongation ceases (van der Weele *et al.*, 2003; Ivanov and Dubrovsky, 2013). Therefore, identification of the boundary between the EZ and DZ is straightforward and is based on either cell length profile data or the appearance of the first root hair bulges, which is a hallmark of termination of elongation (Dolan *et al.*, 1993; Ma *et al.*, 2003; Dolan and Davies, 2004). Despite the importance of being able to fully characterize the apical–basal patterning of the root tip, no consensus on the domains and zones in the arabidopsis root apex has been attained (Ivanov and Dubrovsky,

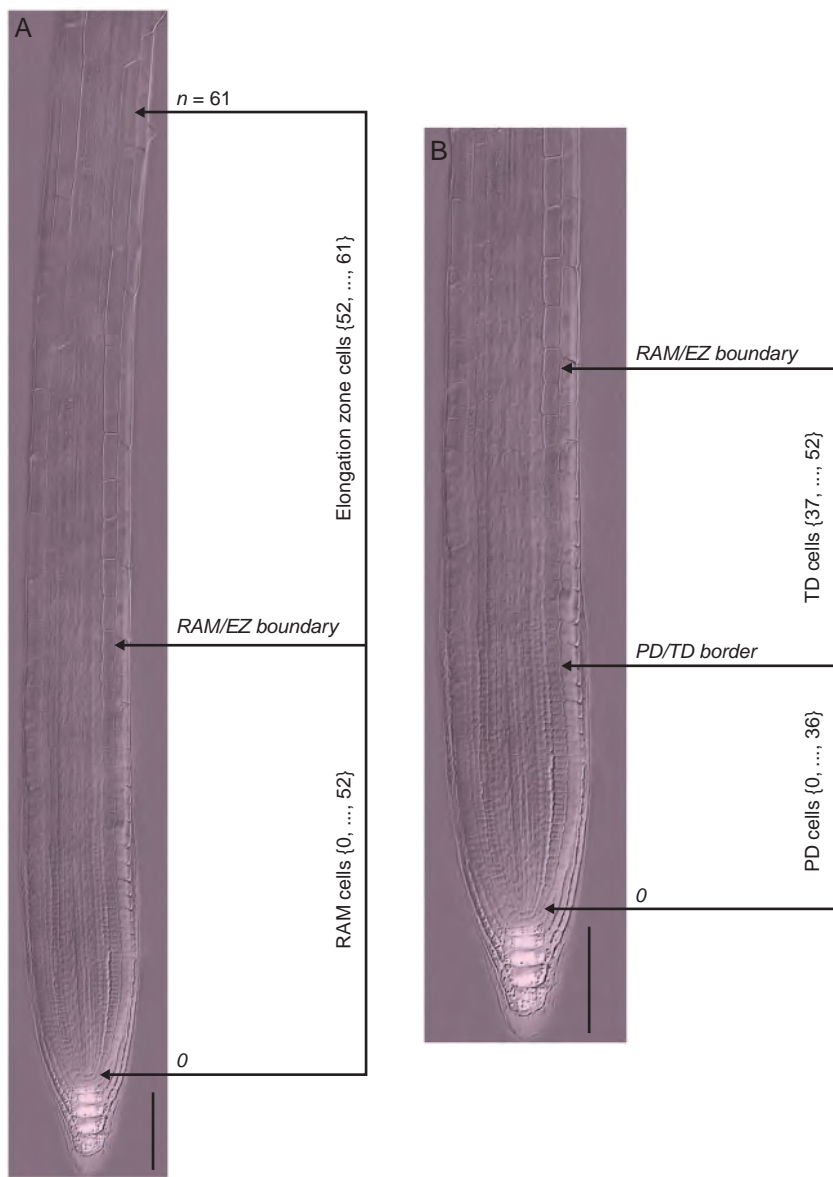


Fig. 1. Anatomical topology of the arabidopsis root. (A) The root apical meristem (RAM) and elongation zone (EZ) of a wt arabidopsis Col-0 seedling root 7 d after sowing; composite image from a cleared root preparation. (B) RAM of the root shown in (A). The numbers represent cell positions with respect to QC (zero position). The n position corresponds to the first cortex cell adjacent to an epidermal cell that started to form a root hair bulge. Scale bars = 100 μ m.

Microphotograph was published in Ivanov V.B., Dubrovsky J.G. 2013. Longitudinal zonation pattern in plant roots: conflicts and solutions. 2013. *Trends in Plant Science*, 18:237–243. Reproduced with permission of Elsevier.

2013). Here we applied a statistical algorithm for determining the number of zones and domains in the growing part of the root and the limits between neighbouring zones and domains. Our results support the existence of three discrete regions in the growing part of the arabidopsis root: the PD, the TD and the EZ.

A rigorous qualitative and quantitative description of these zones and domains and identification of their boundaries are essential for understanding the effects of different genetic, chemical and physical alterations of cell proliferation, growth, and differentiation during root growth and development. Comparisons between different experimental conditions require approaches that enable accurate evaluations of the size and number of cells within the RAM or its PD. This is generally done in the cortex cell layer (Casamitjana-Martínez *et al.*, 2003; Dello Ioio *et al.*, 2007; Tsukagoshi *et al.*, 2010; Zhou *et al.*, 2011; Garay-Arroyo *et al.*, 2013). However, the lack of objective criteria and subjectivity in identifying the boundaries between root growth zones and domains indicates the need for development of new approaches.

Several previous papers have approached this problem. For example, Scheres and collaborators (Casamitjana-Martínez *et al.*, 2003) determined the boundary between the RAM and the EZ as the point where cells begin to increase their lengths significantly. The onset of rapid cell elongation and absence of cell division in the EZ are taken as the only criterion to distinguish between these two regions. Although useful for rough qualitative evaluations, without measuring cell lengths the identification of the point where rapid elongation starts may vary among researchers. A relatively more objective way of determining this boundary implies finding the position at which cell length in a file is more than twice that of the previous cell (González-García *et al.*, 2011). The latter method may yield biased results: before rapid elongation starts, a longer cell can be followed by a shorter cell in the TD, indicating that this criterion is not always sufficient for objective establishment of the RAM/EZ boundary. Recently, a geometric approach for identification of the point at which cell elongation starts was proposed that yields results similar to those obtained arbitrarily (French *et al.*, 2012). This and other studies (Dello Ioio *et al.*, 2007; Moubayidin *et al.*, 2010; Tsukagoshi *et al.*, 2010) do not specify how to identify the border between the PD and the TD of the RAM. Changes in cell proliferation precede the transition to rapid cell elongation: the mitotic index (percentage of dividing cells) decreases drastically (Ivanov and Dubrovsky, 2013) and endoreduplication starts (Hayashi *et al.*, 2013). For this reason, the PD/TD boundary is associated with changes in cell proliferation, whereas the RAM/EZ boundary defines the point where a drastic shift to rapid elongation occurs.

The position of the PD/TD boundary is particularly difficult to establish because it fluctuates in time within a cell file and, additionally, is frequently different among different files of cells of the same type or different types (Baluška and Mancuso, 2013; Ivanov and Dubrovsky, 2013). Because of this, the PD/TD boundary can only be approximated with a certain error, which should be estimated (Ivanov and Dubrovsky, 2013). The position of this boundary can be determined as the point where average cell length along the RAM has slightly increased, or where the distances between nuclei in neighbouring cells along a cell file become greater than the diameter of the nuclei (Rost and Baum, 1988; Dubrovsky *et al.*, 1998a, b; Garay-Arroyo

et al., 2013). It is also possible to locate the beginning of the TD as the position where the mitotic index sharply decreases for the tissue under consideration (Ivanov and Dubrovsky, 2013). Nonetheless, the latter approach is difficult to implement and it is not valid for all species. All such criteria can lead to variable and subjectively defined boundaries and/or require considerable experience from the researcher in order to guarantee reproducible and reliable data. Because of the importance of each of the root developmental domains and/or zones in the cell proliferation/differentiation balance (Dello Ioio *et al.*, 2007; Moubayidin *et al.*, 2010; Tsukagoshi *et al.*, 2010), establishing the PD/TD and RAM/EZ boundaries is essential for a complete phenotypical description of the root. This requires a quantitative approach, which enables the unambiguous identification of the different development stages along the root longitudinal axis.

Here, to identify the location of the PD/TD and RAM/EZ boundaries we applied a multiple structural change algorithm (MSC) to cell length profile data collected on fixed root preparations. Because the position of the EZ/DZ boundary corresponds to the location where root hair formation starts, this location can be used as a qualitative criterion to determine the shootward border of the EZ. For this reason the EZ/DZ boundary can be easily established, and is not considered in this study. We show here that by using the polygonal models obtained from a MSC algorithm it is possible to estimate: (1) the lengths of the PD, the TD and the EZ; (2) the distances from the QC at which the different developmental transitions start; (3) the critical sizes of dividing and transitioning to the EZ cells; and (4) the derivative of cell length as a function of position or gradient in cell length (Silk *et al.*, 1986). We also show that the MSC yields similar results to those obtained with molecular markers that have been used to determine the PD/TD boundary, as well as those obtained by arbitrary estimations made by researchers experienced in root developmental biology.

XANTALI (*XAL1*) or *AGL12* is a member of the MADS box family of genes, which encode transcription factors important for regulating plant and animal development. This gene participates in the regulation of cell proliferation in the arabidopsis RAM (Tapia-López *et al.*, 2008). Loss-of-function allelic mutants have shorter roots and lower root growth rates than wild type (wt), explained by a shorter RAM, lower rates of cell production and a longer cell cycle duration than wt roots (Tapia-López *et al.*, 2008). We used the proposed MSC approach to analyse arabidopsis wt and loss-of-function *xall-2* (hereafter *xall*) mutant roots. We found that *XAL1* is necessary for the increase in length of the PD during the first days after seed germination and its loss of function altered the critical size of dividing cells. This example illustrates that the MSC approach is useful for root phenotyping at the cellular level and for comparing different experimental conditions or genotypes, and can be applied to better understand changes in cell growth rates, the distribution of cell divisions and, changes in the critical size of dividing cells and the longitudinal zonation pattern.

MATERIALS AND METHODS

Plant materials and growth conditions

Arabidopsis wt, *xall*, *CycB1;1_{DB}:GFP* and *pCCS52A1:GUS* are in Col-0 ecotype. C24 and Col-0 were obtained from the

Arabidopsis Biological Resource Center at the Ohio State University. Seeds carrying *pCCS52A1:GUS* were kindly donated by E. Kondorosi and *CycB1;1DB:GFP* was constructed by P. Doerner (Ubeda-Tomás *et al.*, 2009). All lines were homozygous; seeds were surface-sterilized and 2 d after vernalization sown on medium containing 0.2× MS (Murashige and Skoog) salts, 1 % sucrose and 1 % agar (except for *CycB1;1:GFP* seeds; see below). Petri dishes were maintained in vertical position. Plants were grown under long-day (16 h light/8 h dark) conditions in growth chambers at 22–24 °C. Seeds of the *CycB1;1DB:GFP* line were plated on agar media N103 and N3003 that contained 0.3 % sucrose supplemented with 1 (N103) or 30 (N3003) mM of total nitrogen (N) (final concentrations of other components of the media were: CaCl₂ [3 mM], MgSO₄ [1.5 mM], KH₂PO₄ [1.5 mM], 1× MS microelements, MES [5 mM], sucrose, 3 g L⁻¹, pH 5.6). After 2–7 d of vernalization, Petri dishes were transferred to growth chambers with constant light and maintained in vertical position. Root growth increments were recorded daily by marking the root tip position over the surface of the dish and increments were measured using ImageJ (<http://rsb.info.nih.gov/ij>).

Microscopy

In seedlings 7–9 d after sowing (DAS), roots were cleared using Herr's solution (Herr, 1971), which contains lactic acid (85 %), chloral hydrate, phenol, clove oil and xylene (2:2:2:2:1 by weight). Excised roots were transferred to Herr's solution for at least 24 h at room temperature and subsequently mounted in the same solution and visualized using an Olympus BX60 microscope equipped with Nomarski optics and photographed.

pCCS52A1:GUS seedlings were subjected to the β-glucuronidase (GUS) reaction in the dark for 1 h at 37 °C and GUS staining solutions were prepared as described by Malamy and Benfey (1997). To restrict the diffusion of GUS blue precipitate, 2 mM K₃Fe(CN)₆ and K₄Fe(CN)₆ were added to the solution at the beginning. After GUS staining, seedlings were immersed in Herr's clearing solution and stored in the dark at room temperature for 72 h and visualized as described above.

For simultaneous observation of the nuclei and green fluorescent protein (GFP) fluorescence (*CycB1;1DB:GFP*), 7-DAS seedlings were fixed in 4 % formaldehyde in phosphate-buffered saline (PBS) solution supplemented with 0.05 µg mL⁻¹ (final concentrations) of 4',6-diamidino-2-phenylindole (DAPI) overnight at 4 °C. Preliminary experiments showed that this procedure did not quench the fluorescence activity of GFP. Then, material was washed in PBS four times (10 min each), mounted and analysed. Roots were mounted in a drop of PBS, covered with a coverslip and observed under an inverted laser scanning confocal Leica TCS NT microscope with a 63× HCX PL APO water immersion Leica objective. After the optical median section of the apical root portion was found, the intensity of the signal was set by using the look-up tables included in the Leica software. DAPI and GFP channels were set separately and colour intensity was always set to a standard for each individual root at a low scanning speed. These same settings for colour intensity and offset were used for more proximal root portions. Final scanning of each root portion was done sequentially, first for GFP and then for DAPI, and the average of four scans was saved as a TIF file. To improve contrast between the

DAPI and GFP channels, images of GFP fluorescence were pseudo-coloured in magenta. Images of two channels of each root portion were merged and then the whole root tip image was assembled in Adobe Photoshop 5.5. from four to eight originally saved files.

Quantitative analysis

We implemented a semi-automated procedure to systematically and accurately measure cell lengths. The algorithm was constructed based on Java SRE and ImageJ 1.4 libraries. This works properly for multi-platform environments such as Windows, Linux and Mac OS. The software (executable file: Cell_Length_V2.0.jar) and its user manual (Cell_Length_V2.0.pdf) are available at <http://www.ibt.unam.mx/labimage/proyectos/arabidopsis>.

Using Nomarski micrographs, cell length profiles were obtained by measuring a straight line from one end to the other with ImageJ or Cell_Length_V2.0.jar software along a cortex file from the QC to the first cortex cell adjacent to an epidermal cell that had started to form a root hair bulge (Fig. 1A). For confocal images the data on meristem length, number of cells in the meristem, the fraction of GFP-expressing cells and root thickness were collected from assembled images. Root thickness was measured at the level corresponding to the PD/TD boundary for cortex determined by experienced biologists, which implies a subjective method, abbreviated here as the ExpBiol method. The PD/TD boundary determined by an ExpBiol method was defined for epidermis and cortex, arbitrarily based on relative changes in cell lengths or internuclear distances along the root, similar to other studies (Rost and Baum, 1988; Dubrovsky, 1997; Dubrovsky *et al.*, 1998a, b; Tapia-López *et al.*, 2008; Garay-Arroyo *et al.*, 2013).

All statistical analyses were performed using R (R Foundation for Statistical Computing, version 2.15.1). MSC analyses, including estimation of the optimal number of breakpoints with the Bayesian information criterion (BIC) and estimation of breakpoint positions with their 95 % confidence intervals (CI) for all cell length profiles were performed using the breakpoints function of the R 'strucchange' package (Zeileis *et al.*, 2002, 2003). The breakpoints function estimates multiple breakpoints simultaneously, implementing an algorithm that obtains global minimizers of the sum of squared residuals (Bai and Perron, 2003). Examples of MSC analyses using the breakpoints function are provided (Supplementary Data Text S1). The distribution function for the 95 % CI for the breakpoints is given in Bai (1997). For comparison of the results obtained with ExpBiol and MSC analyses, the intraclass correlation coefficient (ICC) was estimated (model, two-way; type, absolute agreement; unit of analysis, average measures) (McGraw and Wong, 1996; Hallgren, 2012). The ICC and its 95 % CI were calculated using the R 'irr' package (Matthias *et al.*, 2012). We also developed a publicly available web site (www.ibiologia.com.mx/MSC_analysis), where the MSC algorithm can be performed.

RESULTS

Previously, van der Weele and collaborators (2003) concluded that the root has a velocity profile with linear phases (RAM, EZ

and differentiation zone) separated by abrupt transitions. Based on this conclusion, we propose that cell length profiles, where cell length (L) is a function of cell position with respect to the QC (i), can be fitted by a polygonal model, also known as piecewise, segmented, broken-line regressions, multi-phase regressions or multiple structural change (MSC) models (Bai and Perron, 2003; Muggeo, 2003). In these models the points where the behaviour or response of the dependent variable, as a function of the independent one, change abruptly are commonly called breakpoints, change points, transition points or switch points (Muggeo, 2003). In the cell length profiles, the breakpoints correspond to the boundary between adjacent developmental zones (Fig. 1A, B).

There is no consensus about the existence of the TD in roots. Thus, the analysis of the longitudinal zonation pattern of the arabidopsis root apex consists of two main problems: establishing the number of domains and zones, and determination of the position of the breakpoints between them. Here, we show that an MSC approach can be productively used for solving these problems and objectively establishing the longitudinal patterning in the arabidopsis growing root portion.

The growing part of the root consists of three discrete regions

The problem of single and multiple structural changes in linear models has been studied mainly in statistics, econometrics and medicine (Auger and Lawrence, 1989; Bai and Perron, 1998, 2003; Kim et al., 2000; Muggeo, 2003). We know that the growing part of the arabidopsis root has at least one

transition or breakpoint that corresponds to the RAM/EZ boundary. Some authors propose also the existence of a TD formed by a group of cells elongating at the same rate as the PD cells but with a very low probability of division. In contrast, other authors consider that such a domain does not exist. If the TD actually exists, then a polygonal model with two breakpoints can be obtained from cell length profiles of single cell files, and such breakpoints would correspond to PD/TD and RAM/EZ boundaries.

There are several procedures to estimate the number of breakpoints in MSC models (Yao, 1988; Liu et al., 1997; Bai and Perron, 1998, 2003; Kim et al., 2000, 2009). Comparing different methods for selecting the number of breakpoints, Bai and Perron (2003) concluded that the BIC (Yao, 1988) works well when there is at least one breakpoint, and Kim et al. (2009) also indicate that the BIC performs well in picking up small changes. This method adjusts the sum of squared residuals for models with different numbers of breakpoints, and the model with the lowest BIC value is accepted as the most parsimonious. To establish the number of regions in the growing part of the root, we analysed arabidopsis Col-0 wt and *xall* roots at two different ages, 7 and 9 DAS, without specifying the number of expected breakpoints. From cleared roots we obtained the cell length profile of a cortex cell file, from the QC to the first cortex cell adjacent to an epidermal cell that formed a root hair bulge (Fig. 1A). For each cell length profile we estimated MSC models with different numbers of breakpoints and their positions.

We found that for 58 % of Col-0 cell length profiles analysed (23 out of 40 cell files) the most parsimonious model was of

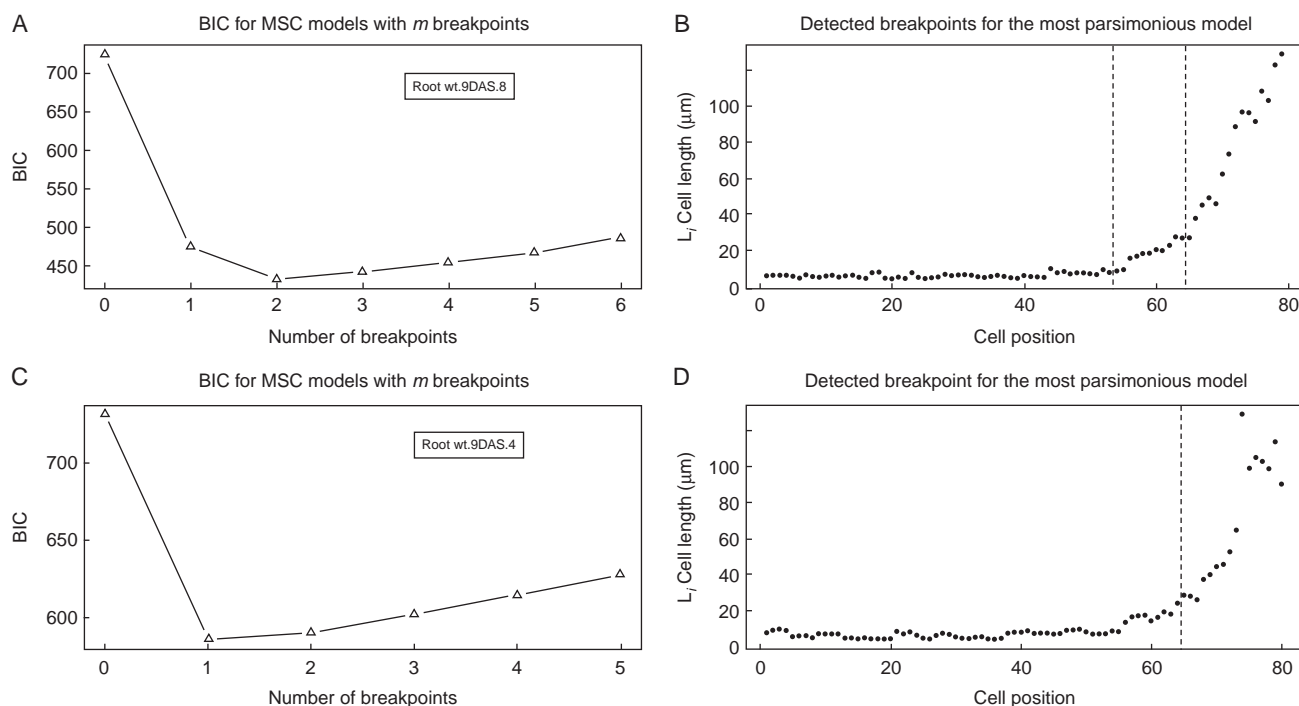


FIG. 2. Estimation of the number of breakpoints and their position by an MSC–BIC approach in Col-0 wt cortical cell length profiles. (A, C) MSC–BIC models with m breakpoints for representative cell length profiles shown in (B) and (D). The lowest value of BIC corresponds to the most parsimonious model for number of breakpoints within a cell file. (B, D) Representative cell length profiles of wt 9-DAS seedlings. Vertical dashed lines represent the breakpoint position estimated by an MSC approach.

TABLE 1. Root growth and meristem characteristics in 7-DAS seedlings of *CycB1;1_{DB}:GFP* (*BJ3*) line grown in media with low and high concentrations of total N

	Low N		High N	
	Mean (s.d.) (n)	95 % CI	Mean (s.d.) (n)	95 % CI
Root length (mm)	43.2 (6.9) (47)	41.2, 45.2	20.7 (5.3) (44)	19.1, 22.3
Rate of root growth during last 24 h ($\mu\text{m h}^{-1}$)	400 (137) (47)	360, 440	160 (66) (44)	140, 180
Root thickness (μm)	146 (11) (29)	142, 150	123 (12) (36)	119, 127
Fraction of GFP-positive cells per cell file (%)				
Epidermis	12.6 (7.5) (39)	10.2, 15.0	12.1 (9.8) (57)	9.5, 14.7
Cortex	11.7 (7.7) (35)	9.1, 14.3	13.9 (9.8) (43)	10.9, 16.9

two breakpoints (Fig. 2A, B). In these cell length profiles the most shootward breakpoint corresponded to the RAM/EZ boundary and the rootward breakpoint corresponded to the PD/TD boundary. In 42 % of cell length profiles analysed in Col-0 (17 out of 40 cell files), the most parsimonious model was of that of one breakpoint. This breakpoint corresponded to the RAM/EZ boundary (Fig. 2C, D). We found also that for these roots the second most parsimonious model was that with two breakpoints. When this model was applied, the same the RAM/EZ boundary was found, and additionally the PD/TD boundary was identified within the RAM.

Similar modelling was performed for the *xall* mutant. Out of 40 cell length profiles analysed, the most parsimonious model was of one, two and three breakpoints in 30, 62 and 8 % of the profiles (Supplementary Data Fig. S1). The small number of profiles with three breakpoints may represent an artefact as a consequence of greater variability in cell lengths. To verify the versatility of the approach, we compared Col-0 wt with a different wt accession, C24. We found that 17, 75 and 8 % of cases ($n = 12$ cortical cell length profiles) showed one, two and three breakpoints respectively (Supplementary Data Table S1).

Overall, our data support the existence of two developmental transitions in the growing part of the root. One of these transitions, the shootward, corresponds to the RAM/EZ boundary (Fig. 1A). In the next section, we will show that the second, rootward, transition corresponds to the PD/TD boundary (Fig. 1B).

The MSC modelling approach identifies the PD/TD boundary

Because the different domains and root growth zones are characterized by distinct and specific developmental processes, the distribution of unambiguous molecular markers for these processes could also be used to define the longitudinal zonation of the root (Ivanov and Dubrovsky, 2013). The distribution of molecular markers for the G2-to-M transition, *CycB1;1_{DB}:GUS* or *CycB1;1_{DB}:GFP*, has been used as a marker for the PD of the RAM (Colón-Carmona *et al.*, 1999; Hauser and Bauer, 2000; Aida *et al.*, 2004; Ticconi *et al.*, 2004; Li *et al.*, 2005; Cruz-Ramírez *et al.*, 2012).

Cell length profiles were obtained from *CycB1;1_{DB}:GFP* roots grown on media with low (1 mm) and high (30 mm) concentration of total N. These cell length profiles were collected from assembled root images obtained under a confocal laser scanning microscope at a high magnification and for this reason did not include EZ cells. The *CycB1;1_{DB}:GFP* reporter detects cells in late G2 and early M phases of the cell cycle

(Colón-Carmona *et al.*, 1999). Therefore, the cell length profile was obtained for a root portion where GFP-positive cells were detected (presumptive PD) and shootward of this zone for a portion of at least half of the presumptive TD. Thus, if a breakpoint is detected, this should correspond to the PD/TD boundary. Roots grown on the media with high and low N content differed significantly in their growth rate and morphology and on medium with low N grew 2.5-fold faster than under high N (Table 1). This observation suggested that the PD would be of different lengths in seedlings grown under these contrasting conditions. Indeed, the PD length determined by the MSC approach was greater in low-N medium (Fig. 3).

The distribution of GFP-positive cells within the meristem was random (Fig. 3A, B). In most cases, those meristematic cells that were in mitosis were GFP-positive. The cells that were not in mitosis but were weakly GFP-labelled were cells in G2, as can be deduced from their size (these cells were approximately twice as long as recently divided cells). The breakpoint values estimated by the MSC approach corresponded to the last PD cells. Cells that expressed *CycB1;1_{DB}:GFP* at the moment of fixation were in most cases located rootward to the breakpoints estimated by the MSC approach (Fig. 3C–F), i.e. within the PD domain. Expression of *CycB1;1_{DB}:GFP* was found in a shootward position with respect to the breakpoint only in 6 % of cell files analysed (5 out of 80). These data indicate that the probability of cell division (GFP-positive cells) after the estimated breakpoint position was low, although rapid cell elongation had not yet started in the measured cell files. Our data indicate that the PD/TD breakpoint estimated by the MSC approach coincided well with the *CycB1;1_{DB}:GFP* expression pattern.

As mentioned above, changes in cell proliferation are associated with the PD/TD boundary before rapid elongation starts, and particularly, before the changes in elongation rates can be detected, cells enter the endoreduplication cycle (Hayashi *et al.*, 2013). Thus, we proposed that the TD can also be defined as the region where cells start endoreduplication but have not yet started rapid elongation. Therefore, a molecular marker for endoreduplication could also be used to establish the PD/TD boundary. The *CELL CYCLE SWITCH52A1* (*CCS52A1*) gene, an isoform of the substrate-specific activator of the anaphase-promoting complex/cyclosome (APC/C), promotes the onset of endoreduplication and its expression correlates with the transition from proliferation to endoreduplication (Vanstraelen *et al.*, 2009). The *pCCS52A1:GUS* reporter gene (Vanstraelen *et al.*, 2009) can be used as a molecular marker of the PD/TD boundary as it is expressed only in the TD and the EZ (Vanstraelen *et al.*, 2009; Takahashi *et al.*, 2013).

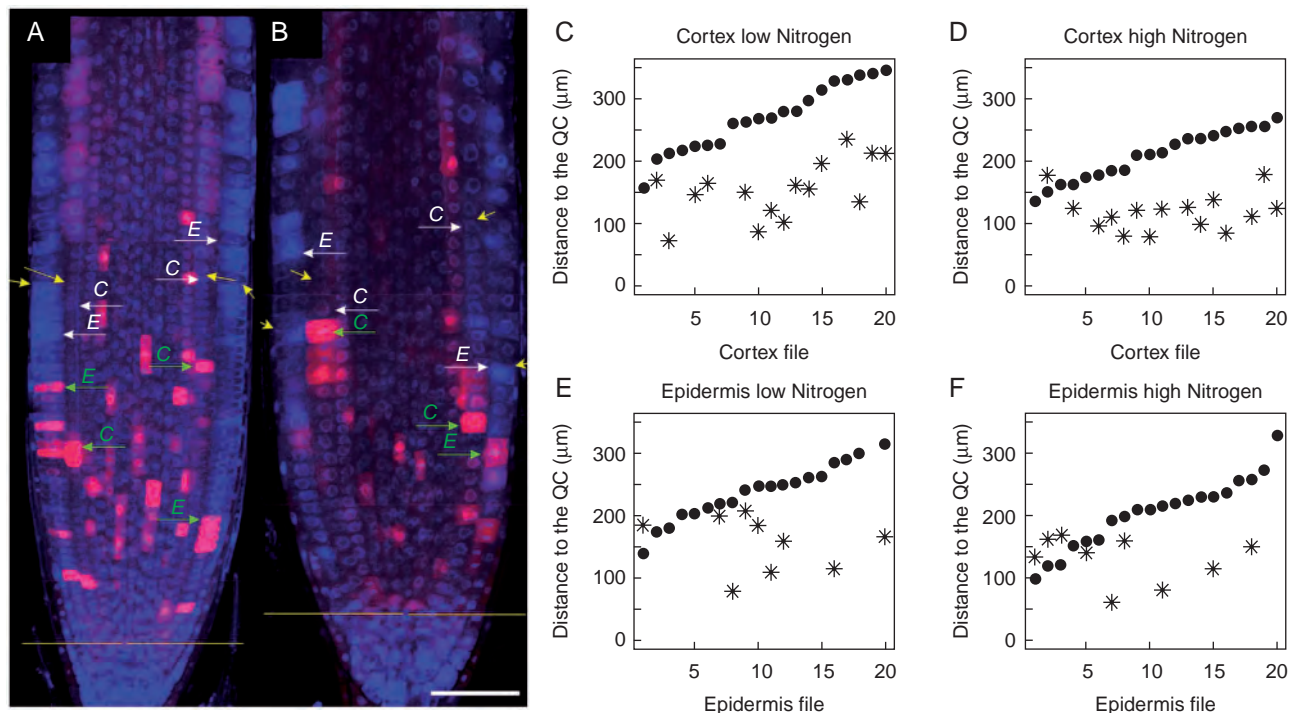


FIG. 3. Distribution pattern of *CycB1;1_{DB}:GFP* expression used as a molecular marker for PD determination and comparison of PD/TD border determinations by the ExpBiol method and MSC approach. (A, B) Root tip longitudinal median sections made by laser scanning confocal microscopy. GFP and DAPI channels were merged and images taken at different levels with respect to the root tip were assembled; the GFP signal is pseudo-coloured as magenta. (A) Roots grown on medium with 1 mm N. (B) Roots grown in medium with 30 mM N. Yellow arrows indicate the PD/TD boundary for cortex and epidermis files determined by ExpBiol based on changes in cell lengths or inter-nuclear distance; green arrows indicate the location within the PD where the cell expresses *CycB1;1_{DB}:GFP* and is closest to the PD/TD boundary in epidermis (E) or cortex (C) files; white arrows indicate the PD/TD boundary determined by the MSC approach. Scale bar = 50 μm. (C–F) X-axis numbers indicate different cell files analysed ($n=10$ roots, one file of cortex and one file of epidermis for each root). The position of the last PD cell determined by the MSC approach (black dots) and the position of the cells closest to the PD/TD boundary which express GFP (asterisks) in epidermis and cortex files for low- and high-N media are shown. Note that not each cell file had cells expressing *CycB1;1_{DB}:GFP* at the moment of fixation. For each condition, cell files are arranged in ascending order of the number of cells in the PD determined by the MSC approach.

To test whether the breakpoint inside the RAM estimated by the MSC approach corresponds with the transition from proliferative state to endoreduplication, we obtained the cortex cell length profile of ten roots of the *pCCS52A1:GUS* reporter line. Using the MSC approach, we determined the breakpoint positions for these roots and estimated the 95 % CI of the position of the last PD cell of each cell file analysed. This position was close to the rootward (distal) border of the GUS-expressing region (seven out of ten cell files, or 70 %) (Fig. 4A–G). In 30 % of the analysed cell files, the last PD cell, estimated by the MSC approach was clearly in a more rootward position than the GUS-expressing region (Fig. 4H–J). Therefore, the PD/TD boundary estimated by MSC coincided with the onset of *pCCS52A1:GUS* expression in the majority of cases.

These data support the conclusion that the MSC approach enabled estimation of the position of the PD/TD boundary and this position coincided with the distribution of cells expressing the *CycB1;1_{DB}:GFP* marker and with the onset of *pCCS52A1:GUS* expression. This PD/TD transition occurred before rapid cell elongation started. Thus we conclude that there are two developmental transitions in the growing part of the root: PD/TD and RAM/EZ (Fig. 1A, B), the former related to changes in proliferation behaviour and the latter to the onset of rapid cell elongation.

Determination of the PD/TD boundary by the MSC approach coincides with subjective determination by an experienced root developmental biologist

In previous studies, the extension of the PD of the RAM was determined based on relative changes in cell length along a root meristem cell file. The PD/TD boundary has been determined at a point from the QC where, in the shootward direction, cell length or inter-nuclear distance increases significantly and where a cell becomes longer than the average cell length within the PD (Dubrovsky, 1997; Dubrovsky *et al.*, 1998a, b; Tapia-López *et al.*, 2008; Garay-Arroyo *et al.*, 2013). Blind experiments to determine this boundary on the same roots by different biologists experienced in this technique (ExpBiol) gave similar results, but students or biologists that are inexperienced in this analysis obtained contrasting results (V.B.I., P.D. and J.G.D., unpubl. res.). Therefore, the ExpBiol is subject to biases depending on the researcher that conducts the analysis. Hence, we were interested in comparing the ExpBiol and MSC approaches to establishing the PD/TD boundary.

The PD/TD boundary was estimated on *CycB1;1_{DB}:GFP* roots grown on media with a low (1 mM) and high (30 mM) concentration of total N. Interestingly, PD length (estimated by ExpBiol) in arabidopsis varied depending not only on N availability but also among roots grown under the same nutrient conditions. The minimum–maximum numbers of cells in a cell file

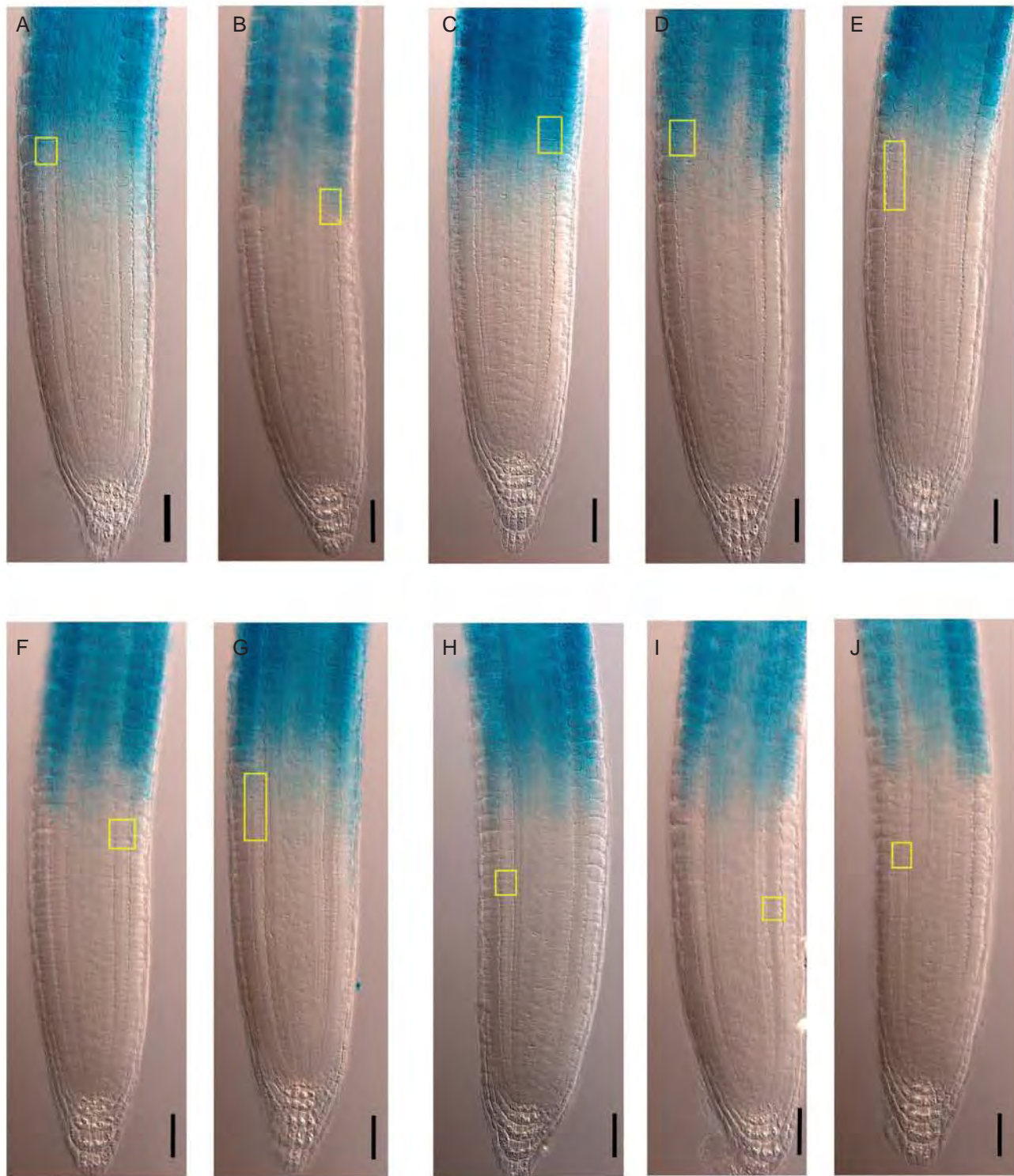


FIG. 4. Determination of the PD/TD boundary in the *CCS2A1:GUS* line using the MSC approach; *GUS* expression marks the beginning of endoreduplication. (A–J) *CCS2A1:GUS* expression in wt roots (7 DAS) occurs in the TD and EZ. Yellow rectangles indicate the 95 % CI of the position of the last PD cell estimated by the MSC approach. Scale bar = 50 μ m.

within the PD (estimated by ExpBiol) in individual roots were 13–41 (epidermis) and 24–48 (cortex) in low N and 9–30 (epidermis) and 10–29 (cortex) in high N. Considering this variation, we analysed the agreement between the PD/TD boundary

estimated for each root when using the ExpBiol method and the MSC approach.

In statistics, inter-rater reliability (IRR) indicates ‘the degree of agreement between two or more coders who made

TABLE 2. Agreement between determinations of the PD/TD boundary by the ExpBiol method and the MSC approach in roots of *CycB1;1_{DB}:GFP* (*BJ3*) line (n=20)

	Distance from the PD/TD boundary to QC (μm)				Number of PD cells			
	ExpBiol		MSC		ExpBiol		MSC	
	Mean (s.d.)	95 % CI	Mean (s.d.)	95 % CI	Mean (s.d.)	95 % CI	Mean (s.d.)	95 % CI
Epidermis, low N	247 (37)	229, 264	241 (47)	218, 263	28 (10)	24, 33	27 (9)	23, 31
Epidermis, high N	199 (20)	190, 209	204 (57)	178, 231	18 (4)	16, 20	18 (5)	16, 21
Cortex, low N	245 (38)	227, 262	270 (54)	245, 295	33 (6)	30, 36	36 (6)	33, 39
Cortex, high N	195 (23)	185, 206	211 (40)	192, 229	22 (4)	20, 24	23 (5)	21, 26

independent ratings about the features of a set of subjects' (Hallgren, 2012). To evaluate IRR for estimates of the number of PD cells obtained by the ExpBiol and MSC approaches, we calculated the intraclass correlation coefficient (ICC) (McGraw and Wong, 1996; Hallgren, 2012). Higher ICC values indicate higher agreement. An ICC estimate of 1 indicates perfect agreement and an estimate of 0 indicates only random agreement. The ICC estimated for all the *CycB1;1_{DB}:GFP* cell files was significantly greater than 0 [ICC = 0.9, $F(79,80) = 10.2$, $P = 2.44e-21$, 95 % CI 0.85, 0.94], and was in the 'excellent' qualitative range proposed by Cicchetti (1994), confirming that the ExpBiol method (which has been traditionally used) and the MSC approach had a high degree of agreement as no statistical differences between the two approaches were detected (Table 2). Importantly, as determined by MSC analysis, in high-N medium the cortex PD length was ~80 % shorter than that in roots grown in low-N medium. This indicates the versatility of the MSC approach. Given that different researchers may reach different results depending on their experience, the use of the MSC approach is recommended as it can eliminate subjective estimates and provide reproducibility within and across laboratories, irrespective of the experience of the observer.

The MSC approach can be used to estimate the critical size of dividing cells and the critical cell size for the initiation of rapid elongation

Organisms from bacteria to higher eukaryotes coordinate cell growth and cell division through size-sensing checkpoint mechanisms in order to maintain a constant cell size. Cells have to reach a certain critical size at which cell-cycle transitions are triggered, such as G1-S or G2-mitosis (Ivanov, 1971; Dobrochaev and Ivanov, 2001; Dolznig *et al.*, 2004; Yang *et al.*, 2006; Turner *et al.*, 2012; Robert *et al.*, 2014). Therefore, along the PD it is expected that cells are equal to or smaller than the critical size of dividing cells (L_{critD}). However, in the TD the probability of cell division is very low (Ivanov and Dubrovsky, 2013); therefore, cells that continue growing at the same relative growth rate as in the PD are longer than the L_{critD} (Hejnowicz, 1959; Hejnowicz and Brodzki, 1960; Ivanov and Maximov, 1999; van der Weele *et al.*, 2003). In the EZ, rapid cell elongation is taking place among other processes due to water uptake into the central vacuole (reviewed by Dolan and Davies, 2004). We addressed in this study whether there is a critical cell length related to the onset of rapid elongation in the

EZ, similar to the L_{critD} near the PD/TD boundary. We denote this cell length as the critical cell size for the initiation of rapid elongation (L_{critE}).

To estimate the maximum cell lengths that correspond to the PD and the TD, we used MSC analysis of sorted cell lengths. We called this analysis the sorted MSC (sMSC). For this procedure, we sorted cell lengths of a root cell file in ascending size order (Fig. 5A, B). Thus, cell length is a function of the cell length rank in the sorted cell length set (Fig. 5B). We assumed that there are three subsets of sorted cell lengths that correspond to the PD, TD and EZ. Then, after estimation of the breakpoints that correspond to the ranks of the longest PD and TD cells (Fig. 5B, C), we found the two linear equations that model the PD and TD cell length subsets after determining the breakpoints by MSC (Fig. 5D). Finally, we used these two linear equations for the PD and TD to estimate the maximum cell length in the PD and TD or the L_{critD} and L_{critE} , respectively (Fig. 5D). In this way the MSC approach can be used to estimate the critical size of dividing cells and the critical size for the initiation of rapid elongation. These parameters were subsequently used for comparison of different genotypes.

MSC analysis of *arabidopsis* wt and *xal1* roots

We generated MSC models with two breakpoints for each cell length profile of wt and *xal1* roots at 7 and 9 DAS. From these models we estimated: (1) the position of RAM/EZ and PD/TD boundaries by the MSC approach; (2) the linear equations for PD, TD and EZ; (3) the number of cells and length of each domain; (4) the derivative of cell length as a function of position (DLP), which corresponds to the slope of each linear equation; and (5) the L_{critD} and L_{critE} . Once the PD/TD and RAM/EZ boundaries were determined by the MSC approach, we compared the sizes of the RAM, PD and TD in wt and *xal1* seedlings 7 and 9 DAS. We found that the number of cells and length of the wt PD and RAM increased from 7 to 9 DAS (Table 3). In contrast, no change was detected in the TD during this growth period in both genetic backgrounds (Table 3). Thus the RAM size increase in the wt was due to a larger population of proliferating cells in the PD at 9 DAS (Table 3).

Interestingly, in the *xal1* mutant we did not detect changes in PD and RAM lengths and corresponding numbers of cells from 7 to 9 DAS under our growth conditions (Table 3). Because accelerated root growth is related mainly to changes in the number of proliferating cells (Beemster and Baskin, 1998), the almost constant growth of *xal1* roots from 3 to 11 DAS

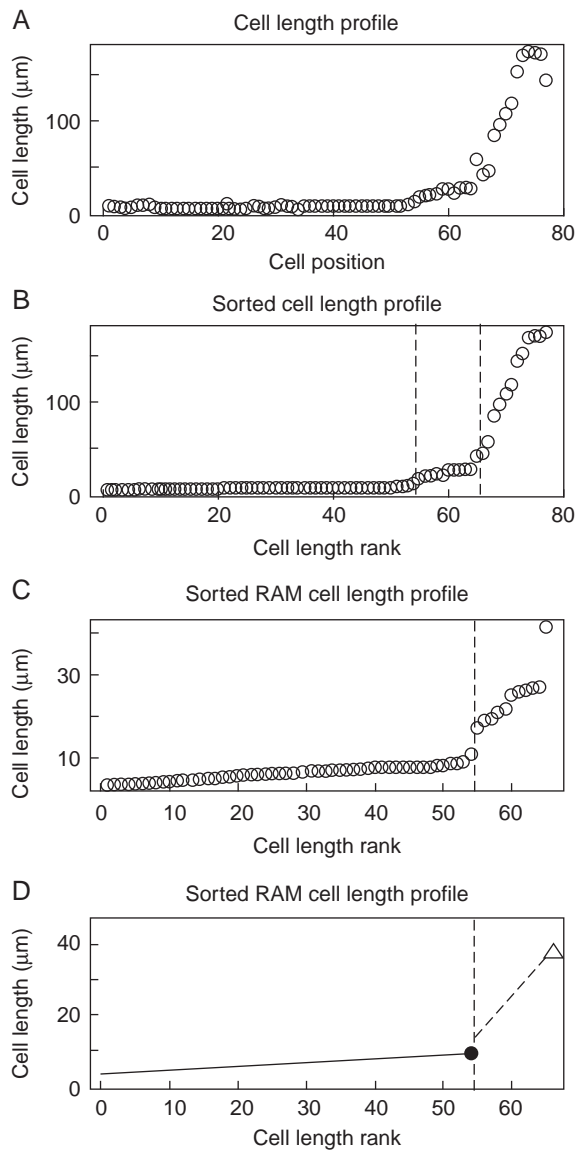


FIG. 5. Estimation of the critical size of dividing and elongating cells by the MSC approach. (A) Cortex cell length profile of the growing part of a representative root of wt Col-0, 9 DAS. (B) Sorted cell length profile in ascending order of the growing part of the root shown in (A). Vertical dashed lines represent positions of breakpoints, estimated by the MSC approach, that correspond to the PD/TD and the RAM/EZ boundaries of sorted cell lengths. (C) Sorted RAM cell length profile of the RAM of the root shown in (A) and (B). Vertical dashed line represents the breakpoint that delimits the PD and TD cell length sets. (D) Linear models for PD and TD cell length sets. The black dot represents the estimated critical size of dividing cells (L_{critD}) and the white triangle represents the critical size for the initiation of rapid elongation (L_{critE}) for the file of the cortex shown in (A).

(Fig. 6A, B) suggested that *xall* PD hardly changes, at least during the first 10 d. Thus, *XAL1* is necessary to maintain the steady increase in the number of cells within the PD, and as a consequence, accelerated root growth.

As *xall* root cells have a longer cell cycle than wt roots (Tapia-López *et al.*, 2008), we asked whether this difference is associated with a change in the L_{critD} . We estimated the mean wt cortex L_{critD} as 8.9 μm (95 % CI 8.5, 9.3, $n = 40$), and the L_{critD} value for *xall* cortex cells as 11.4 μm (95 % CI 10.7,

12.0, $n = 40$). This suggests that the size-sensing mechanism that controls the critical cell size for division is altered by the loss of function of *XAL1* and, as a consequence, the cell cycle duration of *xall* roots is longer, because it takes more time to reach the L_{critD} (assuming the same cell growth rate with respect to time). We also estimated the mean wt cortex cell critical size for the initiation of rapid elongation, L_{critE} , as 25 μm (95 % CI 23, 28, $n = 40$), and for *xall* cortex cells as 38 μm (95 % CI 32, 44, $n = 40$). This analysis showed that the loss of function of *XAL1* altered both critical sizes. In summary, the MSC analysis suggested that *XAL1* may be involved in the regulatory mechanisms that control critical cell size. Alternatively, *XAL1* expression may depend on critical cell size.

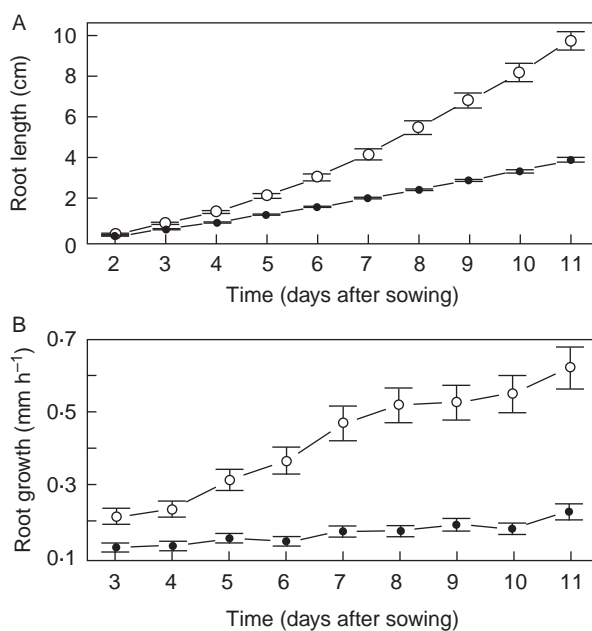
DISCUSSION

We have applied the MSC model to establish the longitudinal zonation pattern of arabidopsis roots. This approach is useful to estimate different parameters, such as (1) the number of longitudinal domains and zones, (2) the number of cells and lengths of each domain and zone, (3) DLP and (4) the critical size of dividing cells (L_{critD}), and the critical size for the initiation of rapid elongation (L_{critE}). Using the BIC to estimate the most parsimonious models for number of breakpoints, we have detected two breakpoints or transitions in cell length profiles of the growing part of the root for the majority of roots. One of these breakpoints corresponds to the RAM/EZ boundary and the other one defines the PD/TD boundary. When one or three breakpoints were detected as the most parsimonious, this was mainly due to internal variability in cell length profiles in arabidopsis roots. Considering that (1) the two-breakpoint model was more common; (2) the one-breakpoint model was a particular case where the PD/TD boundary was not sharp enough; (3) *CycB1;1_{DB}:GFP* was expressed mainly in the PD and (4) *pCCS52AI:GUS* was expressed mainly in the TD, we can conclude that three distinct domains or zones (the PD, the TD and the EZ) should be recognized in the arabidopsis root.

Some authors consider that within individual cell files there is no TD before rapid elongation starts; it is thought that the transition zone is just one point along the root where cells leave the RAM and enter the EZ (Dello Ioio *et al.*, 2007; Moubayidin *et al.*, 2010). These authors also consider that the onset of elongation ‘is different for each cell type, giving a jagged shape to the boundary between dividing and expanding cells’ (Dello Ioio *et al.*, 2007, p. 679). Root tissues stop dividing at different distances from the QC, but they all start rapid elongation at the same distance due to symplastic growth (reviewed in Ivanov and Dubrovsky, 2013). Hence, before rapid elongation, the symplastic nature of plant tissues yields a domain at which cells start endoreduplication but do not start rapid elongation; this region then corresponds to the TD (Baluška *et al.*, 1996; Ivanov and Dubrovsky, 2013). Indeed, experimental evidence has shown that in arabidopsis endoreduplication precedes rapid cell elongation (Hayashi *et al.*, 2013). Thus, for a particular cell file within the arabidopsis root, the TD can also be defined as the region where cells endoreduplicate and continue elongating at the same rate as in the PD. It has also been shown that phospholipase D ζ 2, involved in vesicle trafficking, is strongly expressed in the transition zone (Li and Xue, 2007; Mancuso *et al.*, 2007).

TABLE 3. Quantitative analysis of arabidopsis Col-0 wt and *xal1* roots evaluated at 7 and 9 DAS by MSC analysis (n=20)

	wt				<i>xal1</i>			
	7 DAS		9 DAS		7 DAS		9 DAS	
	Mean (s.d.)	95 % CI	Mean (s.d.)	95 % CI	Mean (s.d.)	95 % CI	Mean (s.d.)	95 % CI
Number of PD cells	40 (7)	36, 43	49 (6)	46, 52	26 (6)	23, 28	28 (7)	24, 31
Number of RAM cells	55 (5)	52, 57	63 (5)	60, 65	36 (5)	34, 38	39 (5)	36, 41
PD length (μm)	245 (53)	220, 270	316 (53)	291, 340	189 (63)	160, 218	210 (63)	181, 240
TD length (μm)	215 (56)	188, 241	216 (56)	189, 242	216 (121)	160, 273	206 (78)	170, 243
RAM length (μm)	460 (61)	431, 488	531 (45)	510, 552	405 (145)	337, 473	417 (90)	375, 459
PD DLP ($\mu\text{m}/\text{cell position}$)	0.0 (0.1)	-0.04, 0.04	0.0 (0.1)	0.0, 0.1	0.1 (0.2)	0.0, 0.1	0.1 (0.2)	0.0, 0.1
TD DLP ($\mu\text{m}/\text{cell position}$)	1.5 (1)	0.8, 2.1	1.3 (1)	1.1, 1.6	2.7 (3.1)	1.2, 4.1	2.6 (2.2)	1.5, 3.6
EZ DLP ($\mu\text{m}/\text{cell position}$)	13 (4)	11, 15	11 (3)	10, 12	13 (11)	8, 18	15 (6)	12, 18
L_{critD} rank	43 (4)	41, 45	50 (5)	48, 53	29 (4)	27, 31	30 (5)	28, 32
L_{critE} rank	55 (5)	52, 57	63 (5)	60, 65	37 (4)	35, 39	38 (5)	36, 41

FIG. 6. Growth of wt and *xal1* roots. (A) Root growth dynamics in wt (white circles) and *xal1* (black dots) roots. (B) Root growth rates over time in wt (white circles) and *xal1* (black dots). Error bars represent 95 % CI, n = 20.

The MSC analysis used here clearly shows that before the onset of rapid elongation all cells within a file, irrespective of the tissue type, are distributed in two subsets separated by an identifiable transition: those in the PD and those in the TD. A clear difference between these two subsets and the difference between the RAM and EZ subsets provide additional evidence that the transition to elongation is not just one point along the root but comprises a domain of cells that have lost or are in the process of losing proliferation activity.

If we consider that the RAM does not include two domains (and the transition to the EZ is not considered to span several cells that constitute an identifiable domain of cells), the estimated RAM linear model should have a slope or DLP greater than zero. This would imply that, along the RAM, the relative cell elongation rate is greater than the relative cell division rate, but cell length profiles do not show a cell length distribution

that corresponds to this scenario (Fig. 2). Within each domain, different relationships between relative elongation and cell division rates (Green, 1976) or DLPs cause a change in the mean cell length. We have found that on average the PD DLP is equal to zero and the TD DLP is greater than zero (Table 3). This implies that in the PD there is a balance between relative cell elongation and division rates (Baskin, 2000), while in the TD relative elongation rates are greater than relative division rates. So, our results support the existence of two domains within the RAM. Thus, cell length profiles that include the RAM and the EZ must be modelled by two-breakpoint MSC models.

The PD/TD boundary is difficult to recognize, partially because relative changes in cell lengths, which do not always steadily increase in the shootward direction, have to be evaluated. Using a molecular marker such as *CycB1;1_{DB};GFP*, we found here that most GFP-expressing cells were within the PD defined by the MSC approach. However, the fact that in 6 % of cases GFP-expressing cells were found in the TD indicates two important aspects: (1) that some TD cells indeed are able to proliferate; and (2) that an estimation error must be considered. This same conclusion might also explain why in some cases *pGUS:CCS52A1* expression is detected shootward of the MSC-determined position of the PD/TD boundary (Fig. 4H–J). Additionally, this discrepancy can be explained by the observation that in arabidopsis roots the endoreduplication cycle can also start in the EZ and that its duration is greater than that of the cell cycle in the RAM (Hayashi *et al.*, 2013).

It is important to point out that the cells at the TD have unique physiological properties such as alterations in their cell-wall structure and the onset of vacuolization, which enables fast cell growth at the EZ (Verbelen *et al.*, 2006; Baluška *et al.*, 2010). It has also been described that cells in the TD are very sensitive to diverse external factors, such as gravity, light, oxidative stress and humidity (Verbelen *et al.*, 2006). Thus, evaluating the extent to which such a domain is altered under different genetic and environmental conditions becomes very relevant. In this paper we propose an approach to the objective establishment of the boundaries between the PD and the TD and between the RAM and the EZ, as well as the sizes and numbers of cells constituting each domain.

Using the MSC, we have found that the PD in wt roots increases after 7 DAS, and such growth is related to an increase in the number of proliferating cells and accelerated root growth,

after 7 DAS. This observation is in accordance with many studies where similar criteria to determine the RAM/EZ boundary have been used, and which report meristem length increase beyond 5 d after germination (DAG) and later (Galinha *et al.*, 2007; Ubeda-Tomás *et al.*, 2009; González-García *et al.*, 2011; Makkena and Lamb, 2013). Moreover, a kinematic analysis of the arabidopsis root showed that accelerated root growth is mainly due to an increased cell production rate during the first 14 DAG and a steady increase in meristem length during the first 2 weeks of growth after germination (Beemster and Baskin, 1998). These results are similar to our observations of accelerated growth from 7 to 11 DAS (Fig. 6A, B), accompanied by an increase in the PD length. However, these results contrast with some previous studies that concluded that wt arabidopsis RAM reaches its maximum size 5 DAG (Dello Ioio *et al.*, 2007; Achard *et al.*, 2009; Moubayidin *et al.*, 2010; Zhou *et al.*, 2011), equivalent to our 7 DAS. This discrepancy about the age at which the RAM reaches its maximum size can be explained by the fact that this age is highly dependent on environmental conditions that vary among studies and by possible methodological differences in meristem length determination. In any case, these variations among laboratories highlight the need for a reliable approach to the identification of root growth zones along the longitudinal axis and their boundaries. In contrast, *xall* roots showed an almost constant root growth rate (Fig. 6A, B), possibly because the PD length hardly changes between, at least, 7 and 10 DAS. This result suggests that *XAL1* is involved in the regulation of the transition from the PD to the TD.

Interestingly, the L_{critD} is altered by the loss of function of *XAL1*, suggesting that the longer cell cycle duration estimated in *xall* roots (Tapia-López *et al.*, 2008) is possibly related to alterations in the size-sensing mechanisms that control the onset of cell division. Fully elongated cells of *xall* roots are shorter on average than wt ones (Tapia-López *et al.*, 2008). Nonetheless, our results show that cells that enter the EZ are larger in *xall* than in wt roots. Cell elongation stops at shorter cell lengths in *xall* than in wt roots, although *xall* cells initiate rapid cell elongation at larger sizes. Our results suggest that the loss of function of *XAL1* alters the two developmental transitions along the root (PD/TD and RAM/EZ), as well as critical cell sizes. Future studies will have to unravel how *XAL1* is involved in the regulation of cell division rate, directly or indirectly, through the regulation of the mechanisms that control the L_{critD} .

In conclusion, the MSC approach for determination of the PD/TD boundary yields similar results to those based on specific molecular markers and those obtained by the ExpBiol subjective method. The MSC approach is an objective and versatile tool for determination of domains and zones and gives reliable results for roots with RAM of different lengths. The use of molecular markers implies genetic crosses and frequently a mixture of different genetic backgrounds. To avoid this problem, the MSC approach permits a direct characterization of the longitudinal zonation pattern. It can be used for different genetic backgrounds and treatments, and can be applied for analysis of developmental changes taking place with age. This approach potentially could also be applied to species other than arabidopsis to better characterize and understand the mechanisms underlying the homeostasis of the RAM in angiosperms.

SUPPLEMENTARY DATA

Supplementary data are available online at www.aob.oxfordjournals.org and consist of the following. Text S1: instructions to analyse the cell length profile of arabidopsis root using the ‘strucchange’ package of R (two examples). Figure S1: estimation of the number of breakpoints and their position by a MSC-BIC approach in *xall* 9 DAS seedling. Table S1: quantitative analysis of arabidopsis C24 wt roots.

ACKNOWLEDGEMENTS

We thank the Arabidopsis Biological Resource Center at Ohio State University for arabidopsis wild-type seeds and Eva Kondorosi for providing the *pCCS52A1:GUS* line. We also thank Diana Romo for help with logistical and laboratory tasks, Marcela Ramírez-Yarza for technical help, graphic designer Francisco José Guijarro Higuera for the root micrograph collage of Fig. 1 and Natalia Doktor for help in confocal microscopy image assemblage and preparation of Fig. 3. The support of B. García Ponce de León (B.G.P.) and M. P. Sánchez Jiménez (M.P.S.J.) is acknowledged. This work was supported by Consejo Nacional de Ciencia y Tecnología, (CONACyT; 180098 and 180380 to E.R.A.B., 167705 to A.G.A., 152649 to M.P.S.J., 237430 and 206843 to J.G.D.); UNAM-DGAPA-PAPIIT (IN203113 to E.R.A.B., IN204011 to B.G.P., IN226510-3 to A.G.A., IN203814 to M.P.S.J. and IN205315 to J.G.D.); the Mexican Academy of Sciences and The Royal Society, UK, to J.G.D. and P.D.; and the Russian Foundation for Basic Research (Grant RFBR-15-04-02502a to V.B.I. and I.A.B.). This work represents partial fulfilment of the requirements for the PhD of M.A.P.E. at the Posgrado en Ciencias Biomédicas, Universidad Nacional Autónoma de México. Financial support for M.A.P.E. was provided by the PhD grant programme of CONACyT.

LITERATURE CITED

- Achard P, Gusti A, Cheminant S, *et al.* 2009. Gibberellin signaling controls cell proliferation rate in Arabidopsis. *Current biology* **19**: 1188–1193.
- Aida M, Beis D, Heidstra R, Willemsen V. 2004. The PLETHORA genes mediate patterning of the Arabidopsis root stem cell niche. *Cell* **119**: 109–120.
- Auger IE, Lawrence CE. 1989. Algorithms for the optimal identification of segmented neighborhoods. *Bulletin of Mathematical Biology* **51**: 39–54.
- Bai J. 1997. Estimation of a change point in multiple regression models. *Review of Economics and Statistics* **79**: 551–563.
- Bai J, Perron P. 1998. Estimating and testing linear models with multiple structural changes. *Econometrica* **66**: 47–78.
- Bai J, Perron P. 2003. Computation and analysis of multiple structural change models. *Journal of Applied Econometrics* **18**: 1–22.
- Baluška F, Mancuso S. 2013. Root apex transition zone as oscillatory zone. *Frontiers in Plant Science* **4**: 354.
- Baluška F, Volkmann D, Barlow PW. 1996. Specialized zones of development in roots: view from the cellular level. *Plant Physiology* **112**: 3–4.
- Baluška F, Mancuso S, Volkmann D, Barlow PW. 2010. Root apex transition zone: a signalling-response nexus in the root. *Trends in Plant Science* **15**: 402–408.
- Baskin TI. 2000. On the constancy of cell division rate in the root meristem. *Plant Molecular Biology* **43**: 545–554.
- Beemster GT, Baskin TI. 1998. Analysis of cell division and elongation underlying the developmental acceleration of root growth in Arabidopsis thaliana. *Plant Physiology* **116**: 1515–1526.
- Casamitjana-Martínez E, Hofhuis HF, Xu J, Liu C-M, Heidstra R, Scheres B. 2003. Root-specific CLE19 overexpression and the sol1/2 suppressors

- implicate a CLV-like pathway in the control of Arabidopsis root meristem maintenance. *Current Biology* 13: 1435–1441.
- Cicchetti D V.** 1994. Guidelines, criteria, and rules of thumb for evaluating normed and standardized assessment instruments in psychology. *Psychological Assessment* 6: 284–290.
- Clowes FAL.** 1956. Nucleic acids in root apical meristems of Zea. *New Phytologist* 55: 29–34.
- Colón-Carmona A, You R, Haimovich-Gal T, Doerner P.** 1999. Spatio-temporal analysis of mitotic activity with a labile cyclin-GUS fusion protein. *Plant Journal* 20: 503–508.
- Cruz-Ramírez A, Diaz-Trivino S, et al.** 2012. A bistable circuit involving SCARECROW-RETINOBLASTOMA integrates cues to inform asymmetric stem cell division. *Cell* 150: 1002–1015.
- Dobrochaev AE, Ivanov VB.** 2001. Variations in the size of mitotic cells in the root meristem. *Ontogenet* 32: 252–262.
- Dolan L, Davies J.** 2004. Cell expansion in roots. *Current Opinion in Plant Biology* 7: 33–39.
- Dolan L, Janmaat K, Willemsen V, et al.** 1993. Cellular organisation of the Arabidopsis thaliana root. *Development* 119: 71–84.
- Dolznig H, Grebien F, Sauer T, Beug H, Müller EW.** 2004. Evidence for a size-sensing mechanism in animal cells. *Nature Cell Biology* 6: 899–905.
- Dubrovsky JG.** 1997. Determinate primary-root growth in seedlings of Sonoran Desert Cactaceae; its organization, cellular basis, and ecological significance. *Planta* 203: 85–92.
- Dubrovsky J, Contreras-Burciaga L, Ivanov VB.** 1998a. Cell cycle duration in the root meristem of Sonoran Desert Cactaceae as estimated by cell-flow and rate-of-cell-production methods. *Annals of Botany* 81: 619–624.
- Dubrovsky J, North G, Nobel P.** 1998b. Root growth, developmental changes in the apex, and hydraulic conductivity for Opuntia ficus-indica during drought. *New Phytologist* 138: 75–82.
- French AP, Wilson MH, Kenobi K, et al.** 2012. Identifying biological landmarks using a novel cell measuring image analysis tool: Cell-o-Tape. *Plant Methods* 8: 7.
- Galinha C, Hofhuis H, Luijten M, et al.** 2007. PLETHORA proteins as dose-dependent master regulators of Arabidopsis root development. *Nature* 449: 1053–1057.
- Garay-Arroyo A, Ortiz-Moreno E, de la Paz Sánchez M, et al.** 2013. The MADS transcription factor XAL2/AGL14 modulates auxin transport during Arabidopsis root development by regulating PIN expression. *EMBO Journal* 32: 2884–2895.
- González-García M-P, Vilarrasa-Blasi J, Zhipanova M, et al.** 2011. Brassinosteroids control meristem size by promoting cell cycle progression in Arabidopsis roots. *Development* 138: 849–859.
- Green PB.** 1976. Growth and cell pattern formation on an axis: critique of concepts, terminology, and modes of study. *Botanical Gazette* 137: 187–202.
- Hallgren K.** 2012. Computing inter-rater reliability for observational data: an overview and tutorial. *Tutorials in Quantitative Methods for Psychology* 8: 23–34.
- Hauser MT, Bauer E.** 2000. Histochemical analysis of root meristem activity in Arabidopsis thaliana using a cyclin: GUS (β -glucuronidase) marker line. *Plant and Soil* 226: 1–10.
- Hayashi K, Hasegawa J, Matsunaga S.** 2013. The boundary of the meristematic and elongation zones in roots: endoreduplication precedes rapid cell expansion. *Scientific Reports* 3: 2723.
- Hejnowicz Z.** 1959. Growth and cell division in the apical meristem of wheat roots. *Physiologia Plantarum* 12: 124–138.
- Hejnowicz Z, Brodzki VY.** 1960. The growth of root cells as the function of time and their position in the root. *Acta Societatis Botanicorum Poloniae* 29: 625–644.
- Herr JM Jr.** 1971. A new clearing-squash technique for the study of ovule development in angiosperms. *American Journal of Botany* 58: 785–790.
- Dello Ilio R, Linh雷斯 FS, Scacchi E, et al.** 2007. Cytokinins determine Arabidopsis root-meristem size by controlling cell differentiation. *Current Biology* 17: 678–682.
- Ivanov VB.** 1971. Critical size and transition of cell to division. Successive transition of sister cells to mitosis and obligatory transition of cell to mitosis in the root tip of maize germling. *Ontogenet* 2: 524–535.
- Ivanov VB, Dubrovsky JG.** 2013. Longitudinal zonation pattern in plant roots: conflicts and solutions. *Trends in Plant Science* 18: 237–243.
- Ivanov VB, Maximov VN.** 1999. The change in the relative rate of cell elongation along the root meristem and the apical region of the elongation zone. *Russian Journal of Plant Physiology* 46: 73–82.
- Kim H-J, Fay MP, Feuer EJ, Midthune DN.** 2000. Permutation tests for joint-point regression with applications to cancer rates. *Statistics in Medicine* 19: 335–351.
- Kim H-J, Yu B, Feuer EJ.** 2009. Selecting the number of change-points in segmented line regression. *Statistica Sinica* 19: 597–609.
- Li C, Potuschak T, Colón-Carmona A, Gutiérrez RA, Doerner P.** 2005. Arabidopsis TCP20 links regulation of growth and cell division control pathways. *Proceedings of the National Academy of Sciences of the USA* 102: 12978–12983.
- Li G, Xue H-W.** 2007. Arabidopsis PLD ζ 2 regulates vesicle trafficking and is required for auxin response. *The Plant Cell* 19: 281–295.
- Liu J, Wu S, Zidek J V.** 1997. On segmented multivariate regression. *Statistica Sinica* 7: 497–525.
- Ma Z, Baskin TI, Brown KM, Lynch JP.** 2003. Regulation of root elongation under phosphorus stress involves changes in ethylene responsiveness. *Plant Physiology* 131: 1381–1390.
- Makkenna S, Lamb RS.** 2013. The bHLH transcription factor SPATULA regulates root growth by controlling the size of the root meristem. *BMC Plant Biology* 13: 1.
- Malamy JE, Benfey PN.** 1997. Organization and cell differentiation in lateral roots of Arabidopsis thaliana. *Development* 124: 33–44.
- Mancuso S, Marras AM, Mugnai S, et al.** 2007. Phospholipase D ζ 2 drives vesicular secretion of auxin for its polar cell-cell transport in the transition zone of the root apex. *Plant Signaling & Behavior* 2: 240–244.
- Matthias G, Jim L, Ian F, Puspendra S.** 2012. irr: Various coefficients of inter-rater reliability and agreement. R package version 0.84. <https://cran.r-project.org/package=irr>.
- McGraw KO, Wong SP.** 1996. Forming inferences about some intraclass correlation coefficients. *Psychological Methods* 1: 30–46.
- Moubayidin L, Perilli S, Dello Ilio R, Di Mambro R, Costantino P, Sabatini S.** 2010. The rate of cell differentiation controls the Arabidopsis root meristem growth phase. *Current Biology* 20: 1138–1143.
- Muggeo VMR.** 2003. Estimating regression models with unknown break-points. *Statistics in Medicine* 22: 3055–3071.
- Robert L, Hoffmann M, Krell N, Aymerich S, Robert J, Doumec M.** 2014. Division in Escherichia coli is triggered by a size-sensing rather than a timing mechanism. *BMC Biology* 12: 17.
- Rost T, Baum S.** 1988. On the correlation of primary root length, meristem size and protoxylem tracheary element position in pea seedlings. *American Journal of Botany* 75: 414–424.
- Sabatini S, Heidstra R, Wildwater M, Scheres B.** 2003. SCARECROW is involved in positioning the stem cell niche in the Arabidopsis root meristem. *Genes & Development* 17: 354–8.
- Silk WK, Hsiao TC, Diedenhofen U, Matson C.** 1986. Spatial distributions of potassium, solutes, and their deposition rates in the growth zone of the primary corn root. *Plant Physiology* 82: 853–858.
- Takahashi N, Kajihara T, Okamura C, et al.** 2013. Cytokinins control endocycle onset by promoting the expression of an APC/C activator in Arabidopsis roots. *Current Biology* 23: 1812–1817.
- Tapia-López R, García-Ponce B, Dubrovsky JG, et al.** 2008. An AGAMOUS-related MADS-box gene, XAL1 (AGL12), regulates root meristem cell proliferation and flowering transition in Arabidopsis. *Plant Physiology* 146: 1182–1192.
- Ticconi CA, Delatorre CA, Lahner B, Salt DE, Abel S.** 2004. Arabidopsis pdr2 reveals a phosphate-sensitive checkpoint in root development. *Plant Journal* 37: 801–814.
- Tsukagoshi H, Busch W, Benfey PN.** 2010. Transcriptional regulation of ROS controls transition from proliferation to differentiation in the root. *Cell* 143: 606–616.
- Turner JJ, Ewald JC, Skotheim JM.** 2012. Cell size control in yeast. *Current Biology* 22: R350–R359.
- Ubeda-Tomás S, Federici F, Casimiro I, et al.** 2009. Gibberellin signaling in the endodermis controls Arabidopsis root meristem size. *Current Biology* 19: 1194–1199.
- Vanstraelen M, Baloban M, Da Ines O, et al.** 2009. APC/C-CCS52A complexes control meristem maintenance in the Arabidopsis root. *Proceedings of the National Academy of Sciences of the USA* 106: 11806–11811.
- Verbel J-P, De Cnodder T, Le J, Vissenberg K, Baluška F.** 2006. The root apex of Arabidopsis thaliana consists of four distinct zones of growth activities: meristematic zone, transition zone, fast elongation zone and growth terminating zone. *Plant Signaling & Behavior* 1: 296–304.
- van der Weele C, Jiang H, Palaniappan K, Ivanov V, Palaniappan K, Baskin T.** 2003. A new algorithm for computational image analysis of deformable

- motion at high spatial and temporal resolution applied to root growth. Roughly uniform elongation in the meristem and also, after an abrupt acceleration, in the elongation zone. *Plant Physiology* **132**: 1138–1148.
- Yang L, Han Z, MacLellan WR, Weiss JN, Qu Z.** 2006. Linking cell division to cell growth in a spatiotemporal model of the cell cycle. *Journal of Theoretical Biology* **241**: 120–133.
- Yao Y-C.** 1988. Estimating the number of change-points via Schwarz' criterion. *Statistics & Probability Letters* **6**: 181–189.
- Zeileis A, Leisch F, Hornik K, Kleiber C.** 2002. strucchange: An R package for testing for structural change in linear regression models. *Journal of Statistical Software* **7**: 1–38.
- Zeileis A, Kleiber C, Walter K, Hornik K.** 2003. Testing and dating of structural changes in practice. *Computational Statistics and Data Analysis* **44**: 109–123.
- Zhou X, Li Q, Chen X, et al.** 2011. The Arabidopsis RETARDED ROOT GROWTH gene encodes a mitochondria-localized protein that is required for cell division in the root meristem. *Plant Physiology* **157**: 1793–1804.

Discusión

XAL1 y XAL2 participan en la regulación del balance proliferación/-diferenciación celular en la raíz de *Arabidopsis*

Las principales aportaciones que se presentan en esta tesis giran alrededor de dos ejes principales: 1) el papel de los factores transcripcionales de dominio MADS en la regulación del balance entre proliferación y diferenciación celular, particularmente *XAL1* y 2) el análisis estadístico del patrón longitudinal de la zona de crecimiento activo, ambos en la raíz de *Arabidopsis*. Estos dos ejes se interrelacionan, principalmente porque el análisis cuantitativo longitudinal de la raíz aportó datos importantes acerca del papel funcional de *XAL1* en la regulación del balance proliferación/diferenciación celular.

En lo que se refiere a la función de los factores transcripcionales de dominio MADS, *XAL1* y *XAL2*, en la regulación del crecimiento de la raíz se encuentran algunos aspectos en común. Morfológicamente alelos de pérdida de función de ambos genes presentan, aunque en grado diferente, raíces más cortas en comparación a las raíces wt; un DP de menor tamaño, tanto en longitud como en número de células, en comparación con las raíces wt; y células de la zona de diferenciación de menor longitud (Tapia-López *et al.*, 2008; Garay-Arroyo *et al.*, 2013).

El tamaño del RAM, o más específicamente el tamaño del DP, es regulado por una compleja red de interacciones entre diversas hormonas (auxinas, citocininas, giberelinas, brasinosteroïdes, ácido absílico y etileno) y factores transcripcionales —miembros de la familia PLETHORA (PLT), SHORT-ROOT (SHR), SCARECROW (SCR), SHORT HYPOCOTYL 2 (SHY2), entre muchos otros— en donde la vía de señalización de las auxinas tiene un papel central (Dello Ioio *et al.*, 2007; Grieneisen *et al.*, 2007; Galinha *et al.*, 2007, 2009; Ubeda-Tomás *et al.*, 2009; Moubayidin *et al.*, 2010; Garay-Arroyo *et al.*, 2012). Dada la importancia que tienen las auxinas en el balance proliferación/diferenciación y el alargamiento celular (Grieneisen *et al.*, 2007; Galinha *et al.*, 2009; Garay-Arroyo *et al.*, 2012), resulta inevitable buscar una relación entre el fenotipo de los alelos de pérdida de función de *xal1* y *xal2* y la vía de señalización de las auxinas o de manera más general ubicar funcionalmente a estos dos factores MADS en la red de regulación del crecimiento de la raíz.

Ambos genes se inducen transcripcionalmente por auxinas, como lo mostraron experimentos de inducción con líneas reporteras y RT-PCR semicuantitativo (Tapia-López *et al.*, 2008; Garay-Arroyo *et al.*, 2013). Además existe un asa de retroalimentación positiva entre XAL2 y la distribución de auxinas, dado que este factor de dominio MADS es un regulador transcripcional directo de los transportadores de auxinas PIN1 y PIN4 (ver: Garay-Arroyo *et al.*, 2013, **Apéndice 1**). Esta asa de retroalimentación positiva puede contribuir a establecer un patrón morfogenético robusto que se ve fuertemente alterado por la pérdida de función de XAL2 (Garay-Arroyo *et al.*, 2013). Es interesante observar que las alteraciones de este patrón morfogenético, si bien presenta algunas modificaciones morfológicas, parece no afectar el establecimiento e identidad del nicho de células troncales, al no observarse cambios en la expresión de genes como *WOX5*, *SCR* y *PLT1*, necesarios para la identidad del CQ (Garay-Arroyo *et al.*, 2013).

Actualmente no se conoce un asa de retroalimentación similar entre las auxinas y XAL1, sin embargo se tienen datos que sugieren que este factor MADS participa en el establecimiento de los patrones morfogenéticos que determinan el crecimiento de la raíz de *Arabidopsis*. Por un lado el patrón de distribución de *PLT1*, uno de los principales componentes de la vía de señalización de las auxinas y cuya función es dosis dependiente —una alta actividad de las proteínas PLT es necesaria para la identidad y mantenimiento del nicho de células troncales; niveles intermedios de actividad promueven la actividad mitótica y bajos niveles de actividad son necesarios para la diferenciación celular (Galinha *et al.*, 2007)— se ve alterada en raíces *xal1*, en donde se observa una menor expresión y una distribución espacial más restringida del reportero *PLT1::GUS* (ver: García-Cruz *et al.*, 2016, **Apéndice 2**).

El tamaño del RAM y el DP a los 7 y 9 dps permanecieron sin cambios significativos en raíces *xal1*, mientras que en raíces wt se pudo observar un crecimiento, en tamaño y número de células en el DP, en el mismo periodo (Pacheco-Escobedo *et al.*, 2016). La velocidad de crecimiento de las raíces está correlacionada positivamente con el número de células proliferativas, por lo que un incremento en la velocidad de crecimiento sugiere un crecimiento del DP (Beemster y Baskin, 1998). Tanto las mediciones del tamaño del DP a los 7 y 9 dps como una aceleración casi de cero desde la germinación hasta el décimo dps, sugieren que en las raíces *xal1* el DP tiene un crecimiento prácticamente constante durante los primeros días de desarrollo, en contraste con las raíces wt en donde el DP aumenta de tamaño (Pacheco-Escobedo *et al.*, 2016). Este dato indica que *XAL1* es necesario para el crecimiento del DP durante los primeros días de desarrollo. Si consideramos que el tamaño del DP depende de un balance entre la tasa de producción celular y la tasa de transición de las células a la ZA, tenemos que en las raíces *xal1*-2 estas dos tasas tienen valores muy similares, mientras que en las raíces wt la tasa de proliferación es mayor que la tasa de transición a la ZA.

En líneas de sobreexpresión de *XAL1* se observa que la ZD comienza a una mayor distancia del CQ que en las raíces wt (ver: García-Cruz *et al.*, 2016, **Apéndice 2**). Por lo tanto, el tamaño de la zona de crecimiento y la

actividad de XAL1 están correlacionados positivamente. La actividad de XAL1 parece determinar la relación entre la proliferación y la diferenciación celular (García-Cruz *et al.*, 2016; Pacheco-Escobedo *et al.*, 2016); a niveles muy bajos de actividad de XAL1, proliferación y diferenciación ocurren en niveles muy similares (como lo muestra el tamaño constante del DP en raíces *xal1*); mientras que a mayor actividad de XAL1 hay una mayor proliferación en relación a la diferenciación celular como lo sugiere la mayor zona de crecimiento de las líneas de sobreexpresión de *XAL1* (García-Cruz *et al.*, 2016).

El crecimiento a velocidad constante, que sugiere un DP que no aumenta de tamaño, no se observa en raíces de alelos de pérdida de función de *XAL2* (datos no mostrados), y la expresión de *PLT1* parece no alterarse a pesar de que hay una fuerte alteración en la distribución de auxinas (ver: Garay-Arroyo *et al.*, 2013, **Apéndice 1**). Es necesario realizar estudios cuantitativos a través de modelos MCE de líneas de ganancia y pérdida de función de *XAL2* para analizar la función de este gen en la regulación del tamaño del RAM y el DP en el tiempo. El hecho de que la distribución de *PLT1* se altera en raíces *xal1*, hace de este gen un candidato interesante para estudios posteriores enfocados a determinar cómo *XAL1* participa en la regulación del balance proliferación/diferenciación celular. Es necesario determinar si *XAL1* es un regulador transcripcional directo de *PLT1* y cómo se afecta la distribución de auxinas en líneas de pérdida y ganancia de función de *XAL1*. Es muy probable que el efecto que ejerce *XAL1* sobre el balance proliferación/diferenciación celular tenga que ver con el establecimiento de los distintos gradientes morfogenéticos que se dan en el eje longitudinal de la raíz.

Por otro lado se determinó, a través de diferentes estrategias, que *XAL1* tiene un papel funcional en la regulación del ciclo celular. Previamente, Tapia-López *et al.* (2008) mostraron que el ciclo celular en el alelo de pérdida de función *xal1* es de una duración mayor respecto a las raíces wt. Apenas se empiezan a descubrir los mecanismos a través de los cuales *XAL1* participa en la regulación del ciclo celular. Por un lado, componentes del ciclo celular como *CYCD3;1*, *CYCA2;3*, *CDKB1;1* y *CDT1a* tienen una expresión a nivel transcripcional menor en relación a las raíces wt (ver: García-Cruz *et al.*, 2016, **Apéndice 2**). Además, utilizando una variante de los modelos MCE se encontró que el tamaño crítico de división (*LCritD*) es mayor en raíces *xal1* (Pacheco-Escobedo *et al.*, 2016). Aún queda por determinar si la regulación transcripcional de los componentes del ciclo celular por *XAL1* es directa o no. ¿Es la alteración de la duración del ciclo celular observada en raíces *xal1* producto de una regulación directa de *XAL1* sobre los componentes del ciclo celular o sobre los mecanismos, aún desconocidos, que determinan el *LCritD*? En el mismo sentido, será importante utilizar la herramienta que proporcionan los modelos MCE para calcular el *LCritD*, para estudiar distintos fondos genéticos con alteraciones en la duración del ciclo celular para poder determinar si está alterado o no el *LCritD*. La respuesta a estas preguntas son de gran importancia y nos aportarán información acerca de la regulación del inicio de la división celular en general, particularmente el papel que juega el *LCritD*, tal como lo han planteado para diferentes sistemas diversos autores (Ivanov, 1971; Dobrochaev y Ivanov, 2001; Dolznig *et al.*, 2004; Yang *et al.*, 2006; Turner *et al.*, 2012; Robert *et al.*, 2014). Es interesante

que el tamaño crítico del inicio del alargamiento rápido ($LCritA$) también es mayor en raíces *xal1* en comparación con las raíces wt. Es curioso observar que a pesar de que las células inician el alargamiento rápido con un mayor tamaño en las raíces *xal1*, el tamaño de las células completamente diferenciadas es menor que en las raíces wt. Esto se puede deber a que la tasa de alargamiento en la ZA es menor en raíces *xal1* que en raíces wt, al tiempo en que las células permanecen en la ZA y por lo tanto en alargamiento rápido o a una combinación de la velocidad y tiempo del alargamiento rápido.

Finalmente es importante recordar que los factores de dominio MADS forman complejos proteicos de orden superior, en donde se unen tanto a otras proteínas MADS como a proteínas de otras familias. Es necesario continuar en esta área de investigación para poder determinar la estructura y funcionamiento de estos complejos proteicos. La caracterización de estos complejos no solo es necesaria para comprender la función de las proteínas MADS en la regulación del balance proliferación/diferenciación, sino que serán esenciales para entender cómo participan en la regulación transcripcional en general, principalmente a nivel de la topología de la cromatina y dinámica nuclear. La identificación de genes que son regulados transcripcionalmente por *XAL1* y *XAL2* (Garay-Arroyo *et al.*, 2013; García-Cruz *et al.*, 2016), permitirán en un futuro poder identificar a otros miembros de los complejos proteicos que forman estas dos proteínas MADS. El conocer la conformación de estos complejos quizás ayude a entender por qué en el caso de *XAL1* y *XAL2* no se observa la redundancia funcional presente en otros genes MADS-box en la raíz.

La zona de crecimiento de la raíz de *Arabidopsis* está compuesta de tres regiones discretas

A través de los modelos MCE y el criterio de información bayesiana (BIC) se encontró que en la mayor parte de los perfiles de longitudes celulares los modelos poligonales más parsimoniosos son aquellos que poseen dos puntos de rompimiento o transiciones (Pacheco-Escobedo *et al.*, 2016). Lo anterior tiene como consecuencia que la zona de crecimiento de la raíz está compuesta de tres zonas discretas, en relación a la longitud celular, que coinciden con las regiones longitudinales consideradas por Ivanov y Dubrovsky (2013): El dominio de proliferación (DP), el dominio de transición (DT) y la zona de alargamiento (ZA). Es importante destacar que en aquellos perfiles en los que según el BIC el modelo más parsimonioso era aquel con una sola transición (RAM/ZA), no significa que no se hayan detectado otras transiciones; simplemente que el modelo con una transición fue más parsimonioso que aquel modelo con dos transiciones.

¿Qué representa esta segunda transición detectada por los modelos MCE? Este segundo punto de rompimiento o transición siempre se ubicó entre el CQ y la transición RAM/ZA, es decir, es una transición que se encuentra dentro

del RAM. Mediante el análisis de la distribución de las líneas reporteras *CycB1;1DB:GFP* y *pCCS52A1:GUS* se determinó que esta transición detectada por los modelos coincide con un cambio en el comportamiento proliferativo de las células. Por un lado, la expresión de *CycB1;1DB:GFP*, que es un marcador de la transición G2/M del ciclo celular, se observa en la mayor parte de los casos en una posición distal con respecto a la transición detectada por el modelo (Pacheco-Escobedo *et al.*, 2016), lo que significa que esta transición coincide o es muy cercana con el límite proximal de la región en que las células mantienen un estado proliferativo.. Previamente, Hayashi *et al.* (2013) demostraron que el establecimiento del ciclo endorreduplicativo se establece antes de que se puedan detectar cambios en la tasa de alargamiento celular. El producto del gen *CELL CYCLE SWITCH52A1 (CCS52A1)* promueve el establecimiento del ciclo endorreduplicativo y la expresión de este gen tiene una correlación con la transición de proliferación a endorreduplicación (Vanstraelen *et al.*, 2009). Así, la expresión del reportero *pCCS52A1:GUS* se podrá detectar en el DT y la ZA pero no en el DP (Vanstraelen *et al.*, 2009; Takahashi *et al.*, 2013). A través de los modelos MCE se calcularon los intervalos de confianza ($\alpha = 0.05$) de la posición de la última célula del DP. En el 70 % de los casos analizados (siete de diez raíces) esta posición se encontró cerca del límite distal de la región que expresa el reportero *pCCS52A1:GUS*; mientras que en el 30 % restante de las raíces analizadas el límite calculado se encontró claramente en una posición más distal que el límite de la región que expresa el *pCCS52A1:GUS*. Esto significa en conjunto que esta segunda transición detectada coincide con el establecimiento del ciclo endorreduplicativo de las células y el cese de la proliferación celular.

El DT se puede definir como la región del RAM donde la probabilidad de división celular es muy baja y en donde las células no presentan un cambio drástico en la velocidad de alargamiento (Ivanov y Dubrovsky, 2013). La segunda transición detectada por los modelos MCE coincide con un cambio en el estado proliferativo de las células dentro del RAM, previamente van der Weele *et al.* (2003) demostraron que la misma velocidad de alargamiento se registra desde la punta de la raíz hasta el inicio de la zona de alargamiento rápido o transición RAM/ZA; por lo tanto se puede concluir que este límite detectado es la transición DP/DT. Lo anterior implica que cuando se utilicen modelos MCE para la zona de crecimiento de la raíz se deben elegir aquellos con dos transiciones o puntos de rompimiento, aunque en algunas ocasiones no sean los más parsimoniosos según el BIC.

Los modelos MCE permiten determinar la posición de las diferentes transiciones con resultados relativamente confiables. Al comparar los resultados de la determinación de la posición de la transición DP/DT obtenida a partir de modelos MCE y la realizada por un investigador con experiencia en el método que analiza cambios en la longitud promedio de las células —basado principalmente en la relación entre las distancias de los núcleos de células contiguas y el diámetro de los núcleos (Rost y Baum, 1988; Dubrovsky *et al.*, 1998a; Garay-Arroyo *et al.*, 2013)—, no se encontraron diferencias significativas (Pacheco-Escobedo *et al.*, 2016). Esto significa que los modelos MCE son una alternativa objetiva y que necesita de poco entrenamiento para determinar la posición de las transiciones longitudinales de la raíz de *Arabidopsis* y así obtener datos como el tamaño y número de células del DP, DT y ZA;

Cuadro 1: Coeficientes de determinación de cada una de las regiones longitudinales de raíces wt y *xal1-2* a los siete y nueve dps ($n = 20$).

	wt 7dps		wt 9 dps		<i>xal1-2</i> 7 dps		<i>xal1-2</i> 9 dps	
	media (d.t)	95 % I.C	media (d.t)	95 % I.C	media (d.t)	95 % I.C	media (d.t)	95 % I.C
R ² DP	0.3 (0.2)	0.21, 0.38	0.2 (0.1)	0.13, 0.22	0.3 (0.2)	0.15, 0.38	0.3 (0.2)	0.26, 0.4
R ² DT	0.7 (0.2)	0.66, 0.83	0.7 (0.2)	0.64, 0.79	0.8 (0.2)	0.66, 0.88	0.8 (0.2)	0.75, 0.91
R ² ZA	0.9 (0.1)	0.79, 0.92	0.8 (0.1)	0.73, 0.86	0.7 (0.3)	0.6, 0.9	0.8 (0.2)	0.76, 0.95

los tamaños críticos de división y transición al alargamiento rápido ($LCritD$ y $LCritA$); y la derivada de la longitud celular en función de la posición (DLP) (Green, 1976) para cada región, que corresponde a la pendiente de la ecuación lineal que modela una región longitudinal.

Una vez determinadas las posiciones de las transiciones DP/DT y RAM/ZA es posible analizar el comportamiento de las células en cada región. El análisis de residuales (datos no mostrados) y los coeficientes de determinación de cada una de las zonas de las raíces estudiadas indica que el DT y la ZA efectivamente tienen un comportamiento lineal, sin embargo el DP no tiene un comportamiento lineal (Cuadro 1). Lo anterior concuerda con lo observado previamente en maíz, en donde la media de la longitud de las células en división decrece primero de la parte distal del DP a la parte media, y se incrementa después de la parte media a la parte basal del DP (Dobrochaeve y Ivanov, 2001). Estos cambios se deben a que disminuye la proporción de células de menor longitud en división al principio y al final del DP, lo cual afecta el valor de la media, pero no implica un cambio en el tamaño crítico de división, ya que los límites de variación del tamaño de las células en división no cambian (Dobrochaeve y Ivanov, 2001). Además hay que considerar que las células iniciales son por lo general más largas que las células de córtex, y que en los perfiles analizados se incluyen estas células iniciales.

El cálculo del $LCritD$ por medio de los modelos MCE de perfiles de células ordenados permite establecer diferencias importantes entre el DP y el DT. Dentro del DP es muy raro encontrar células con una longitud mayor al $LCritD$, mientras que en el DT la mayor parte de las células son mayores al $LCritD$. Esto se debe a que en el DP si una célula alcanza el $LCritD$, se divide. Por lo tanto, en el DP prácticamente la totalidad de las células están en estado proliferativo. En cambio, en el DT donde la probabilidad de división celular es muy baja es frecuente encontrar células mayores al $LCritD$. Lo anterior se mantuvo tanto en raíces wt y *xal1-2* a pesar del cambio en el $LCritD$ observado, lo que pone de manifiesto que esta longitud crítica sí está relacionada con cambios en el comportamiento de las células. La estrategia presentada en este trabajo representa una herramienta muy útil que permitirá incluir datos acerca del $LCritD$ en futuros estudios en raíz (en la actualidad es un dato que casi o nunca se reporta) que podrán aportar mayor información importante acerca de este parámetro y su importancia en el desarrollo de la raíz y el control en el inicio de la mitosis en general.

La existencia del DT se demuestra en este trabajo a través de los modelos MCE, los cuales son capaces de calcular la posición de sus límites, y por lo tanto determinar su tamaño. Al analizar el tamaño del DT en raíces de diferentes condiciones experimentales (raíces wt y *xal1-2*, siete y nueve dps, ecotipo Col-0; raíces wt, 15 días posteriores a la germinación, ecotipo C24) la media se mantuvo sin cambios significativos (ver: Pacheco-Escobedo *et al.* 2016 y **Apéndice 5**), a pesar de los cambios observados en el tamaño del DP y en el *LCrtiD*. Lo que sugiere que el tamaño del DT es un parámetro robusto que se mantiene relativamente constante a pesar de que se hayan alterado diversos aspectos del crecimiento de las raíces. El DT prácticamente no se ha considerado en ningún estudio previo, sin embargo, dada la evidencia que se presenta en esta tesis, será importante que en el futuro se incluya información acerca de esta región como parte de la caracterización del RAM en diferentes condiciones experimentales, esto nos permitirá saber qué condiciones pueden alterar su tamaño, o las razones que lo hacen tan robusto.

La utilización de modelos MCE para el análisis del patrón de regionalización longitudinal de la raíz tiene un gran potencial, no solo como herramienta en la caracterización morfológica de la zona de crecimiento, sino por las preguntas que se plantean a partir de su utilización en la identificación y delimitación de las distintas regiones longitudinales de la raíz. El patrón de regionalización longitudinal que se observa en la raíz de *Arabidopsis* conformado por DP, DT, ZA y zona de diferenciación, ¿está conservado en las raíces de otras especies? ¿Cómo es la regulación del tamaño del DT? ¿Qué funciones fisiológicas tiene el DT? ¿Qué características fisiológicas y genético-moleculares tienen las células que pertenecen al DT? Al considerar la existencia del DT se abre todo un conjunto de preguntas acerca de esta región.

A partir de la modelación de los perfiles de longitud celular la caracterización morfológica de la zona de crecimiento activo de la raíz no se limitará, como en la mayor parte de las publicaciones a reportar el número de células meristemáticas o tamaño del RAM, sino que pueden incluir información acerca de las tres regiones y los tamaños críticos de división e inicio del alargamiento rápido. Si estos parámetros se analizan en series de tiempo la información que se puede obtener de raíces en diferentes condiciones experimentales aumenta de manera considerable. Así, los modelos MCE son una herramienta que puede tener un impacto considerable en futuros estudios acerca del crecimiento de la raíz que es, además, relativamente fácil de aplicar ya sea con los paquetes existentes en R u otros programas estadísticos o como los códigos presentados en los **Apéndices 3 y 4** y el sitio web: www.ibiologia.com.mx/MSC_analysis.

A futuro, será necesario realizar modelos de la dinámica de la zona de crecimiento de la raíz «*in vivo*» a través de técnicas tipo *time lapse* y las diversas técnicas cinemáticas que se han desarrollado para la raíz anteriormente, pero tomando en cuenta la existencia del DT. Finalmente, lograr la integración de la dinámica celular con la dinámica de las redes de regulación genética y su interacción con el ambiente nos permitirá tener una visión más realista e integral del desarrollo de la raíz y así poder explotar todo su potencial como sistema modelo.

Conclusiones

- Los modelos de múltiple cambio estructural (MCE) junto con el criterio de información Bayesiana (BIC) identifican tres regiones discretas en la región de crecimiento: El dominio de proliferación (DP), el dominio de transición (DT) y la zona de alargamiento (ZA).
- La posición de la transición DP/DT determinada por los modelos MCE corresponde con la distribución de la expresión de los marcadores moleculares *CycB1;1DB:GFP* y *pCCS52A1:GUS*, los cuales indican cambios en el comportamiento proliferativo de las células. Por lo tanto, la transición DP/DT detectada por los modelos coincide con cambios fisiológicos y no es un artefacto.
- Los modelos MCE se pueden usar para determinar el tamaño de las distintas regiones longitudinales de la raíz (DP, DT, RAM, ZA) de manera objetiva y sin la necesidad de adquirir experiencia previa.
- *XAL1* es necesario para el crecimiento del DP durante los primeros días de desarrollo.
- La pérdida de función de *XAL1* altera los tamaños críticos de división (L_{CritD}) e inicio del alargamiento rápido (L_{CritE}).

Apéndice 1. El factor transcripcional
MADS XAL2/AGL14 modula el
transporte de auxinas a través de la
regulación transcripcional de los
transportadores PIN

The MADS transcription factor XAL2/AGL14 modulates auxin transport during *Arabidopsis* root development by regulating PIN expression

Adriana Garay-Arroyo^{1,8}, Enrique Ortiz-Moreno^{1,8}, María de la Paz Sánchez¹, Angus S Murphy², Berenice García-Ponce¹, Nayelli Marsch-Martínez³, Stefan de Folter⁴, Adriana Corvera-Poiré¹, Fabiola Jaimes-Miranda¹, Mario A Pacheco-Escobedo¹, Joseph G Dubrovsky⁵, Soraya Pelaz^{6,7} and Elena R Álvarez-Buylla^{1,9,*}

¹Depto. de Ecología Funcional. Laboratorio de Genética Molecular, Desarrollo y Evolución de Plantas, Instituto de Ecología, Universidad Nacional Autónoma de México, 3er Circuito Ext. Junto a J. Botánico, Ciudad Universitaria, UNAM, México DF, México, ²Department Plant Science and Landscape Architecture, 2104 Plant Science Bldg, University of Maryland, College Park, USA, ³Departamento de Biotecnología y Bioquímica, CINVESTAV-IPN Unidad Irapuato, Irapuato, México, ⁴Laboratorio Nacional de Genómica para la Biodiversidad (Langebio), Centro de Investigación y de Estudios Avanzados del IPN (CINVESTAV-IPN), Irapuato, México, ⁵Depto. de Biología Molecular de Plantas, Instituto de Biotecnología, Universidad Nacional Autónoma de México, Morelos, UNAM., Cuernavaca, México, ⁶Centre for Research in Agricultural Genomics, CSIC-IRTA-UAB, Barcelona, Spain and ⁷ICREA (Institució Catalana de Recerca i Estudis Avançats), Barcelona, Spain

Elucidating molecular links between cell-fate regulatory networks and dynamic patterning modules is a key for understanding development. Auxin is important for plant patterning, particularly in roots, where it establishes positional information for cell-fate decisions. PIN genes encode plasma membrane proteins that serve as auxin efflux transporters; mutations in members of this gene family exhibit smaller roots with altered root meristems and stem-cell patterning. Direct regulators of PIN transcription have remained elusive. Here, we establish that a MADS-box gene (*XANTAL2*, *XAL2/AGL14*) controls auxin transport via PIN transcriptional regulation during *Arabidopsis* root development; mutations in this gene exhibit altered stem-cell patterning, root meristem size, and root growth. *XAL2* is necessary for normal shootward and rootward auxin transport, as well as for maintaining normal auxin distribution within the root. Furthermore, this MADS-domain transcription factor upregulates *PIN1* and *PIN4* by direct binding to regulatory regions and it is required for *PIN4*-dependent auxin response. In turn, *XAL2* expression is regulated by auxin levels thus establishing a positive

feedback loop between auxin levels and PIN regulation that is likely to be important for robust root patterning.

The EMBO Journal (2013) 32, 2884–2895. doi:10.1038/emboj.2013.216; Published online 11 October 2013

Subject Categories: development; plant biology

Keywords: MADS proteins; root development; PIN regulation; stem cell niches; auxin

Introduction

Plant and animal development is guided by transcriptional networks that control cell-fate decisions in conjunction with dynamic patterning modules, such as those that regulate the differential distribution (gradients) of hormones (Davidson and Erwin, 2006; Newman *et al.*, 2009). Establishing the molecular links between such networks and hormone or nutrient distribution is a key for understanding cell patterning. Our current comprehension of how these two types of processes are linked spatially and temporally *in vivo* is limited (Newman *et al.*, 2009).

The root of *Arabidopsis thaliana* has become an exemplar for *in vivo* studies of molecular developmental mechanisms, particularly of the molecular basis of stem-cell niche patterning and dynamics (van den Berg *et al.*, 1997; Aida *et al.*, 2004; Sarkar *et al.*, 2007; Fulcher and Sablowski, 2009). The root stem-cell niche is a part of the cell proliferation domain (Ivanov and Dubrovsky, 2013) and, like that of other multicellular organisms, has in the centre an organizer, called the Quiescent Centre (QC) in roots. Tissue-specific progenitor cells, multipotent stem cells or initial cells, surround the QC. The derivatives of the initial cells exhibit a brief period of rapid cell proliferation shootward of the root apical region. After 4–6 rounds of division, cells begin elongation and ultimately differentiation (Dolan *et al.*, 1993; van den Berg *et al.*, 1998).

Expression of GRAS family SCARECROW and SHORTROOT (SCR/SHR) and AP2 family PLETHORA (PLT) transcription factors is necessary for the formation and maintenance of the stem-cell niche in *Arabidopsis* roots (Sabatini *et al.*, 1999, 2003; Helariutta *et al.*, 2000; Aida *et al.*, 2004). Auxins are fundamental plant hormones in embryonic development (Möller and Weijers, 2009), organogenesis (Vanneste and Friml, 2009), and root cell patterning (Friml *et al.*, 2003). An auxin gradient with a maximum level at the QC is required for correct specification of the stem-cell niche. Moreover, the cellular levels of auxin define root cell fate: intermediate auxin concentrations are found in the cell proliferation zone and low auxin levels characterize the zones of elongation and differentiation along the root longitudinal axis (Burstrom, 1957; Friml and Palme, 2002; Petersson *et al.*, 2009; Jurado *et al.*, 2010). Directional auxin

*Corresponding author. ER Alvarez-Buylla, Instituto de Ecología, Universidad Nacional Autónoma de México, 3er Circuito Exterior, Junto a Jardín Botánico, CU, Coyoacán, México DF 04510, México. Tel.: +52 55 5622 9013; Fax: +52 55 5622 9013;

E-mail: eabuylla@gmail.com

⁸These authors contributed equally to this work.

⁹Present address: 431 Koshland Hall, University of California, Berkeley, CA 94720, USA.

Received: 25 April 2012; accepted: 28 August 2013; published online: 11 October 2013

transport between cells, partially mediated by PIN auxin-efflux carriers, is crucial for generating these auxin gradients (Blilou *et al*, 2005; Vieten *et al*, 2005; Wisniewska *et al*, 2006). Differential PIN expression has been explored extensively (Aida *et al*, 2004; Vieten *et al*, 2005; Ruzicka *et al*, 2009), but little is known about the factors that directly regulate PIN gene transcription or PIN expression in response to auxins, as well as how this regulation impacts PIN-dependent developmental processes.

Initial studies suggested that the *PLT* and *SHR/SCR* genes constituted the main components of root stem-cell niche patterning; based on the recent gene discoveries and a new gene regulatory network (GRN) model it is hypothesized that additional components remain undiscovered (Sarkar *et al*, 2007; Welch *et al*, 2007; Azpeitia *et al*, 2010). Plant MADS-box genes have been extensively characterized as regulators of reproductive development, flower transition, and organ identity (Coen and Meyerowitz, 1991; Alvarez-Buylla *et al*, 2000a; Álvarez-Buylla *et al*, 2000b; Burgeff *et al*, 2002), and recent studies suggest that auxin-regulated MADS-box genes, such as *XANTAL1/AGL12* (*XANTAL* is the Mayan word for ‘go slower’ in recognition of the retarded root growth phenotypes of *xaantal* mutants), also regulate root development (Gan *et al*, 2005; Tapia-López *et al*, 2008). We report here that the *Arabidopsis* MADS-box gene, *AGL14/XANTAL2*, closely related to the flowering gene, *SUPPRESSOR OF OVEREXPRESSION OF CONSTANS1 (SOC1)* (Martinez-Castilla and Alvarez-Buylla, 2003) is required for root stem-cell niche and meristem patterning. Furthermore, *AGL14/XAL2* regulates auxin transport and gradients in the root via direct regulation of PIN transcription.

Results

XANTAL2 (XAL2/AGL14) controls root stem-cell niche delimitation and cell proliferation

We sought to test the role of MADS-box gene *XAL2* in *Arabidopsis* root development. We obtained lines with loss-of-function mutations in *XAL2*, a type II MADS-box gene that belongs to the *SOC1* clade (Figure 1A) and is highly expressed in roots (Figure 1B). ‘*in situ*’ data of RNA expression derived from both ‘*in situ*’ PCR and dig-labelled ‘*in situ*’ experiments demonstrated that mRNA is found in lateral root cap, epi-

dermis, endodermis, and columella of the root meristematic region, as well as in the vascular cylinder in differentiated zones of the primary root and in emerged lateral root primordia (Figures 1C–H; Supplementary Figures S1B–H and S2). In addition, we generated a 1-kb *XAL2* promoter that also recovers the expression of the gene promoter in the vascular tissue and in the lateral roots. This line recovers only a scanty and light expression in the root meristematic tissues after a few hours of GUS staining, maybe because the cloned promoter fraction misses some important enhancer sequences. This genetic marker is strongly expressed in the root meristem only after several days of staining (data not shown). Nonetheless, both this and the ‘*in situ*’ data show clear and strong expression of *XAL2* in the central cylinder and the emerging lateral roots. These data parallel the reports by Birnbaum *et al* (2003) and Nawy *et al* (2005) for *XAL2*; who report expression in the meristematic tissues as our ‘*in situ*’ assays, and in the QC (see Supplementary Figure S1A). We isolated two loss-of-function alleles for this *XAL2* (called hereafter *xaantal2-1* and *xaantal2-2*). Both mutants develop shorter wild-type roots in the Columbia background, similar in length to *XAL1* mutants (Figure 1I; Tapia-López *et al*, 2008). The *xal2-2* allele exhibited the most pronounced retarded root growth and altered cellular structure at the stem-cell niche, and concordantly lacked detectable levels of *XAL2* mRNA, whereas the *xal2-1* allele exhibited intermediate phenotypes between wild type and *xal2-2*, and exhibited residual *XAL2* expression (Figures 1I–K). The root growth and stem-cell niche phenotypes, as well as the correlated levels of expression of *XAL2* in these two independent alleles demonstrate that the observed phenotype can be attributed to the loss of *XAL2* function (Figure 2A). For the rest of the functional analyses, we therefore focused on the strong allele *xal2-2*.

Quantitative growth analyses of *xal2-2* roots (Table I) showed that the mutant displays a significantly lower number of meristematic cells and lower rate of cell production, fewer cells in the elongation zone and shorter fully elongated cells compared with wild-type roots (Figures 2B–D; Table I) and the *xal2-2* line exhibits normal cell-cycle duration and *pCYCB1;1DB::GUS* expression (Supplementary Figures S3A and B). Consequently, decreased root growth in plants with this strong loss-of-function *xal2-2* allele results from

Table I Quantitative cellular analysis of root development for wild-type and *xal2-2* seedlings (7 d.p.s.)

	Root growth rate ($\mu\text{m h}^{-1}$)	Proliferation domain (PD) length (μm)	Cortical cell number within PD	Cortical cell length within PD (μm)	Combined length of the transition domain and the elongation zone (μm)
	*****	*	***		**
WT	265 ± 11	173 ± 12	33.3 ± 2.14	5.2 ± 0.1	510 ± 32
<i>xal2-2</i>	163 ± 3	142 ± 5	26.5 ± 1.43	5.4 ± 0.1	385 ± 22
Length of the growing part of the root (μm)	Length of completely elongated cortical cells (μm)	Cell-cycle duration (h)	Cell production rate (1/h)	Cortical cell number in the elongation zone	
****	*****	*****	*****	**	
WT	683 ± 32	156 ± 6	12.3 ± 0.7	1.9 ± 0.1	20.1 ± 1.0
<i>xal2-2</i>	528 ± 22	113 ± 4	12.7 ± 1.03	1.5 ± 0.6	16.5 ± 1.12

Average (marked with bold letters) \pm s.d. with $\alpha < 0.1$, $\alpha < 0.05$, $\alpha < 0.02$, $\alpha < 0.005$, $\alpha < 0.002$, and $\alpha < 0.001$ indicated as *, **, ***, ****, *****; and ******, respectively; $n = 30$.

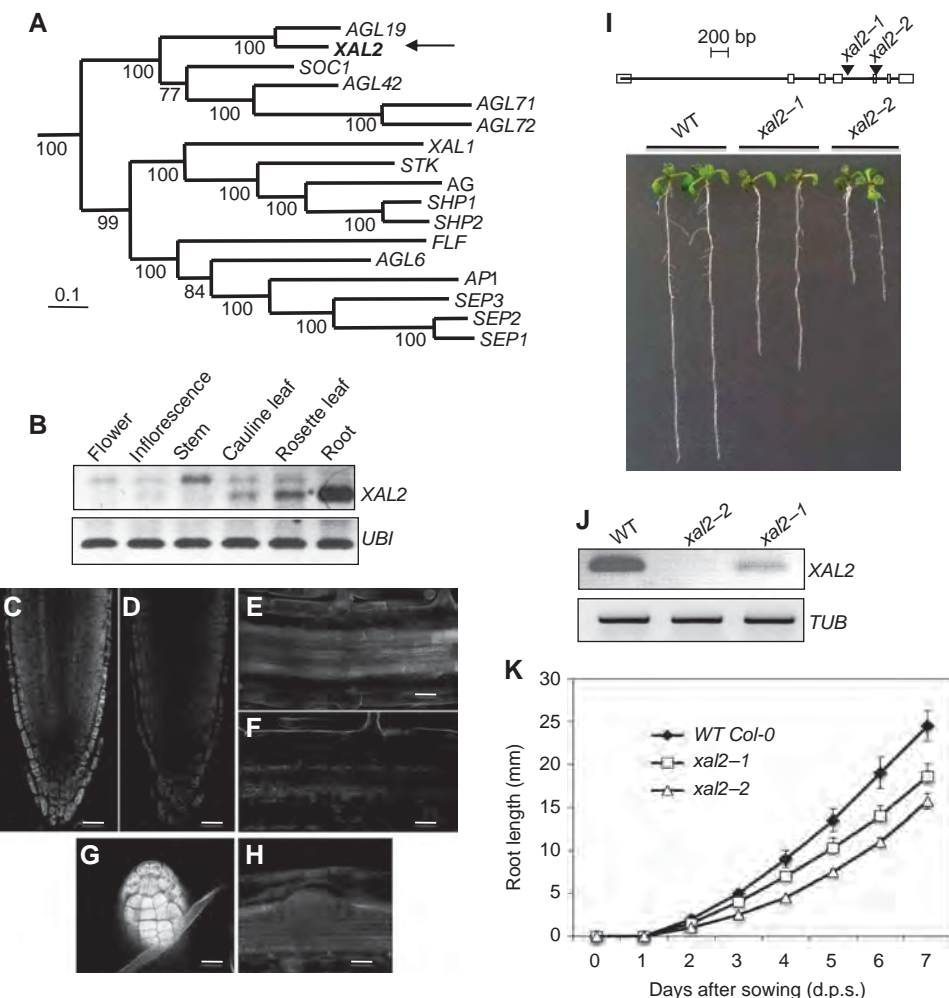


Figure 1 *XAL2*, a MADS-box gene, is highly expressed in roots and affects root growth. (A) Bayesian reconstruction of the phylogenetic relationships among selected type II *A. thaliana* MADS-box genes, with *XAL2* position indicated by an arrow. (B) RT-PCR used to visualize *XAL2* expression in different tissues from 7 days post sowing (d.p.s.) in wild-type. Ubiquitin (*UBI*) was used as an internal control. (C–H) Whole-mount *in situ* RT-PCR hybridization (see Materials and methods for details of procedures used) of *XAL2* in columella cells and lateral root cap (C), in the vascular bundle in differentiated cells (E) and in the primordia of lateral roots (G). (D, F, and H) Negative sense controls (Bar = 50 µm). (I) *XAL2* gene structure schematic model with the sites of transposon insertions. Squares correspond to exons while lines represent introns. Root length phenotypes of seedlings at 7 d.p.s. of Col-0 wild type, *xal2-1*, and *xal2-2* ($n = 60$). Tubulin (*TUB*) was used as an internal control. (J) RT-PCR of *XAL2* at 7 d.p.s. in wild type, *xal2-1*, and *xal2-2*. (K) Root growth curves of wild-type, *xal2-1*, and *xal2-2* plants grown in medium supplemented with 2% sucrose for 10 days ($n = 30$). Average and s.d. are shown.

a combination of decreased cell production and shorter cell length in the differentiation zone. The diminished size of the completely elongated cells observed in *xal2-2* accounts for up to 86% of the decrease in root length in the mutant, while only 14% of such length decrease could be attributed to changes in a number of cells in the root apical meristem (RAM) proliferation domain (Table I). In addition, we documented that the diameter of the stele (provascular tissues) of wild-type plants is not larger (see Supplementary Figures S4A–E), in the root meristem compared to that of *xal2-2* plants. In wild type, a greater number of pericycle cells are present in the transverse plane of the wild-type roots in comparison to the mutant ones (14.8 cells in wild type and 12.0 cells in *xal2-2*, Supplementary Figures S4C, D, and F). It is important to note, that wild-type and *xal2-2* mutant lines had roots and steles with the same width also in the differentiation zone (see Supplementary Figure S4G). We can conclude that *xal2-2* loss-of-function mutation significantly affects the proliferation of the pericycle

cells, particularly the radial anticlinal divisions at the fifth cortical cell.

To determine whether *XAL2* is necessary for QC identity and stem-cell niche patterning, we analysed whole mount optical and thin plastic sections of roots for each allele. We identified an altered stem-cell niche phenotype characterized by altered shapes and distributions of the QC, initial, and columella cells. *XAL2* does not seem to be necessary for QC identity, as *WOX5*, *SCR*, and *PLT1* (*COL148* (*plt1-1-GUS*); Aida *et al*, 2004) were properly expressed in the *xal2-2* mutants (Supplementary Figure S5) and *xal2-2* roots continued growth until day 10, although at a lower rate than wild-type roots (Figure 1K). The domains of expression of the QC-specific markers *QC25* and *QC46* were abnormally expanded in *xal2-2* mutants towards the columella cells and provascular initials, respectively (Figure 3A; Supplementary Figure S5), suggesting that *XAL2* is necessary for restriction of the QC to its normal spatial domain. Expression of the columella initial marker *J2341* was expanded as well in 25% of the *xal2-2*

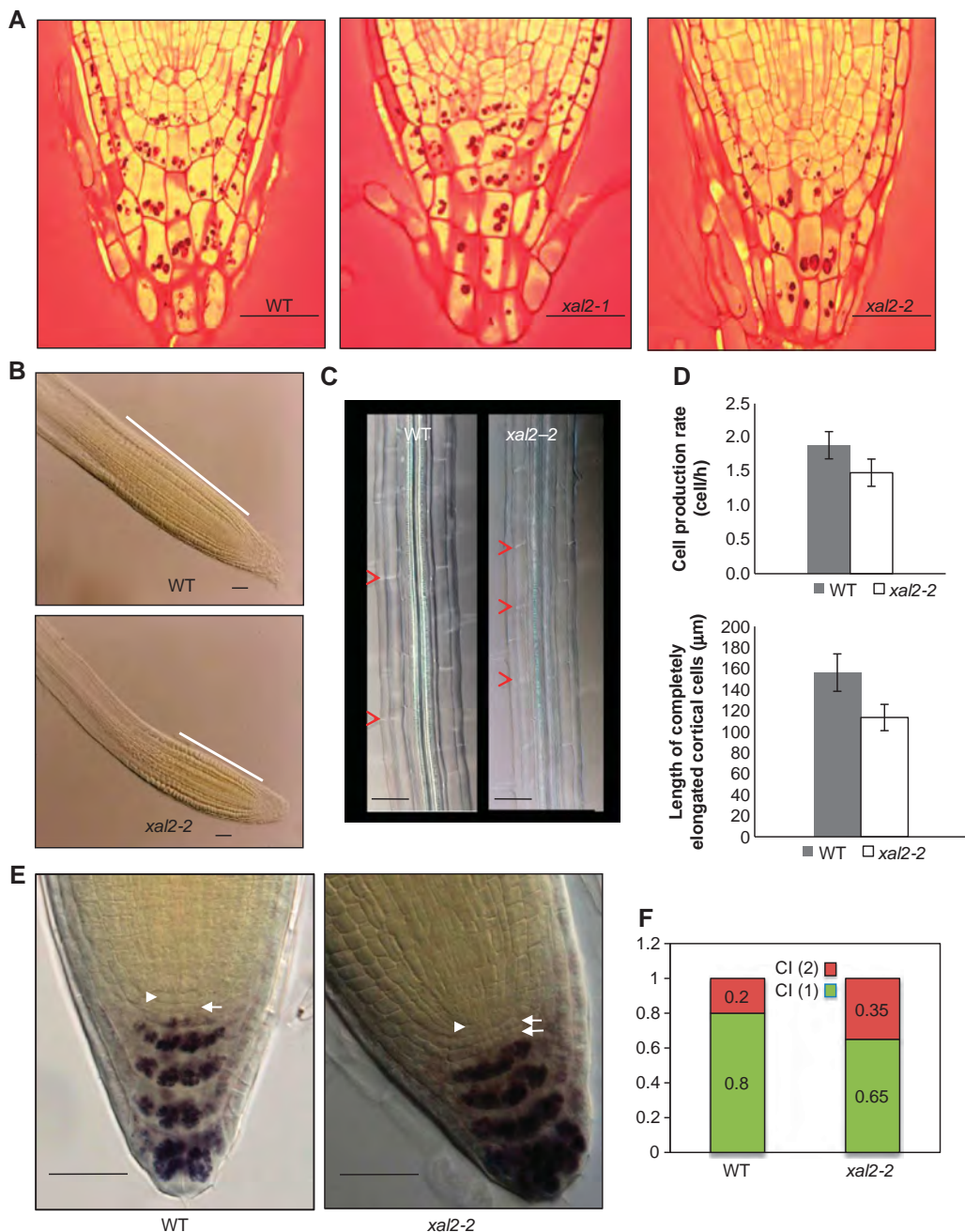


Figure 2 XAL2 controls meristem size and patterning of the root apical meristem. (A) Organization of the quiescent center and initial cells in the stem-cell niche from representative phenotypes for wild-type and *XAL2* mutants in longitudinal root sections (100%; $n = 30$) (Bar = 50 μm). (B) Meristem length of wild-type and *xal2-2* plants at 7 d.p.s.; the white line indicates the size of the meristematic region (Bar = 50 μm). (C) Cell length of fully elongated cells (see red arrowheads) at 7 d.p.s. ($n = 30$) in cleared roots observed with Nomarski optics (Bar = 50 μm). (D) Cell production rate and length of completely elongated cortical differentiated cells; quantifications are described in detail in Materials and methods. All data were analysed with the JMP 5.1.1 version statistical package. Measurements were obtained directly by measuring 10 cortical cells from 10 plants. Average and s.d. are shown. (E) Nomarski photographs of wild-type and *xal2-2* plants. The position of the QC is indicated (see white arrowhead) and white arrows indicate position of columella initial tiers. Lugol staining marks starch granules observed in mature wild-type and *xal2-2* columella-differentiated cells (Bar = 50 μm). (F) Percentage of one or two tiers of columella initials (CI) in wild-type plants and *xal2-2* mutants ($n = 56$ for wild type; $n = 69$ for *xal2-2*).

mutant roots (Figure 3A), and in these plants a super-numerary columella layer lacking starch granules was observed (Figures 2E and F); the rest of the mutant roots did not show this phenotype. We interpret this as indicating a delayed transition to columellar cell differentiation. The above results suggest that XAL2 seems to be required for normal spatial organization and patterning of the root stem-cell niche, as well as for maintaining meristem homeostasis.

XAL2 controls auxin transport and concentration

Auxin is required for normal cell proliferation and elongation: intermediate auxin levels are associated with highest cell proliferation, while lower levels with cell elongation and differentiation along the root (Burstrom, 1957; Grieneisen *et al*, 2007; Jurado *et al*, 2010). Given the growth defects of *xal2-2* mutant roots, we hypothesized that XAL2 could be important for maintaining auxin gradients along the root

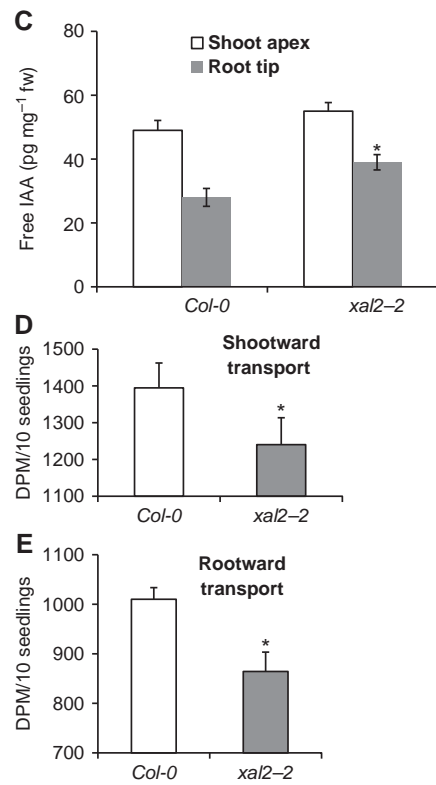
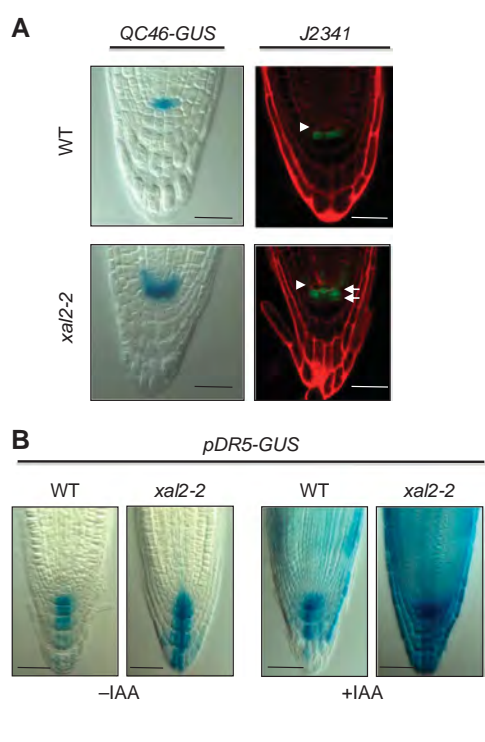


Figure 3 XAL2 is necessary to restrict QC and auxin distribution to its normal spatial domain in *Arabidopsis* root tip. **(A)** Two different markers in wild-type and *xal2-2* mutant plants: *QC46* expression (95%; $n=50$) and specific enhancer trap *J2341* expression (25%; $n=30$). In the latter marker, two tiers of columella initials were observed in *xal2-2* (white arrowheads) and the position of the QC is indicated (white arrowhead). For this line, red signal is emitted by propidium iodide that was used as a counterstain. 7 d.p.s. plants were used for the experiment with *QC46* transgenic lines and 5 d.p.s. plants for the *J2341* marker (Bar = 50 μ m). **(B)** *pDR5-GUS* (90%; $n=80$) expression of wild-type and mutant *xal2-2* plants with or without an auxin treatment (IAA 1 μ M, 4 h) (Bar = 50 μ m). **(C)** Quantification of free IAA levels in the root of wild-type and *xal2-2* plants ($P<0.01$, $n=50$). **(D)** Direct measurements of 3 H-IAA transport in shootward transport capacity from the root apex to the first 2 mm section ($P=0.052$, $n=10$). **(E)** Direct measurements of 3 H-IAA transport in rootward transport capacity in the hypocotyl to root-shoot transition zone ($P<0.001$, $n=10$). In (C–E), bars represent standard errors (s.e.) and the * indicates significant differences ($P<0.01$, $n=50$).

longitudinal axis. Visualization of the auxin-responsive *DR5* promoter (Sabatini *et al.*, 1999; Friml *et al.*, 2003) reporter suggests that auxin levels or responses are elevated in the QC, provascular initials, and columella cells of *xal2-2* mutants compared with normal siblings (Figure 3B). Moreover, exogenous indole acetic acid (IAA) treatment of *xal2-2* roots resulted in increased *pDR5::GUS* expression throughout the root (Figure 3B; Supplementary Figure S6A) compared with wild-type treated roots. We performed several experiments to distinguish whether these effects reflected alterations in downstream signalling, free auxin levels, or auxin transport. First, we tested several auxin responsive markers in the wild-type and *xal2-2* plants with or without auxin treatment and found that all these markers were similarly induced by auxin treatment in both genotypes (Supplementary Figure S6B), implying that auxin response is not altered in the mutant.

Next, direct quantification of free IAA levels in *xal2-2* seedlings confirmed that auxin levels are significantly increased in the *xal2-2* root compared with wild type (Figure 3C). A reduction in rootward 3 H-IAA transport, similar to levels seen in *pin1* mutants (Blakeslee *et al.*, 2007), was also observed (Figure 3E). Diminished shootward transport from the root apex (Figure 3D) is consistent with the increased *pDR5::GUS* signal observed in *xal2-2*. These results indicated that XAL2 is a positive regulator of auxin transport towards and within the root. We then addressed

whether such alterations were a consequence, at least in part, of the misregulation of the transcription of PIN auxin transporters, in the *xal2-2* background.

XAL2 regulates the transcript accumulation of several PIN genes

Despite functional redundancy, each PIN protein has been implicated in particular developmental processes (Gälweiler *et al.*, 1998; Luschnig *et al.*, 1998; Friml *et al.*, 2002a, b, 2003; Mravec *et al.*, 2009). For example, PIN4 has been associated with root meristem activity and patterning (Friml *et al.*, 2002b). Interestingly, roots with *pin4* loss-of-function alleles are strikingly similar to *xal2-2* roots, with altered stem-cell niches, two files of columella initials, expanded expression domains of QC markers, and altered auxin gradients (Friml *et al.*, 2002b). Hence, we addressed whether XAL2 is involved in regulation of PIN4 expression. We crossed *xal2-2* with a *pPIN4::GUS* line to assay an impact on RNA accumulation and a *pPIN4::PIN4-GFP* translational fusion line. The progeny of these crosses displayed clearly diminished GUS and GFP signals, respectively (Figures 4A and B). Consistent with this result, *PIN4* transcript abundance in response to auxin was also decreased by this visual assay in *xal2-2* mutants compared to wild type (Figures 4A and D).

Lower expression of *PIN4* in *xal2-2* mutants is insufficient to explain the shorter roots and the rootward and shootward

auxin transport alterations observed in this mutant. Hence, we decided to analyse the expression of other *PIN* genes. *xal2-2* exhibits similar root growth alterations observed in double and triple *pin* mutants (Blilou *et al*, 2005). *PIN1* is preferentially expressed in the stele and is fundamental for rootward auxin transport (Blilou *et al*, 2005; Vieten *et al*, 2005; Blakeslee *et al*, 2007); *pPIN1:GFP* signals in *xal2-2* are lower in comparison with the wild-type roots (Figures 4C and D; Supplementary Figure S7). To distinguish whether the observed differences reflected anatomical differences in

stele width between wild-type plants and the *xal2-2* mutant, transverse sections were analysed by light and confocal microscopy. As can be seen in Supplementary Figures S4F and G, there were no differences between these plants in terms of width of the root and the stele in the differentiation zone although we can see more rounded cortical cells in some *xal2-2* mutant roots (Supplementary Figure S4F). We also observed that there were a significantly lower number of pericycle cells at the level of the fifth cortical cell from the QC in *xal2-2* compared to wild-type plants (see Supplementary

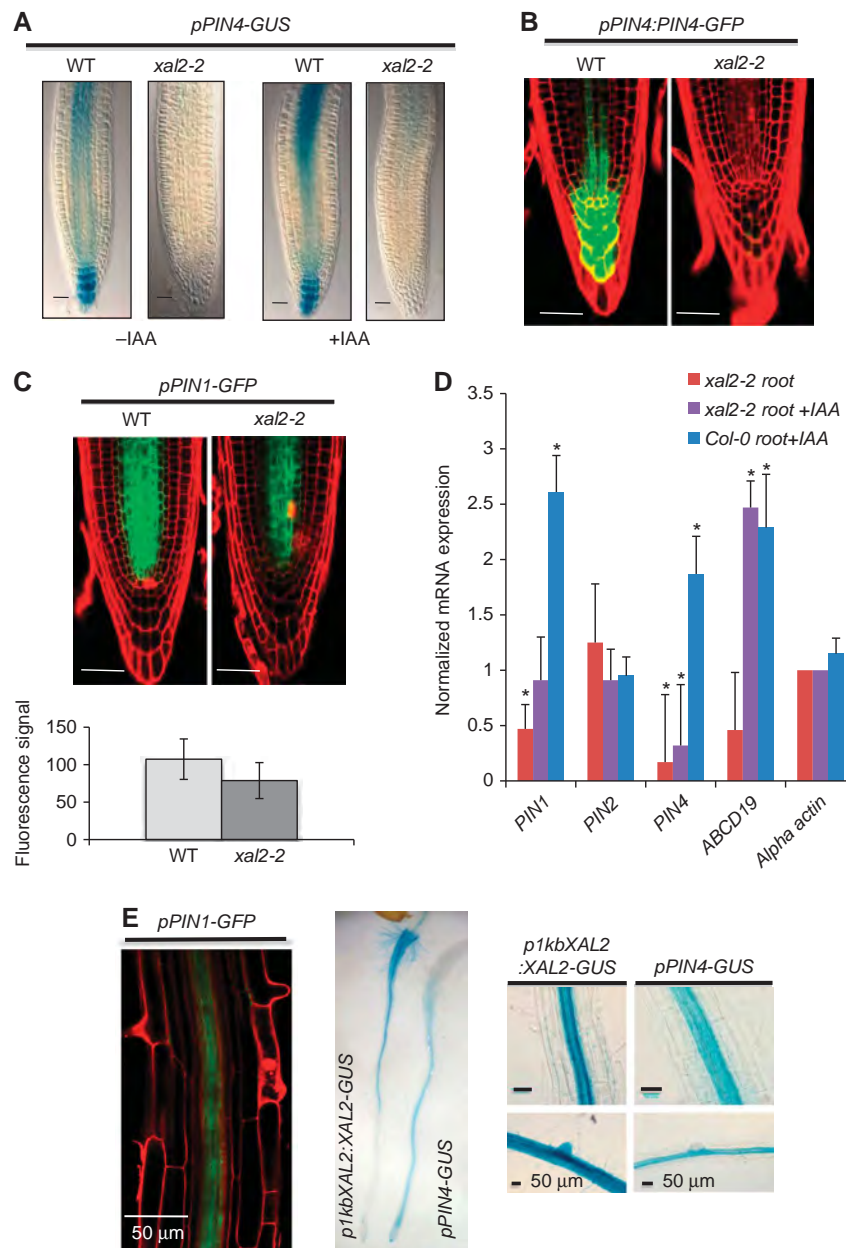


Figure 4 XAL2 upregulates *PIN1* and *PIN4* gene expression and controls *PIN4* auxin response. (A) *pPIN4-GUS* (100%; $n=60$) expression of wild-type and mutant *xal2-2* plants with or without an auxin treatment (IAA 1 μ M, 4 h) (Bar = 50 μ m). (B) *pPIN4:PIN4-GFP* (30%; $n=6$) expression in wild-type and *xal2-2* mutant plants. In these lines, confocal image of longitudinal optical sections of root meristem and red signal is emitted by propidium iodide that was used as a counterstain (Bar = 50 μ m). (C) *pPIN1-GFP* (50%; $n=80$) expression in wild-type and *xal2-2* mutant plants (Bar = 50 μ m). Quantification of the fluorescent signal of the *pPIN1-GFP* reporter (shown above) for wild-type and *xal2-2* plants ($n=57$ for wild type and $n=52$ for *xal2-2* plants) Average and s.d. are shown. (D) qRT-PCR analysis of *PIN1*, *PIN2*, *PIN4*, and *ABCD19* normalized to actin expression in 5 d.p.s. wild-type and *xal2-2* plants. Bars represent standard deviation (s.d.). *Marks that the change is significant at $P<0.001$ by Student's *t*-test followed by Neuman Keuls *post hoc* ANOVA. (E) Co-localization of expression of *PIN1*, *PIN4*, and *XAL2* in different tissues of the root: *pPIN1-GFP*, *pPIN4-GUS*, and *p1kbXAL2:XAL2-GUS*.

Figures S4A–E). Nonetheless, the magnitude of the difference is insufficient to explain the decrease found in the expression of *PIN1* in *xal2-2* mutant. Moreover, we did not find that XAL2 regulates *PIN7* expression despite the latter is expressed also in the vascular tissue (see Supplementary Figure S8A) but we found that *PIN7* has two overlapping phenotypes (see Supplementary Figure S8A); in one of them, the expression of *PIN7* was expanded to the xylem root axis in both wild-type and *xal2-2* plants, thus suggesting that the mutation in XAL2 is not the causal factor of such patterns. The decrease in *PIN1* and *PIN4* expression was further confirmed quantitatively by qRT-PCR measurements. Confirming the qualitative assessment with visual *PIN* reporter lines, transcripts of *PIN1* and *PIN4* genes were reduced in *xal2-2* compared with wild-type plants (Figure 4D). As can be seen in Figure 4E, *PIN1*, *PIN4*, and XAL2 are strongly expressed and their expression overlaps in the vascular tissue in the differentiation zone of the root; *PIN4* and XAL2 expression also overlaps in the columella and the three genes seem to have coincident patterns of expression in the root meristem (Blilou *et al*, 2005; Vieten *et al*, 2005; Figures 1C and 4E). XAL2 is not a general regulator of *PIN* genes, because we found that this MADS transcription factor does not regulate *PIN2* or *PIN7* (Supplementary Figure S8). We conclude that XAL2 is a positive regulator of the mRNA expression of *PIN1* and *PIN4* in the root. It is important to note that *xal2-2* loss-of-function allele has several phenotypes that cannot be explained by the loss of function of *PIN1* and *PIN4*, thus suggesting that XAL2 is a regulator of several additional genes involved in the networks important for root development.

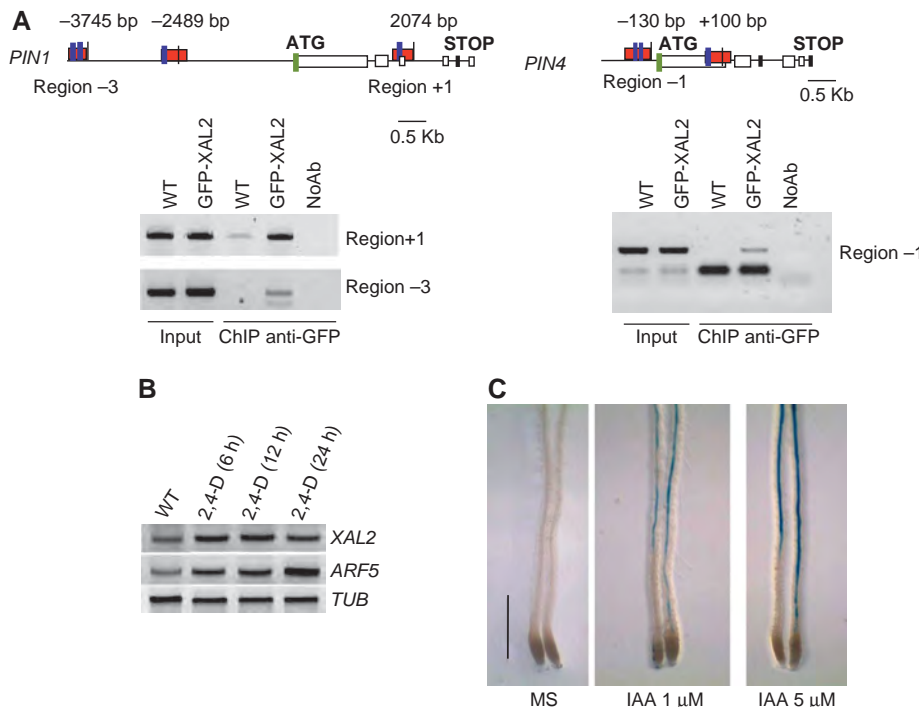


Figure 5 XAL2 directly regulates *PIN1* and *PIN4* gene expression and is induced by auxin treatment. **(A)** Scheme of *PIN1* and *PIN4* genes; blue boxes indicate putative CArG-boxes, red boxes indicate the XAL2 binding sites, and green box indicates the translation start site. PCR on total DNA (Input) and on DNA recovered by immunoprecipitation with (ChIP anti-GFP) or without (NoAb) GFP antibody from 5 d.p.s. roots of wild-type and 35S-GFP:XAL2 lines, using primers to amplify region -3, -1 and +1. **(B)** RT-PCR of XAL2, ARF5, and TUB2. RNA was isolated from 4 d.p.s. seedlings subject to 96 hours of 1-N-naphthylphthalimide acid (NPA) treatment and then transferred to 10 μM 2,4-D for 6, 12, or 24 h as indicated. **(C)** *p1KbXAL2:XAL2-GUS* line induced by different auxin treatments. Plants were grown for 6 d.p.s. in hormone-free medium and then transferred to growth media supplemented with 1 and 5 μM IAA (indole acetic acid) ($n=4$) (Bar = 0.5 mm).

XAL2 directly binds to PIN regulatory sequences

Both *PIN1* and *PIN4* have several MADS DNA binding motifs (CArG boxes; Riechmann *et al*, 1996) in their regulatory regions and hence we tested whether XAL2 is able to directly bind to any of such CArG boxes. Chromatin immunoprecipitation (ChIP) assays with 35S:GFP-XAL2 were performed (Supplementary Figure S9). Three CArG box-containing fragments, one in the promoter region of *PIN1*, another one in the second intron of *PIN1*, and the third in the promoter region of *PIN4* were consistently enriched in three different biological experiments in the IP, indicating that XAL2 directly binds to and presumably regulates the expression of both *PIN1* and *PIN4* (Figure 5A). We also tested whether XAL2 recognizes additional CArG boxes present in upstream regions of these genes (two for *PIN1* and one for *PIN4*) and confirmed that XAL2 does not bind to all CArG boxes found in these regions (see –2489 bp in the *PIN1* promoter and +100 pb in the *PIN4* promoter in Figure 5A).

Do the observed *xal2-2* phenotypes result from the down-regulation of *PIN1* and *PIN4* that, in turn, alter auxin distribution and transport in the root? The extent of decrease (1010 ± 23.51 in wild type and 864 ± 39 in *xal2-2*) in rootward transport in *xal2-2* mutant (Figure 3E) is approximately what we would expect for the loss of *PIN1* and *PIN4* activity (20–40% in Blakeslee *et al*, 2007). Ectopic auxin accumulation observed in *xal2-2* also appears to induce compensatory auxin efflux mechanisms, as expression of the auxin-inducible *ABCB19* auxin transporter gene (Noh *et al*, 2001) was significantly increased in auxin-treated roots compared with the wild-type roots (Figure 4D; Supplementary Figure S10); this result parallels what is

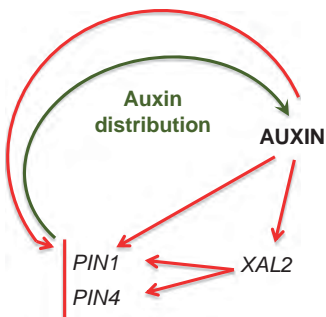


Figure 6 Positive feedback loop between XAL2 gene transcription and auxin distribution. Auxin upregulates XAL2 gene transcription and this MADS regulates efflux auxin carriers controlling auxin distribution/participation in the proliferation of the root meristematic cells. It is shown that while the response to auxin of PIN4 is mediated by XAL2, the auxin response of PIN1 does not depend on XAL2. Red arrows indicate transcript regulation based on the experimental data and green arrow indicates proteins involved in auxin distribution.

observed in the weak *pin1-5* allele (Supplementary Figure S10). In conclusion, decreased PIN1 expression (and by implication, function) in *xal2-2* appears to increase local auxin concentrations, which, in turn, increases ABCB19 abundance to compensate for the partial *PIN1* loss-of-function in the *xal2-2* background.

XAL2 gene responds to exogenous auxins

According to TGA (<http://bioinformatics.psb.ugent.be/webtools/plantcare/html>), there are several auxin response elements (AREs) in the regulatory regions of XAL2. Does this gene respond to auxin resulting in increased transcript abundance, similar to *XANTAL1*? (Tapia-López et al., 2008). Expression analysis using RT-PCR after 2,4-Dichlorophenoxyacetic acid (2,4-D) (Figure 5B) or IAA induction of *p1Kb::XAL2::gXAL2-GUS* reporter lines (Figure 5C) indicates that this XAL2 is positively regulated by auxins. Therefore, there is a positive feedback loop between auxin levels and PIN regulation via XAL2, which in turn, affects auxin levels and distribution in the root meristem (Figure 6).

Discussion

The focus of this study is XAL2, a MADS-box gene belonging to the SOC clade (Martinez-Castilla and Alvarez-Buylla, 2003). We establish that XAL2 is a component of the *Arabidopsis* GRNs underlying root stem-cell and meristem patterning and that XAL2 can control auxin transport via direct regulation of *PIN1* and *PIN4* genes. XAL2 directly binds to discrete motifs within the regulatory regions of *PIN1* and *PIN4* and results in increased transcript abundance; this activity is selective, because XAL2 does not affect *PIN2* and *PIN7*. Furthermore, *PIN4* response to auxin depends on XAL2. Thus, we have uncovered a direct molecular link between auxin transport dynamics, which is a key plant hormone, and transcriptional MADS-box GRNs that underpin cell-fate decisions.

xal2-2 roots showed an increased free auxin accumulation in comparison to wild-type roots. Although this could appear to contradict the observation of lower *PIN1* and *PIN4* expression in the mutant, redundant auxin efflux mechanisms must compensate, which in turn could explain augmented ABCB19 expression levels. Such compensatory mechanisms are

expected from the reported complexity of phenotypic effects with multiple *PIN* mutations (Blilou et al., 2005). The magnitude of ABCB19 overexpression in *xal2-2* mutant could be important for auxin accumulation in the root tip, especially when the mutants are treated with IAA. The fact that *xal2-2* roots showed increased free auxin levels along the entire length of the *Arabidopsis* seedling root could explain the decreased size of completely elongated and differentiated cells in the mutant in comparison to wild-type cells.

Because both XAL2 and XAL1 (Tapia-López et al., 2008) are auxin-responsive genes, we hypothesize that a complex MADS network functions to regulate auxin transport, distribution patterns, and auxin levels within root cells. Auxin levels in turn modulate PIN expression via at least one of these MADS factors. Such feedback may contribute to the establishment of a robust auxin and morphogenetic pattern along the root axis, because it has been shown that positive feedback loops amplify a received signal or stimulus and can generate robust and precise patterns as it has been suggested by theoretical dynamical systems (Kitano, 2004; Jaeger et al., 2008; Mitrophanov and Groisman, 2008). In *Arabidopsis* roots, the complete mechanism likely involves XAL1 and XAL2 plus additional MADS-box proteins that form heterodimeric transcriptional activators and repressors (Honma and Goto, 2001). MADS proteins already identified as important regulators of root development include AGL16, AGL20, and AGL21; XAL1 can interact by yeast two and three hybrid, with all three of these AGLs and XAL2 with AGL16 and AGL20 (de Folter et al., 2005; Immink et al., 2009). We propose that both MADS-domain heteromultimeric complexes and yet to be identified transcription factors are involved in the control and readout mechanisms of auxin gradients along the root. Those with maximum impact on auxin distribution should be factors expressed primarily at the root stem-cell niche.

The PLETHORA genes have been reported to be crucial genes to root patterning and auxin readout mechanisms (Aida et al., 2004; Galinha et al., 2007). Future studies should search directly for biochemical evidence of MADS-PLT interactions combined with tests of functional relevance in stem-cell patterning and auxin control and readout mechanisms. In fact, XAL and PLT mutants are quite similar in root length and organization of stem-cell niche (Aida et al., 2004; Galinha et al., 2009) although the loss-of function or the gain-of-function of PLT genes shows more drastic effects than those observed in the MADS mutant lines.

A recent GRN model of root stem-cell niche patterning suggests that additional components of the mechanisms involved in root stem-cell patterning remain undiscovered (Azpeitia et al., 2010). Here, we have provided data for XAL2 mutants, which have altered cellular patterns in the stem-cell niche and apical meristem of *Arabidopsis* roots. We also showed that this MADS factor is an important regulator of transport and distribution of auxin, a hormone required for stem-cell patterning. Future models should incorporate the role of these and other MADS factors utilizing ChIP-Seq data to define their target genes and detailed phenotypic quantification to clarify their roles in controlling cell patterning and proliferation in the root apex. Indeed, the relatively more drastic alterations in the stem-cell and meristem cellular patterns of *xal2-2*, in comparison to *pin* mutants (Blilou et al., 2005), suggest that XAL2 regulates other genes in addition to *PIN1* and *PIN4*.

Materials and methods

Plant materials, DNA constructs, and growth conditions

Arabidopsis thaliana wild-type, *xal2-1*, and *xal2-2* plants, *pPIN1-GFP*, *pPIN2:PIN2-GFP*, *pPIN4:PIN4-GFP*, *pPIN4-GUS*, *pWOX-GFP*, and *pSCR-GFP* constructs and *DR5-GUS* auxin reporter lines are in a Col-0 genetic background. *QC25-GUS*, *QC46-GUS*, and *PLT1-GUS* are in the Ws ecotype, and *J2341* is in C24 ecotype. All lines were homozygous. The *xal2-1* and *xal2-2* alleles were identified by screening for En-I insertions among a collection of *Arabidopsis* plants carrying ~50 000 independent insertions of the autonomous maize transposable element (En; Baumann *et al.*, 1998). The collection was screened in pools using the En-I transposon primer En8130 and the internal XAL2 primers: XAL2F and XAL2R (see Supplementary Table S1 for primer sequences) and single insertion lines were confirmed with Southern blot analyses and propagated for further analysis. For the *35S:GFP-XAL2* construction, an (AGL14) XAL2 cDNA entry clone (de Folter *et al.*, 2005) was recombined using the Gateway system (Invitrogen) in the pK7WG2 destination vector (Karimi *et al.*, 2002). In the case of the *35S:XAL2* construction, an (AGL14) XAL2 cDNA entry clone (de Folter *et al.*, 2005) was recombined using the Gateway system (Invitrogen) in the pH7WG2 destination vector (Karimi *et al.*, 2007). For the *pXAL2-GUS* promoter construction, *Arabidopsis* (Col-0 ecotype) genomic DNA was used as a template to amplify a 1-kb fragment upstream of the XAL2 start codon. The oligonucleotides used were up-p14-FW and Atg-14-RV (+NcoI; see Supplementary Table S1 for primer sequences). The PCR product was purified by using a kit (Qiagen; Cat. no. 28104) and cloned in pENTR/D, followed by sequencing and recombination with pBGWFS7 (Karimi *et al.*, 2007). *Arabidopsis thaliana* plants were transformed using the floral dip method (Clough and Bent, 1998), the transgenic lines were selected based on their antibiotic resistance (different for each line), and expression analysis was carried out on T3 homozygous lines. All seeds were sown on vertical plates with 0.2X MS salts, 1% sucrose and 1% agar (unless otherwise indicated). Plants were grown under long-day (LD; 16 h light/8 h dark) conditions in growth chambers at 22°C and with a 16-h photo/8-h dark period (110 $\mu\text{E m}^{-2} \text{s}^{-1}$).

Seed carrying *pPIN1-GFP* was obtained from J Friml; *pPIN4:PIN4-GFP* and *pPIN4:GUS* were obtained from E Benková; *QC25-GUS*, *pPIN2:PIN2-GFP*, *pPIN7:PIN7-GFP*, *pDR5-GUS*, *pWOX5-GFP*, *plt1-1-GUS*, and *QC46-GUS* were obtained from B Scheres; *pSCR-GFP* was obtained from P Benfey, *pCYCB1;1DB::GUS* was obtained from P Doerner and *J2341* was obtained from the *Arabidopsis* Stock Center.

Phylogenetic analysis

We performed a Bayesian reconstruction of the phylogenetic relationships among selected type II *Arabidopsis thaliana* MADS-box genes using the complete cDNA sequences from Martinez-Castilla and Alvarez-Buylla (2003). Bayesian methods with Mr Bayes (Huelsenbeck and Ronquist, 2001) were used with a Markov chain Monte Carlo exploration of the tree likelihood surface. Four independent Markov chains (three heated) were used according to the Metropolis coupled scheme. The codon substitution model used was that of Goldman and Yang (1994). Four independent runs of 2 500 000 generations each were performed, and every 100th tree was saved. After checking for Markov chain convergence, we discarded the first 15 000 trees and used the remaining trees to calculate Bayesian posterior probabilities of the clades. Results from every independent run were similar.

Histological analysis

Roots were fixed, embedded in Historesin (Leica Instruments GmbH) as described previously (Dubrovsky *et al.*, 2000) and 2.5 μm sections obtained on a Leica RM2155 microtome (Cambridge Instruments, Nussloch, Germany). Sections were mounted on gelatin-coated slides (Baum and Rost, 1996), and after 30 min of hydrolysis in 5N of HCl at room temperature, were stained by the Feulgen technique (De Tomasi, 1936) for 1 h. The same material subsequently was stained by periodic Acid-Schiff reaction (Baum and Rost, 1996).

'In situ' hybridization

For whole-mount 'in situ' RT-PCR hybridization, we used the protocol of Ruiz-Medrano *et al.* (1999); probes were chosen to avoid the presence of the MADS-box sequence and to have an

average length of 200 bp. Sense probes were used as negative controls for XAL2 in all experiments performed for different tissues.

GUS staining

Plant material for light microscopy and GUS staining was prepared as previously described by Malamy and Benfey (1997) and visualized microscopically (see below). Seedlings were subjected to GUS reaction in the dark during 40 min at room temperature for *pDR5-GUS* and *plt1-1-GUS*, 1 h at 37°C for *pPIN4-GUS*, 5 h at 37°C for *QC25-GUS*, overnight at 37°C for *QC46-GUS*, 24 or 48 h, 4 or 6 days at 37°C for *p1KbXAL2:XAL2-GUS*. To restrict the diffusion of GUS blue staining, 2 mM of K₃FE(CN)₆ and K₄FE(CN)₆ was added in the GUS solution at the beginning.

GFP quantification

Fluorescence intensity of green channel was measured using the FV10-ASW 1.7 Software (Olympus, USA). To measure the intensity of GFP, we used the same region shown in Figure 4C of WT and *xal2-2* plants. The figure shows the mean and standard deviation.

Microscopy

Plant material for light microscopy was cleared using a modified Malamy and Benfey protocol (1997). Roots were visualized using Nomarski optics under an Olympus BX60 microscope and photographed with a Leica camera. Confocal images were acquired using an inverted Zeiss LSM 510 Meta microscope (Carl Zeiss, Oberkochen, Germany) with a dry $\times 40$ or a $\times 63$ water immersion C-Apochromat objectives after root tissue was stained with 5 or 10 g μl^{-1} propidium iodide. For starch staining, live roots were stained for 5 min in Lugol (Sigma Aldrich) solution 1 \times , washed in 30% glycerol for 1 min, mounted into the Nal solution without DMSO as described previously (Dubrovsky *et al.*, 2009) and immediately analysed using Nomarski optics.

Quantitative analysis of cellular parameters of root growth

Length of the cell proliferation domain of the RAM was determined for the cortex cells as a point where the distances between nuclei in neighbouring cells in a cell file became greater than the diameter of the nuclei (Dubrovsky *et al.*, 1998). The combined length of the elongation zone and the transition domain defined as in Ivanov and Dubrovsky (2013) was measured as the distance between the shootward border of the RAM proliferation domain and the location of the most distal root-hair bulge. The number of cortical cells in the cell proliferation domain in 7-day and 8-day plants (a period during which the rate of the root growth was estimated) was similar in wild-type and mutant plants, which enabled us to consider root growth to be at steady state and apply the rate of cell production method (Ivanov and Dubrovsky, 1997) for estimation of average cell-cycle duration in the RAM of 8-day plants. Cell-cycle duration (*T*, hours) was calculated as $T = (N_{PD} l_e \ln 2) V^{-1}$ where N_{PD} is the number of cells in the cell proliferation domain, l_e (μm) is the average length of 10 fully elongated cells and V ($\mu\text{m h}^{-1}$) is the rate of root growth during last day of growth (Ivanov and Dubrovsky, 1997). As the transition domain of the RAM previously has not been defined, the number of meristematic cells in the cited work corresponds to the N_{PD} in the current study. The rate of cell production was estimated as $V(l_e)^{-1}$ (Baskin, 2000). Student's *t*-test or the Tukey-Kramer test (depending on the sample size) was calculated by the JMP program version 5.1.1 at different confidence level (see Table I).

Expression analysis by RT-PCR

Total RNA was isolated from seedlings using the Trizol reagent (Invitrogen). Columbia wild-type, *xal2-1*, and *xal2-2* seedlings were grown for 7 days post sowing (d.p.s.); for *PIN1* expression analysis Columbia wild-type, *xal2-2*, and *35S:GFP-XAL2* plants were grown for 5 d.p.s.; in both cases, the seedlings were grown in MS plates. RT-PCR was done starting from 1 μg of total RNA to obtain cDNA using Super Script II (Invitrogen). *TUBULIN* or *UBIQUITIN* was amplified as an internal positive control; primer sequences of PCR primers are included in Supplementary Table S1. The primers for XAL2 were XAL2F1 and XAL2R2, for *PIN1* were PIN1F and PIN1R, for *ARF5* were ARF5F1 and ARF2R2; for *TUB2* were TUB2F and TUB2R and for *UBI* were UBIF and UBIIR; primer sequences are described in Supplementary Table S1. For auxin induction assays, seeds were germinated in plates with 10 μM 1-N-naphthalylphthalamic acid (NPA) for 96 h and then were transferred to fresh plates with or without 10 μM 2,4-D and incubated for 6, 12, and 24 h, as indicated.

Real-time PCR

Seedlings were grown as described by Murphy and Taiz (1995). RNA extraction and PCR conditions were as described by Blakeslee and collaborators (2004). See http://www.psla.umd.edu/faculty/Murphy/index_files/Page530.htm for complete details and Supplementary Table S1 for primer sequences. Primer sequences for quantitative PCR are marked with a *q* at the beginning of the primer name. The qRT-PCR data were analysed using the value of the wild-type amplification cycle divided by the internal standard compared to the value of *xal2-2* against the same standard for *PIN1*, *PIN2*, *PIN4*, *ABCB19*, and *alpha actin*. The standard deviations are the sum of standard deviations for *N* biological replicates with *N* technical replicates of each sample. Quantification and data acquisition was done using the iCycler Real Time system (Bio-Rad) using Syber Green I as a fluorophor. Real-time PCR was run using 1:50 dilution of first strand at 95°C for 40 s (denaturation), 54°C for 40 s (annealing), and 72°C for 20 s (extension) for 35 cycles. The ABI program was setup with an s.d. threshold for three replicates and was set to <0.25. If data are ≥0.25, then they are not significant.

Chromatin immunoprecipitation

ChIP assays were carried out as previously described (Sanchez and Gutierrez, 2009) with several modifications. For immunoprecipitation, 4 µl of an anti-GFP antibody (sc-8334; Santa Cruz Biotechnology) was incubated in phosphate-buffered saline (PBS) with Protein A agarose; 500 ng of root fixed-chromatin extracts from 5-day-old 35S:GFP-XAL2 complementation plants or wild-type plants was added to the IP reaction. The immunoprecipitated DNA was resuspended in 30 µl of TE and 1 µl of this DNA and a 1/5 dilution of INPUT samples were used for each PCR. The primers sequences are described in Supplementary Table S1.

Hormone treatments

Plants of the lines harbouring the *1KbXAL2:XAL2-GUS* or *PIN4-GUS* constructs were grown for 7 days in hormone-free medium plates and then transferred to growth media supplemented with 1 or 5 µM of IAA for 1 day. For the RT-PCR experiment, plants were grown in 2,4-D for 4 days in NPA and then transferred to 10 µM of 2,4-D for 6, 12, and 24 h as indicated. After IAA treatment, some seedlings were subjected to GUS staining, *pDR5-GUS* (40 min at room temperature) and *pPIN4-GUS* (1 h at 37°C). In parallel, duplicate samples were subjected to RNA extraction for RT-PCR experiments. T3 seeds of two representative independent *p1KbXAL2:XAL2-GUS* transformants were surface sterilized and sown in plates containing 0.2XMS medium with 1% sucrose and 1% micropagation grade agar. After three nights at 4°C, the plates were placed in a growth cabinet (Percival) at 16 h photoperiod at 22°C.

Quantification of endogenous-free auxin

Seedlings were grown as described by Murphy and Taiz (1995). The protocol for quantification of free IAA is described in Kim et al (2007).

Auxin transport assays

Seedlings were grown as described by Murphy and Taiz (1995). Protocols for quantifying auxin transport are provided in Blakeslee and collaborators (2007) and in Peer and Murphy (2007). A detailed protocol can be found at http://www.psla.umd.edu/faculty/Murphy/index_files/Page530.htm.

References

- Aida M, Beis D, Heidstra R, Willemsen V, Blilou I, Galinha C, Nussaume L, Noh YS, Amasino R, Scheres B (2004) The PLETHORA genes mediate patterning of the *Arabidopsis* root stem cell niche. *Cell* **119**: 109–120
- Alvarez-Buylla ER, Pelaz S, Liljegren SJ, Gold SE, Burgeff C, Ditta GS, Ribas de Pouplana L, Martínez-Castilla L, Yanofsky MF (2000a) An ancestral MADS-box gene duplication occurred before the divergence of plants and animals. *Proc Natl Acad Sci* **97**: 5328–5333

Supplementary data

Supplementary data are available at *The EMBO Journal* Online (<http://www.embojournal.org>).

Acknowledgements

We thank M Yanofsky for his help, guidance, and support during the early stages of this work. We also thank C Gutiérrez for support and advice during the final phase of this study. Thanks to B Scheres, V Ivanov, E Azpeitia, and M Benítez who provided insightful comments on the manuscript, and to R Pérez, G Coello, D Romo, T Romero, S Napsucialy-Mendivil, A Saralegui, X Alvarado-Affantranger, JA Pimentel-Cabrera, JM Hurtado-Ramírez, K Jiménez-Durán and L Rodríguez who helped with logistical and laboratory tasks. We also thank J Lin for assistance with the preliminary set of transport assays, Professor Wendy Peer for statistical evaluation and validation of qRT-PCR results and A Chase for preparing the materials and plants for auxin transport assays. We thank Dr Virginia Walbot for her careful editing and overall revision of the paper. Any remaining mistake is our responsibility. This work was supported by grants from CONACYT, México: (1) Red Temática de Investigación: ‘Complejidad, Ciencia y Sociedad’ (124909; ERAB; BGP; AGA) and (2) 81542 and 105678 (ERAB), 167705 (AGA), 152649 (MPS), 81433 (BGP), 177739 (SF) and 127957 (JGD), from PAPIIT-UNAM, IN204011-3 (BGP), IN229009-3 (ERAB), IN226510-3 (AGA), IB201212 (MPS), and IN204312 (JGD), from the Spanish Government BFU2012-33746 (SP) and from the National Science Foundation (NSF-IOS) 0820648 (ASM). ERAB acknowledges the support of the Miller Institute for Basic Research in Science, University of California, Berkeley while spending a sabbatical leave in the laboratory of Chelsea Specht at UC-B.

Author contributions: ERA-B designed and coordinated this study, designed many experiments, performed the initial experiments, analysed all experimental results, and wrote the paper; AG-A conceptualized and performed most of the genetic experiments and some of the qRT-PCR assays, analysed data, and wrote the paper; EO-M conceptualized and performed the mutant line characterizations and some of the crosses, made whole-mount *in situ* hybridization experiments, performed root histology and assisted with data analysis. AC-P participated in the genetic and molecular biology experiments and analysis. MPS, NM-M, and SF conceptualized, performed, and analysed ChIP experiments and made the overexpression constructs and the prom-GUS fusion construct. NM-M also performed the auxin induction experiments for long periods of time. ASM conceptualized, performed, and analysed auxin transport, response, and level experiments, as well as qRT-PCR assays for PINs and auxin responsive markers and participated in writing the manuscript. BGP conceptualized genetic and molecular biology experiments, helped analyse them and participated in writing the paper. FJ-M participated in genetic and molecular experiments and MAP-E participated in the visualization of roots and analysis of results. JGD established and helped coordinate the quantitative cellular, histological, and confocal microscopy analyses of wild-type and mutant roots, participated in analysis of genetic experiments, and participated in manuscript preparation. SP performed some of the first experiments and helped in the isolation of the transposon mutants of XAL2.

Conflict of interest

The authors declare that they have no conflict of interest.

- Alvarez-Buylla ER, Liljegren SJ, Pelaz S, Gold SE, Burgeff C, Ditta GS, Vergara-Silva L, Yanofsky MF (2000b) MADS-box gene evolution beyond flowers: expression in pollen, endosperm, guard cells, roots and trichomes. *Plant J* **24**: 457–466
- Azpeitia E, Benítez M, Vega I, Villarreal C, Alvarez-Buylla E (2010) Single-cell and coupled GRN models of cell patterning in the *Arabidopsis thaliana* root stem-cell niche. *BMC Syst Biol* **4**: 134

- Baskin TI (2000) On the constancy of cell division rate in the root meristem. *Plant Mol Biol* **43**: 545–554
- Baum SF, Rost TL (1996) Root apical organization in *Arabidopsis thaliana*: 1. Root cap and protoderm. *Protoplasma* **192**: 178–188
- Baumann E, Lewald J, Saedler H, Schultz B, Wisman E (1998) Successful PCR-based reverse genetic screen using an En-1 mutagenised *Arabidopsis thaliana* population generated via single-seed descent. *Theor Appl Genet* **97**: 729–734
- Birnbaum K, Shasha DE, Wang JY, Jung JW, Lambert GM, Galbraith DW, Benfey PN (2003) A gene expression map of the *Arabidopsis* root. *Science* **302**: 1956–1960
- Blakeslee JJ, Bandyopadhyay A, Lee OR, Mravec J, Titapiwatanakun B, Sauer M, Makam SN, Cheng Y, Bouchard R, Adamec J, Geisler M, Nagashima A, Sakai T, Martinoia E, Friml J, Peer WA, Murphy AS (2007) Interactions among PIN-FORMED and P-glycoprotein auxin transporters in *Arabidopsis*. *Plant Cell* **19**: 131–147
- Blakeslee JJ, Bandyopadhyay A, Peer WA, Makam SN, Murphy AS (2004) Relocalization of the PIN1 auxin efflux facilitator plays a role in phototropic responses. *Plant Physiol* **134**: 28–31
- Blilou I, Xu J, Wildwater M, Willemse V, Paponov I, Friml J, Heidstra R, Aida M, Palme K, Scheres B (2005) The PIN auxin efflux facilitator network controls growth and patterning in *Arabidopsis* roots. *Nature* **433**: 39–44
- Burgeff C, Liljegren SJ, Tapia-Lopez R, Yanofsky MF, Alvarez-Buylla ER (2002) MADS-box gene expression in lateral primordia, meristems and differentiated tissues of *Arabidopsis thaliana* roots. *Planta* **214**: 365–372
- Burstrom H (1957) Auxin and the mechanism of root growth. *Symp Soc Exp Biol* **11**: 44–62
- Clough SJ, Bent AF (1998) Floral dip: a simplified method for Agrobacterium-mediated transformation of *Arabidopsis thaliana*. *Plant J* **16**: 735–743
- Coen ES, Meyerowitz EM (1991) The war of the whorls: genetic interactions controlling flower development. *Nature* **353**: 31–37
- Davidson EH, Erwin DH (2006) Gene regulatory networks and the evolution of animal body plans. *Science* **311**: 796–800
- de Folter S, Immink RG, Kieffer M, Parenicová L, Henz SR, Weigel D, Busscher M, Kooiker M, Colombo L, Kater MM, Davies B, Angenent GC (2005) Comprehensive interaction map of the *Arabidopsis* MADS Box transcription factors. *Plant Cell* **17**: 1424–1433
- De Tomasi JA (1936) Improving the technic of the Feulgen stain. *Stain Technol* **11**: 137–144
- Dolan L, Janmaat K, Willemse V, Linstead P, Poethig S, Roberts K, Scheres B (1993) Cellular organization of the *Arabidopsis thaliana* root. *Development* **119**: 71–84
- Dubrovsky JG, Doerner PW, Colón-Carmona A, Rost TL (2000) Pericycle cell proliferation and lateral root initiation in *Arabidopsis*. *Plant Physiol* **124**: 1648–1657
- Dubrovsky JG, North GB, Nobel PS (1998) Root growth, developmental changes in the apex, and hydraulic conductivity for *Opuntia ficus-indica* during drought. *New Phytol* **138**: 75–82
- Dubrovsky JG, Soukup A, Napsucialy-Mendivil S, Jeknic Z, Ivanchenko MG (2009) The lateral root initiation index: an integrative measure of primordium formation. *Annu Bot* **103**: 807–817
- Friml J, Benková E, Blilou I, Wisniewska J, Hamann T, Ljung K, Woody S, Sandberg G, Scheres B, Jürgens G, Palme K (2002b) AtPIN4 mediates sink-driven auxin gradients and root patterning in *Arabidopsis*. *Cell* **108**: 661–673
- Friml J, Palme K (2002) Polar auxin transport—old questions and new concepts? *Plant Mol Biol* **49**: 273–284
- Friml J, Vieten A, Sauer M, Weijers D, Schwarz H, Hamann T, Offringa R, Jürgens G (2003) Efflux-dependent auxin gradients establish the apical-basal axis of *Arabidopsis*. *Nature* **426**: 147–153
- Friml J, Wiśniewska J, Benková E, Mendgen K, Palme K (2002a) Lateral relocation of auxin efflux regulator PIN3 mediates tropism in *Arabidopsis*. *Nature* **415**: 806–809
- Fulcher N, Sablowski R (2009) Hypersensitivity to DNA damage in plant stem cell niches. *Proc Natl Acad Sci USA* **106**: 20984–20988
- Galinha C, Hofhuis H, Luijten M, Willemse V, Blilou I, Heidstra R, Scheres B (2007) PLETHORA proteins as dose-dependent master regulators of *Arabidopsis* root development. *Nature* **449**: 1053–1057
- Gan Y, Filleur S, Rahman A, Gotensparre S, Forde BG (2005) Nutritional regulation of ANR1 and other root-expressed MADS-box genes in *Arabidopsis thaliana*. *Planta* **222**: 730–742
- Goldman N, Yang Z (1994) A codon-based model of nucleotide substitution for protein-coding DNA sequences. *Mol Biol Evol* **11**: 725–736
- Grieneisen VA, Xu J, Marée AF, Hogeweg P, Scheres B (2007) Auxin transport is sufficient to generate a maximum and gradient guiding root growth. *Nature* **449**: 1008–1013
- Gälweiler L, Guan C, Müller A, Wisman E, Mendgen K, Yephremov A, Palme K (1998) Regulation of polar auxin transport by AtPIN1 in *Arabidopsis* vascular tissue. *Science* **282**: 2226–2230
- Helariutta Y, Fukaki H, Wysocka-Diller J, Nakajima K, Jung J, Sena G, Hauser MT, Benfey PN (2000) The SHORT-ROOT gene controls radial patterning of the *Arabidopsis* root through radial signaling. *Cell* **101**: 555–567
- Honma T, Goto K (2001) Complexes of MADS-box proteins are sufficient to convert leaves into floral organs. *Nature* **409**: 525–529
- Huelsbeck JP, Ronquist F (2001) MRBAYES: Bayesian inference of phylogenetic trees. *Bioinformatics* **17**: 754–755
- Immink RG, Tonaco IA, de Folter S, Shchennikova A, van Dijk AD, Busscher-Lange J, Börst JW, Angenent GC (2009) SEPALLATA3: the ‘glue’ for MADS box transcription factor complex formation. *Genome Biol* **10**: R24
- Ivanov VB, Dubrovsky JG (1997) Estimation of the cell-cycle duration in the root meristem: a model of linkage between cell-cycle duration, rate of cell production, and rate of root growth. *Int. J. Plant Sci* **158**: 757–763
- Ivanov VB, Dubrovsky JG (2013) Longitudinal zonation pattern in plant roots: conflicts and solutions. *Trends Plant Sci* **18**: 237–243
- Jaeger J, Irons D, Monk N (2008) Regulative feedback in pattern formation: towards a general relativistic theory of positional information. *Development* **135**: 3175–3183
- Jurado S, Abraham Z, Manzano C, López-Torrejón G, Pacios LF, Del Pozo JC (2010) The *Arabidopsis* cell cycle F-box protein SKP2A binds to auxin. *Plant Cell* **22**: 3891–3904
- Karimi M, Depicker A, Hilson P (2007) Recombinational cloning with plant gateway vectors. *Plant Physiol* **145**: 1144–1154
- Karimi M, Inzé D, Depicker A (2002) GATEWAY vectors for Agrobacterium-mediated plant transformation. *Trends Plant Sci* **7**: 193–195
- Kim JI, Sharkhuu A, Jin JB, Li P, Jeong JC, Baek D, Lee SY, Blakeslee JJ, Murphy AS, Bohnert HJ, Hasegawa PM, Yun DJ, Bressan RA (2007) *yucca6*, a dominant mutation in *Arabidopsis*, affects auxin accumulation and auxin-related phenotypes. *Plant Physiol* **145**: 722–735
- Kitano H (2004) Biological robustness. *Nat Rev Genet* **5**: 826–837
- Luschnig C, Gaxiola RA, Grisafi P, Fink GR (1998) EIR1, a root-specific protein involved in auxin transport, is required for gravitropism in *Arabidopsis thaliana*. *Genes Dev* **12**: 2175–2187
- Malamy JE, Benfey PN (1997) Organization and cell differentiation in lateral roots of *Arabidopsis thaliana*. *Development* **124**: 33–44
- Martinez-Castilla LP, Alvarez-Buylla ER (2003) Adaptive evolution in the *Arabidopsis* MADS-box gene family inferred from its complete resolved phylogeny. *Proc Natl Acad Sci USA* **100**: 13407–13412
- Mitrophanov AY, Groisman EA (2008) Positive feedback in cellular control systems. *Bioessays* **30**: 542–555
- Mravec J, Skúpa P, Bailly A, Hoyerová K, Krecek P, Bielach A, Petrásek J, Zhang J, Gaykova V, Stierhof YD, Dobrev PI, Schwarzerová K, Rolcik J, Seifertová D, Luschnig C, Benková E, Zázimalová E, Geisler M, Friml J (2009) Subcellular homeostasis of phytohormone auxin is mediated by the ER-localized PIN5 transporter. *Nature* **459**: 1136–1140
- Murphy A, Taiz L (1995) A new vertical mesh transfer technique for metal-tolerance studies in *Arabidopsis*-ecotypic variation and copper-sensitive mutants. *Plant Physiol* **108**: 29–38
- Möller B, Weijers D (2009) Auxin control of embryo patterning. *Cold Spring Harb Perspect Biol* **1**: a001545 Review
- Nawy T, Lee JY, Colinas J, Wang JY, Thongrod SC, Malamy JE, Birnbaum K, Benfey PN (2005) Transcriptional profile of the *Arabidopsis* root quiescent center. *Plant Cell* **17**: 1908–1925
- Newman SA, Bhat R, Mezentseva NV (2009) Cell state switching factors and dynamical patterning modules: complementary

- mediators of plasticity in development and evolution. *J Biosci* **34**: 553–572
- Noh B, Murphy AS, Spalding EP (2001) Multidrug resistance-like genes of *Arabidopsis* required for auxin transport and auxin-mediated development. *Plant Cell* **13**: 2441–2454
- Peer WA, Murphy AS (2007) Flavonoids and auxin transport: modulators or regulators? *Trends Plant Sci* **12**: 556–563 Review
- Petersson SV, Johansson AI, Kowalczyk M, Makoveychuk A, Wang JY, Moritz T, Grebe M, Benfey PN, Sandberg G, Ljung K (2009) An auxin gradient and maximum in the *Arabidopsis* root apex shown by high-resolution cell-specific analysis of IAA distribution and synthesis. *Plant Cell* **21**: 1659–1668
- Riechmann JL, Krizek BA, Meyerowitz EM (1996) Dimerization specificity of *Arabidopsis* MADS domain homeotic proteins APETALA1, APETALA3, PISTILLATA, and AGAMOUS. *Proc Natl Acad Sci USA* **93**: 4793–4798
- Ruiz-Medrano R, Xoconostle-Cázares B, Lucas WJ (1999) Phloem long-distance transport of CmNACP mRNA: implications for supracellular regulation in plants. *Development* **126**: 4405–4419
- Ruzicka K, Simáková M, Duclercq J, Petrásek J, Zázimalová E, Simon S, Friml J, Van Montagu MC, Benková E (2009) Cytokinin regulates root meristem activity via modulation of the polar auxin transport. *Proc Natl Acad Sci USA* **106**: 4284–4289
- Sabatini S, Beis D, Wolkenfelt H, Murfett J, Guilfoyle T, Malamy J, Benfey P, Leyser O, Bechtold N, Weisbeek P, Scheres B (1999) An auxin-dependent distal organizer of pattern and polarity in the *Arabidopsis* root. *Cell* **99**: 463–472
- Sabatini S, Heidstra R, Wildwater M, Scheres B (2003) SCARECROW is involved in positioning the stem cell niche in the *Arabidopsis* root meristem. *Genes Dev* **17**: 354–358
- Sanchez MP, Gutierrez C (2009) *Arabidopsis* ORC1 is a novel PHD-containing H3K4me3 effector that regulates transcription. *Proc Natl Acad Sci USA* **106**: 2065–2070
- Sarkar AK, Luijtjen M, Miyashima S, Lenhard M, Hashimoto T, Nakajima K, Scheres B, Heidstra R, Laux T (2007) Conserved factors regulate signalling in *Arabidopsis thaliana* shoot and root stem cell organizers. *Nature* **446**: 811–814
- Tapia-López R, García-Ponce B, Dubrovsky JG, Garay-Arroyo A, Pérez-Ruiz RV, Kim SH, Acevedo F, Pelaz S, Alvarez-Buylla ER (2008) An AGAMOUS-related MADS-box gene, XAL1 (AGL12), regulates root meristem cell proliferation and flowering transition in *Arabidopsis*. *Plant Physiol* **146**: 1182–1192
- van den Berg C, Weisbeek P, Scheres B (1998) Cell fate and cell differentiation status in the *Arabidopsis* root. *Planta* **205**: 483–491
- van den Berg C, Willemse V, Hendriks G, Weisbeek P, Scheres B (1997) Short-range control of cell differentiation in the *Arabidopsis* root meristem. *Nature* **390**: 287–289
- Vanneste S, Friml J (2009) Auxin: a trigger for change in plant development. *Cell* **136**: 1005–1016 Review
- Viéte A, Vanneste S, Wisniewska J, Benková E, Benjamins R, Beeckman T, Luschnig C, Friml J (2005) Functional redundancy of PIN proteins is accompanied by auxin-dependent cross-regulation of PIN expression. *Development* **132**: 4521–4531
- Welch D, Hassan H, Blilou I, Immink R, Heidstra R, Scheres B (2007) *Arabidopsis* JACKDAW and MAGPIE zinc finger proteins delimit asymmetric cell division and stabilize tissue boundaries by restricting SHORT-ROOT action. *Genes Dev* **21**: 2196–2204
- Wisniewska J, Xu J, Seifertová D, Brewer PB, Ruzicka K, Blilou I, Rouquié D, Benková E, Scheres B, Friml J (2006) Polar PIN localization directs auxin flow in plants. *Science* **312**: 883

Apéndice 2. El factor transcripcional XAANTAL1 participa en la regulación de la proliferación y la transición a la diferenciación

The MADS-box *XAANTAL1* increases proliferation at the *Arabidopsis* root stem-cell niche and participates in transition to differentiation by regulating cell-cycle components

Karla V. García-Cruz^{1,†}, Berenice García-Ponce^{1,†}, Adriana Garay-Arroyo¹, María De La Paz Sanchez¹, Yamel Ugartechea-Chirino², Bénédicte Desvoyes³, Mario A. Pacheco-Escobedo¹, Rosalinda Tapia-López¹, Ivan Ransom-Rodríguez¹, Crisanto Gutierrez³ and Elena R. Alvarez-Buylla^{1,*}

¹Laboratorio de Genética Molecular, Epigenética, Desarrollo y Evolución de Plantas, Instituto de Ecología, Universidad Nacional Autónoma de México, Ciudad Universitaria, Av. Universidad 3000, Coyoacán, México D.F. 04510, México, ²Centro de Investigación en Dinámica Celular, Facultad de Ciencias, Universidad Autónoma de Morelos, Av. Universidad 1001, Col Chamilpa, Cuernavaca, Morelos, 62209, México and ³Centro de Biología Molecular Severo Ochoa, Consejo Superior de Investigaciones Científicas, Universidad Autónoma de Madrid, Nicolás Cabrera 1, 28049 Madrid, Spain

*For correspondence. E-mail eabuylla@gmail.com

†These authors contributed equally to this work.

Received: 15 December 2015 Returned for revision: 4 May 2016 Accepted: 16 May 2016

• **Background** Morphogenesis depends on the concerted modulation of cell proliferation and differentiation. Such modulation is dynamically adjusted in response to various external and internal signals via complex transcriptional regulatory networks that mediate between such signals and regulation of cell-cycle and cellular responses (proliferation, growth, differentiation). In plants, which are sessile, the proliferation/differentiation balance is plastically adjusted during their life cycle and transcriptional networks are important in this process. MADS-box genes are key developmental regulators in eukaryotes, but their role in cell proliferation and differentiation modulation in plants remains poorly studied.

• **Methods** We characterize the *XAL1* loss-of-function *xall-2* allele and overexpression lines using quantitative cellular and cytometry analyses to explore its role in cell cycle, proliferation, stem-cell patterning and transition to differentiation. We used quantitative PCR and cellular markers to explore if *XAL1* regulates cell-cycle components and *PLETHORA1* (*PLT1*) gene expression, as well as confocal microscopy to analyse stem-cell niche organization.

• **Key Results** We previously showed that *XAANTAL1* (*XAL1/AGL12*) is necessary for *Arabidopsis* root development as a promoter of cell proliferation in the root apical meristem. Here, we demonstrate that *XAL1* positively regulates the expression of *PLT1* and important components of the cell cycle: *CYCD3;1*, *CYCA2;3*, *CYCB1;1*, *CDKB1;1* and *CDT1a*. In addition, we show that *xall-2* mutant plants have a premature transition to differentiation with root hairs appearing closer to the root tip, while endoreplication in these plants is partially compromised. Coincidentally, the final size of cortex cells in the mutant is shorter than wild-type cells. Finally, *XAL1* overexpression-lines corroborate that this transcription factor is able to promote cell proliferation at the stem-cell niche.

• **Conclusion** *XAL1* seems to be an important component of the networks that modulate cell proliferation/differentiation transition and stem-cell proliferation during *Arabidopsis* root development; it also regulates several cell-cycle components.

Key words: MADS-box, *XAANTAL1* (*XAL1*), cell-cycle, cyclins, CDKs, endoreplication, *PLETHORA*, proliferation/differentiation, root development, *Arabidopsis thaliana*.

INTRODUCTION

Development depends on the dynamic spatio-temporal modulation of cell proliferation and differentiation during morphogenesis. When such modulation is perturbed, aberrant morphologies, such as tumours, may emerge (Dick and Rubin, 2013). In plants, tumours are rare, in comparison with in animals, probably due to the existence of plant cell walls (Sablowski and Carnier Dornelas, 2014), and also because plant morphogenesis has evolved to plastically adjust to environmental conditions, while maintaining patterns within functional limits (Lempe *et al.*, 2013). In contrast to animals, which largely

terminate development during embryogenesis, plants produce new organs during their whole life cycle. Plant growth and morphogenesis rely on two main meristems that maintain a pool of undifferentiated cells at the shoot (shoot apical meristem, SAM) and the root (root apical meristem, RAM) tips (Sarkar *et al.*, 2007; Sablowski, 2011).

The root of *Arabidopsis thaliana* (*Arabidopsis*) has become a useful system to address the molecular genetic components of the networks underlying the modulation of cell proliferation and differentiation during development (Moubayidin *et al.*, 2010). Within the root stem-cell niche (SCN), the stem or initial cells surrounding the organizer or quiescent centre (QC)

eventually give rise to the cells of the differentiated tissues of the root, which from its outermost to inner layers are: epidermis, cortex, endodermis, pericycle and vascular cylinder (van den Berg *et al.*, 1997). In addition, columella cells formed in the root apex are differentiated from the initials beneath the QC (Dolan *et al.*, 1993). As the initial cells divide, daughter cells are displaced outside the SCN where they form the proliferation domain (PD) of the RAM, in which cells attain maximum division rates (Ivanov and Dubrovsky, 2013). After several division cycles, cells start dividing at lower rates at the transition domain (TD) within the meristem, and then stop dividing and start to enlarge at the elongation zone (EZ). Progressively, at the differentiation zone (DZ), cells acquire their final size and differentiated cellular features that are characteristic of each root tissue layer (Dolan *et al.*, 1993; Dello Ioo *et al.*, 2007; Ivanov and Dubrovsky, 2013).

Cell proliferation and differentiation are modulated by transcriptional regulatory networks that integrate external and internal signals (Boye and Nordstrom, 2003; Farkas *et al.*, 2006; Slavov and Botstein, 2011). MADS-domain transcription factors have been shown to be key regulators of plant development (Alvarez-Buylla *et al.*, 2000a; Messenguy and Dubois, 2003; Smaczniak *et al.*, 2012), but their role in modulating cell proliferation and differentiation has not been fully addressed. In previous studies we showed that XAANTAL1 (*XAL1*/AGL12) and XAANTAL2 (*XAL2*/AGL14) two MADS-box factors, are necessary for normal root development and cell proliferation control (Tapia-Lopez *et al.*, 2008; Garay-Arroyo *et al.*, 2013). *xall* mutants have shorter roots than wild-type plants with fewer meristematic cells and longer cell-cycle duration, resulting in a diminished cell production rate. Moreover *xall* differentiated cells are smaller than in wild-type roots (Tapia-Lopez *et al.*, 2008).

Understanding the specific role of MADS-domain transcription factors and the networks in which they participate in the modulation of proliferation/differentiation requires exploring if they regulate cell-cycle progression. The network underlying the cell-cycle is complex and seems also to be involved in regulating the transition of cells to endoreplication cycles during cell differentiation (Vanstraelen *et al.*, 2009; Fox and Duronio, 2013; Edgar *et al.*, 2014). Cell-cycle progression is regulated by cyclin-dependent kinases (CDKs), which associate with cyclins (CYCs) that confer substrate specificity (Lim and Kaldis, 2013). Different CDK/CYC complexes act throughout the cell cycle. The CDKA/CYCD complexes trigger the G1–S phase transition. After DNA replication during G2, CDKA and CDKB associated with A- and B-type CYCs induce G2/M transition and then, at later stages of the M phase, CYCA and CYCB must be degraded by APC/C complex to exit mitosis (Menges *et al.*, 2005; Eloy *et al.*, 2011).

When RAM cells exit from the proliferative mitotic cycle to the EZ, plant cells may enter into endoreplicative cycles during which their DNA content and cell size increase as a result of DNA synthesis without mitotic cell division (Kondorosi *et al.*, 2000; Inze and De Veylder, 2006; De Veylder *et al.*, 2011; Edgar *et al.*, 2014). Endoreplication is in part induced by inhibition of the activity of mitotic CDK–CYC activity by Kip-related proteins (KRPs) or SIAMESE (SIM) proteins (Morgan, 1997; Walker *et al.*, 2000; Schnittger *et al.*, 2002; Verkest *et al.*, 2005; Boudolf *et al.*, 2009).

Here we show that *XAL1* is necessary to promote the transition to differentiation during root development as meristematic cells in the *xall*-2 mutant prematurely transit to the EZ and next to the DZ but are unable to reach the final size of wild-type cells, probably because they attain a limited number of endoreplication cycles at the TD–EZ. We also found, in accordance with our previous data in which the mutant *xall* showed a longer cell-cycle (Tapia-Lopez *et al.*, 2008), that *XAL1* positively regulates *CYCD3;1*, *CYCA2;3*, *CYCB1;1*, *CDKB1;1* and *CHROMATIN LICENSING AND DNA REPLICATION FACTOR 1* (*CDT1a*; Castellano *et al.*, 2004) expression, as well as *PLETHORAI* (*PLTI*; Aida *et al.*, 2004). *XAL1* overexpression lines show a higher number of meristematic cells. Interestingly, some plants of these lines also showed altered SCN with abnormal cell divisions under and at the QC. Hence, *XAL1* seems to be an important component of a network that underlies the modulation of cell proliferation/differentiation in root development, and is responsible for regulating some components of the mitotic and endoreplicative cycles (Ishida *et al.*, 2009). Furthermore, our results suggest that such a network is involved in both SCN maintenance and apical–basal root development zonation (proliferation, elongation and differentiation) in *Arabidopsis*. This network also involves *PLTI* (Aida *et al.*, 2004; Galinha *et al.*, 2007; Mahonen *et al.*, 2014). Alternatively, *XAL1* could be an important link between the two networks.

MATERIALS AND METHODS

Plant materials and growth conditions

The *Arabidopsis* plants used are Columbia-0 ecotype, except for the *PLTI*::GUS (Aida *et al.*, 2004) reporter line which is in WS background. Seedlings were grown on vertical plates with 0.2× Murashige Skoog (Murashige and Skoog, 1962) salts (MP Biomedicals) and 1 % sucrose, as described by Tapia-Lopez *et al.* (2008).

XAL1 overexpression lines

XAL1 cDNA was amplified from the pSR102 clone (Rounslley *et al.*, 1995) with the primers CB5F (5'-CGGATCC TCTATGGCTCGTGGAAAGATTCA-3') and CB6R (5'-CCG GATCCGCTAGAACTGAAATATTCAC-3') that include *Bam*H1 restriction sites. This DNA fragment was transferred to pGEM-T Easy (Promega, Madison, WI, USA) to generate the RT150 plasmid. After sequence confirmation the *Bam*H1 cut fragment was cloned into the pBIN-JIT plasmid. Plants were transformed via *Agrobacterium tumefaciens* by floral dipping and plants resistant to kanamycin were selected.

RNA extraction and RT-qPCR

Plants were grown for 5 d post-germination (dpg) and roots from three independent biological replicates (25 plants each) were collected. Total RNA was extracted using Trizol reagent (Invitrogen, Carlsbad, CA, USA) and it was reverse-transcribed using Superscript II (Invitrogen). We amplified *PDF2* (AT1G13320) and *UPL7* (AT1G13320) as housekeeping

control genes (Czechowski *et al.*, 2005), and their stability across the compared samples was confirmed using NormFinder (<http://moma.dk/normfinder-software>; Vandesompele *et al.*, 2002). Amplification efficiencies were analysed using real-time PCR Miner (Zhao and Fernald, 2005), and relative expression was calculated as in Perez-Ruiz *et al.* (2015). Primer sequences are included in Supplementary Data Table S1.

Microscopy

GUS-stained roots were cleared with Herr solution (Herr, 1971) and visualized by Nomarsky microscopy in an Olympus BX60. For quantification of *CYCB1;1::GUS*-stained cells, wild-type, *xall-2* and *XAL1*-OE 5.2.5 plants were grown for 1, 3, 5 and 7 dpg and 15 roots for each genotype were mounted on slides and all the spots visualized along the cortex tissue file were counted and used for further statistical analysis (Hacham *et al.*, 2011). Root meristem organization was visualized using an Olympus FV1000 confocal microscope after roots were fixed and stained using the pseudo-Schiff protocol (Napsucialy-Mendivil *et al.*, 2014).

Quantitative analysis of cellular parameters

For quantitative cellular analysis, roots were mounted in 30 % chloral hydrate and examined with Nomarsky optics. Measurements were performed according to Ivanov and Dubrovsky (1997) and Tapia-Lopez *et al.* (2008). Cell size profiles along the apical–basal axis of the root were obtained by cell size measurements along the cortex file of the root from QC to the adjacent cell of the first primordial hair cell.

Flow cytometry analysis

Arabidopsis complete roots of 1 and 3 dpg and root tips 1 cm long of 6 and 9 dpg were chopped and then incubated in Galbraith's buffer (Galbraith *et al.*, 1983). The extracts were filtered with nylon filters of 30 µm (Millipore, Billerica, MA, USA), and nuclei were stained with propidium iodide for 10 min and treated with RNAase (10 µg mL⁻¹). Finally 10000 events were measured, and DNA histograms were generated with the cytometer FACS Calibur package (Becton Dickinson, Franklin Lakes, NJ, USA).

RESULTS

XAL1 is a positive transcriptional regulator of cell-cycle components

The fact that *xall-2* mutants have fewer root meristem proliferating cells and a longer cell-cycle duration in comparison with wild-type roots (Tapia-Lopez *et al.*, 2008) suggest that *XAL1* could be a regulator of cell-cycle components. Hence we assayed mRNA levels of several cell-cycle components in *xall-2* roots in comparison with wild-type (Fig. 1A). We found that cyclin *CYCD3;1*, which participates in the G1–S transition (Menges *et al.*, 2006), as well as *CYCA2;3* and *CDKB1;1*, which participate in the G2–M transition (Doerner *et al.*, 1996; Menges *et al.*, 2003; Li *et al.*, 2005; Inze and De Veylder,

2006; Boudolf *et al.*, 2009), are significantly down-regulated in *xall-2* in comparison with wild-type roots (Fig. 1B). However, other cell-cycle components as *HISH4*, *CYCA2;1*, *CDKA* and *KRP2* are not significantly affected at their mRNA accumulation levels in the mutant background, indicating that *XAL1* regulation is specific for some of the cell-cycle components (Fig. 1B). *CDKB1;1* interacts with *CYCB1;1* to perform its activity (Weingartner *et al.*, 2004). Hence, it is not surprising that *CYCB1;1::GUS* (Colon-Carmona *et al.*, 1999) was also diminished in the *xall-2* background and up-regulated in the overexpression line (*XAL1*-OE 5.2.5), in comparison with wild-type roots (Fig. 2A; Supplementary Data Fig. S1). We also found that *CDT1a*, an essential component for the pre-replication complex during the S phase (Castellano *et al.*, 2004), was down-regulated in *xall-2* mutant compared with wild-type roots (Fig. 2B).

The transcription factors *PLT1* and *PLT2* are important for meristem function in a dose–response fashion in response to auxins regulating proliferation and endocycle onset (Aida *et al.*, 2004; Galinha *et al.*, 2007; Ishida *et al.*, 2009; Zhou *et al.*, 2011). *XAL1* is also induced by auxin (Tapia-Lopez *et al.*, 2008). Therefore, we tested if *PLT1* is altered in *xall-2* roots. We found that *PLT1::GUS* (Aida *et al.*, 2004) is down-regulated in *xall-2* roots in comparison with the wild-type (Fig. 2C), particularly at the QC and initial cells, indicating that *XAL1* is a positive regulator of *PLT1* as well.

XAL1 overexpression lines have increased cell proliferation in the root SCN

To corroborate the role of *XAL1* in the establishment of SCN (Tapia-Lopez *et al.*, 2008), we generated several *XAL1* overexpression (OE) lines under the 35S promoter. We analysed seven 100 % kanamycin-resistant OE lines and focused on two of them, *XAL1*-OE 5.2.5 and *XAL1*-OE 7.9.1, that showed high *XAL1* mRNA expression levels (Supplementary Data Fig. S2). Quantitative cellular analyses of these lines showed that *XAL1* overexpression increases the meristem size and the number of meristematic cells at 5 dpg (Fig. 3A, B). In contrast, cell production rate and the final length of cortex cells in these overexpressing lines were similar to wild-type roots (Supplementary Data Fig. S3). Interestingly, over 50 % of the plants of both OE lines showed roots with cellular pattern alterations in the SCN with increased cell divisions (Fig. 3C).

XAL1 participates in modulating the transition to cell differentiation in roots

To test if *XAL1* is involved in regulation of the cell transition from the RAM to the EZ and DZ, we analysed the distance from the QC at which root hairs, which are clear markers of differentiation (Foreman and Dolan, 2001), first appear in *XAL1* loss- and gain-of-function lines. We found that root hairs appeared at shorter distances from the QC in *xall-2* (Fig. 4A, B, D), while these appeared farther away from the QC in the *XAL1*-OE 7.9.1 line in comparison with wild-type plants (Fig. 4A, C, D). Interestingly, root hairs in the mutant are longer and in the OE line are shorter than in wild-type roots (Fig. 4A–C).

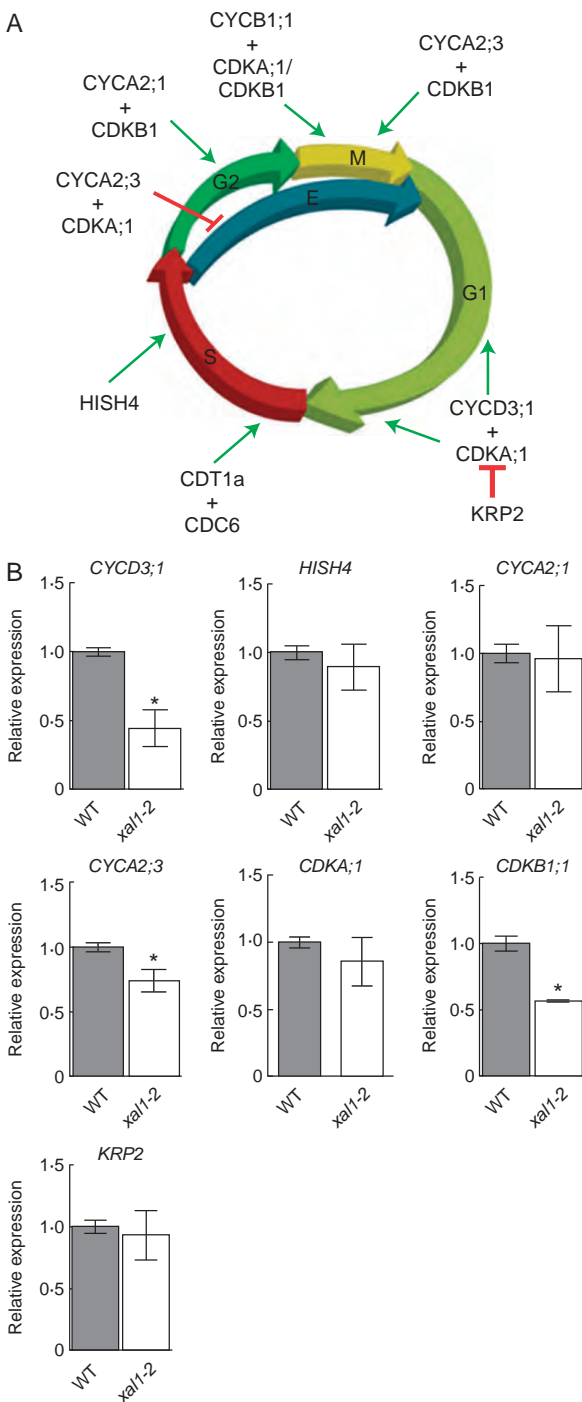


FIG. 1. XAL1 is necessary for *CYCD3;1*, *CYCA2;3* and *CDKB1;1* transcriptional regulation. (A) Schematic representation of the participation of some genes in Arabidopsis cell-cycle transitions. The *CYCD3;1/CDKA1* complex triggers G1–S phase by phosphorylation of RB-E2F pathway (not shown) and is essential for cell proliferation. This complex could be inhibited by *KRP2* depending on hormonal conditions. *CDT1a* and *CDC6* form the pre-replication complex performing in S phase. During G2 phase, cyclins *CYCA2;3*, *CYCB1;1* and *CYCB1;4* are associated with other CDK types (A or B), promoting transition to G2–M and their regulation is important for repressing the endoreplicative cycle. (B) Relative expression levels of some cell-cycle components in *xall-2* compared with wild-type (WT) roots at 5 dpg, showing that *CYCD3;1*, *CYCA2;3* and *CDKB1;1* are down-regulated in the mutant. Relative expression data are expressed as the mean \pm s.d. and statistically significant differences from WT ($*P < 0.05$) were obtained by the Kruskal–Wallis test.

In the transition between the RAM and the EZ, cells exit from the mitotic cycle and go into endoreplicative cycles (Van Straelen *et al.*, 2009). In fact, differentiated cells, such as those with already formed root hairs, show the highest levels of endoreplication in *Arabidopsis* roots (Abel *et al.*, 1995; Guimil and Dunand, 2007; Takahashi *et al.*, 2013). Hence, we hypothesized that *xall-2* roots, in which cells prematurely transit into the EZ and DZ, should also prematurely enter the endoreplication cycle. We used flow cytometry analysis to determine the ploidy levels found in *xall-2* and the *XAL1*-OE 5.2.5 line compared with wild-type complete roots at 1 and 3 dpg, and root tips (1 cm long) at 6 and 9 dpg to avoid interference caused by lateral roots at these ages (Fig. 4E). Our data showed that 16C ploidy was reduced in *xall-2* compared with wild-type roots, at 3, 6 and 9 dpg (Fig. 4E). These results suggest that the lack of *XAL1* causes diminished proportions of cells with higher ploidy levels, at the same time that it causes a premature differentiation of cells, with root hairs formed at shorter distances to the QC than in wild-type roots (Fig. 4D). Ploidy levels in the *XAL1*-OE 5.2.5 line are similar to those of wild-type roots (Fig. 4E), although in the former, root hairs appeared farther away from the QC than in wild-type roots (Fig. 4D).

We have previously reported (Tapia-Lopez *et al.*, 2008) and corroborated here (Supplementary Data Fig. S2B) that totally differentiated cells in *xall-2* roots are shorter than wild-type cells, so it is possible that in this mutant, during transition to differentiation, cells are unable to attain normal sizes due to relatively lower ploidy levels (16C) compared with wild-type roots. We measured all the cortex lineage cells from the initial to the first differentiated cell that presented a root hair in *xall-2* and wild-type roots (Fig. 4F). We found that *xall-2* cells started to elongate sooner than wild-type cells, but at the equivalent wild-type TD distance from the QC they stopped growing. These data further suggest that *xall-2* cells transit faster to the elongation and differentiation zones, in comparison with wild-type root cells, but they are unable to endoreplicate at the same rate as in wild-type roots, in correlation with the smaller sizes that they attain in comparison with cells in wild-type roots.

DISCUSSION

We had previously shown that *XAL1* is necessary for normal root growth and development by positively regulating cell proliferation rates and cell elongation, and modulating cell-cycle duration in *Arabidopsis* roots (Tapia-Lopez *et al.*, 2008). Hence, we tested here if *XAL1* regulates cell-cycle regulators.

XAL1 regulates some cell-cycle components

We found that expression levels of G1–S factors *CYCD3;1* and *CDT1a* (Menges *et al.*, 2006) and G2–M check-point factors *CYCA2;3*, *CYCB1;1* and *CDKB1;1* (Doerner *et al.*, 1996; Menges *et al.*, 2003; Li *et al.*, 2005; Inze and De Veylder, 2006; Boudolf *et al.*, 2009) are significantly diminished in *xall-2* mutant roots in comparison with wild-type (Figs 1 and 2). Also, we found that overexpression of *XAL1* results in up-regulation of *CYCB1;1::GUS* expression (Fig. 2A; Fig. S1). In agreement with these results, *xall* mutant alleles have shorter meristems with fewer meristematic cells and the *XAL1*-OE lines

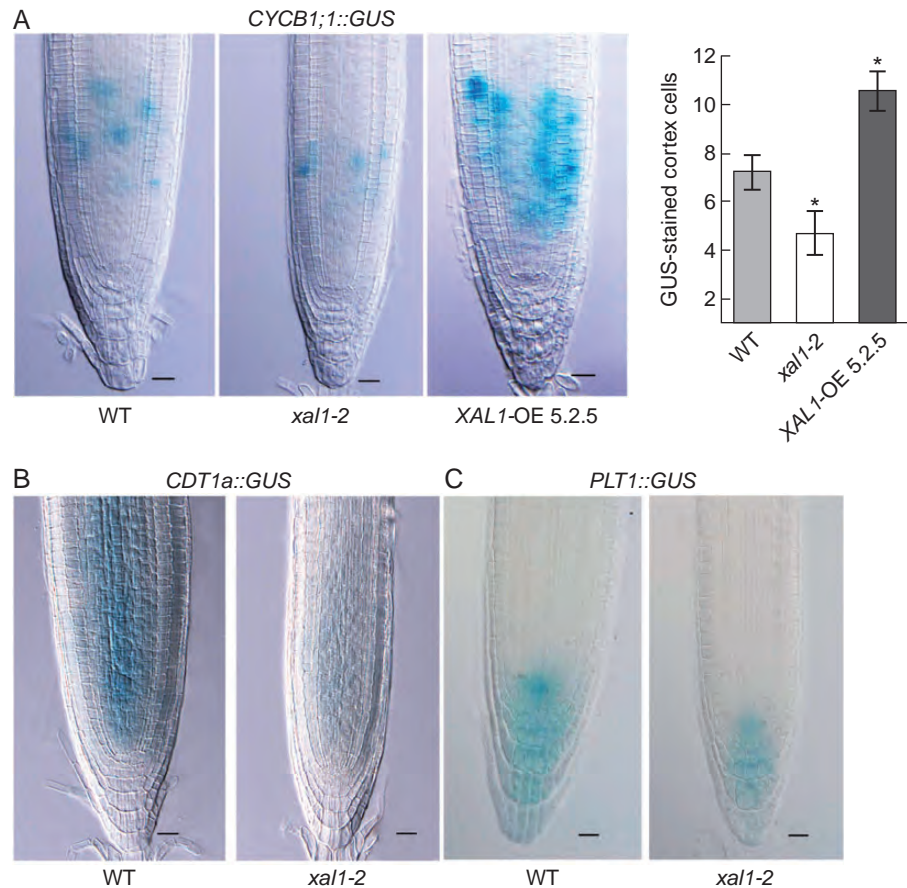


FIG. 2. XAL1 positively regulates *CYCB1*, *CDT1* and *PLT1* in the RAM. (A) Lower and higher levels of *pCYCB1;1::GUS* expression in *xal1-2* roots and *XAL1-OE 5.2.5* respectively, compared with WT. The number of GUS-stained cortex cells is shown on the right. Data correspond to mean \pm s.e. and statistically significant (*) differences from WT ($P < 0.05$) were determined with the Kruskal-Wallis test. (B, C) Expression of *pCDT1a::GUS* (B) and *PLT1::GUS* (C) is diminished in *xal1-2* roots compared with WT roots. All plants are 5 dpg, $n = 10$ per line. Scale bars = 20 μ m.

have a higher meristematic cell number than wild-type plants (Fig. 3A, B; Tapia-López *et al.*, 2008).

CYCD3;1 forms a complex with *CDKA;1* to phosphorylate RBR1, which in turn releases it from E2F transcription factors. This process regulates entry to the cell-cycle and it is required for cell-cycle transitions (Nakagami *et al.*, 1999, 2002; Uemukai *et al.*, 2005; Magyar *et al.*, 2012). The triple mutant *cyclinD3;1 cyclinD3;2 cyclinD3;3* has smaller organs with fewer cells (Dewitte *et al.*, 2007), thus confirming the role of *CYCD3* proteins in cell proliferation. Therefore, it is possible that XAL1, a MADS-box transcription factor, promotes cell proliferation by up-regulating *CDKB1;1*, *CYCB1;1*, *CYCA2;3* and *CYCD3;1* at least. Also, lower levels of *CDT1a* in *xal1-2*, a component of the pre-replication complex (Castellano *et al.*, 2004; Sanchez *et al.*, 2012), could explain the longer cell-cycle observed in *xal1* root meristem (Tapia-Lopez *et al.*, 2008).

Down-regulation of *CYCA2;3*, *CYCB1;1* and *CDKB1;1* in *xal1-2* should also favour endocycle entry (Schnittger *et al.*, 2002; Boudolf *et al.*, 2004; Sablowski and Carnier Dornelas, 2014), but as mentioned above, premature enlargement of the meristematic cells does not affect the first rounds of endoreplication. Also we did not find alterations in *KRP2* or *CDKA;1* mRNA expression levels (Fig. 1). These latter components

participate in endocycle/mitosis decisions, indicating that at least their transcriptional regulation is independent of XAL1.

Our results suggest that XAL1 regulates both cell proliferation at the meristem and endocycle maintenance during differentiation and it seems that this transcription factor is one of the interconnecting players of the networks underlying these two processes, or they are both regulated by the same network in which XAL1 participates.

MADS-domain factors seem to share some functions among all eukaryotes as suggested by the high conservation of the DNA-binding domain sequence in all lineages of the MADS-domain protein family (Alvarez-Buylla *et al.*, 2000b). In animals, MEF-related MADS-domain factors, as is XAL1, have been also identified as critical components of the mechanisms involved in cell proliferation/differentiation decisions in myoblasts by regulating E2F (Naya and Olson, 1999).

XAL1 mediates the transition to cell differentiation

We analysed cells transition from the RAM to EZ to the DZ in loss- and gain-of-function lines of *XAL1*. Cells in the *xal1-2* mutant showed premature transition to the elongation and differentiation zones, while this transition was delayed in the

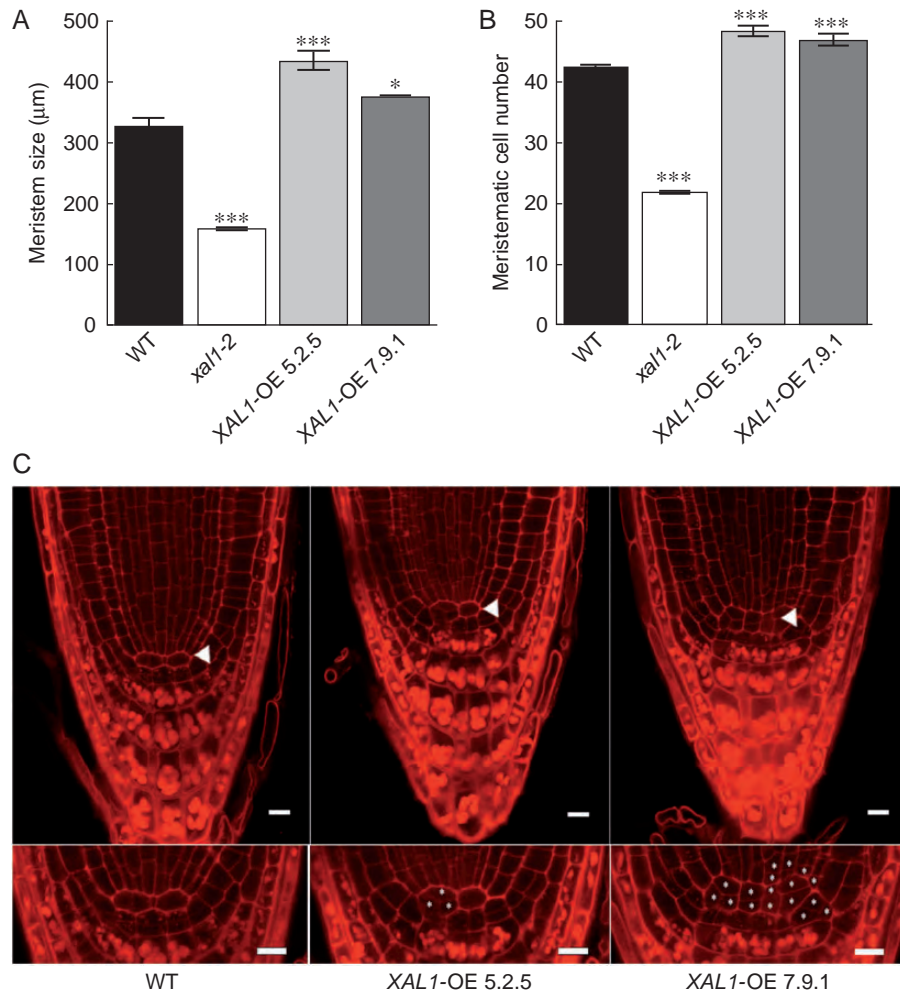


Fig. 3. Overexpression of *XAL1* is sufficient to promote root cell proliferation. (A, B) Meristem size (A) and meristematic cell number (B) are higher in the overexpression lines (*XAL1*-OE 5.2.5 and *XAL1*-OE 7.9.1) while *xal1*-2 has both parameters diminished compared with WT roots at 5 dpg. Data correspond to mean \pm s.e. Statistical significance (**P < 0.001, *P < 0.05) was obtained using the Kruskal–Wallis test (n = 30). (C) *XAL1*-overexpression increases cell divisions at the SCN. Confocal microscopy showing atypical divisions of the QC (arrowheads) and initial cells (labelled cells in the insets) in 50 % of the *XAL1*-OE 5.2.5 and 7.9.1 plants compared with WT roots. Seedlings of 3 dpg were stained with the pseudo-Schiff technique. n = 35 (WT), 20 (*XAL1*-OE 5.2.5) and 32 (*XAL1*-OE 7.9.1) plants. Scale bars = 10 μ m.

XAL1-OE lines (Fig. 4), where we found smaller and larger meristems in the *XAL1* loss- and gain-of-function lines, respectively (Fig. 3A, B). Concordantly, we found that in *xal1*-2, root cells start to elongate and differentiate at positions closer to the QC, in comparison with wild-type roots, and we observed the opposite in the *XAL1*-OE lines (Fig. 4). These results imply that *XAL1* participates in the network that underlies the correct timing at which cells transit to a differentiation state.

Some mutants with short root phenotypes that are involved in DNA replication mechanisms show smaller meristems and differentiated cells similar to *xal1*, but with overall diminished ploidy levels and an accumulation of 2–4C cells in comparison with wild-type roots (Breuer *et al.*, 2007; Dittmer *et al.*, 2007; Kirik *et al.*, 2007; Zhou *et al.*, 2011). Here we demonstrated premature and delayed transitions to differentiation in the mutant and OE lines of *XAL1*, respectively. Therefore, we expected to find a correlation with larger proportions of cells with

higher ploidy levels in the former and lower in the latter, in agreement with studies that have demonstrated that prematurely differentiated cells present higher ploidy levels in their nuclei (Perilli *et al.*, 2012). Contrary to this expectation, we found lower proportions of 16C in the *xal1* mutant and no change in ploidy levels in the OE line compared with wild-type roots (Fig. 4E), thus indicating that *XAL1* is necessary for maintaining normal high ploidy levels in the root cells but is not sufficient to alter them. It has been established that there is a correlation between cell size and high ploidy levels (Kondorosi *et al.*, 2000; Sugimoto-Shirasu and Roberts, 2003; Inze and De Veylder, 2006). Our results indicate that cells in *xal1*-2 start elongating earlier than wild-type cells and as a consequence they differentiate earlier as well, affecting their normal final size (Fig. 4F; Supplementary Data Fig. S3B). Mutants in components of the topoisomerase VI and II are unable to progress into endoreplicative cycles beyond 8C ploidy. Thus, mutants

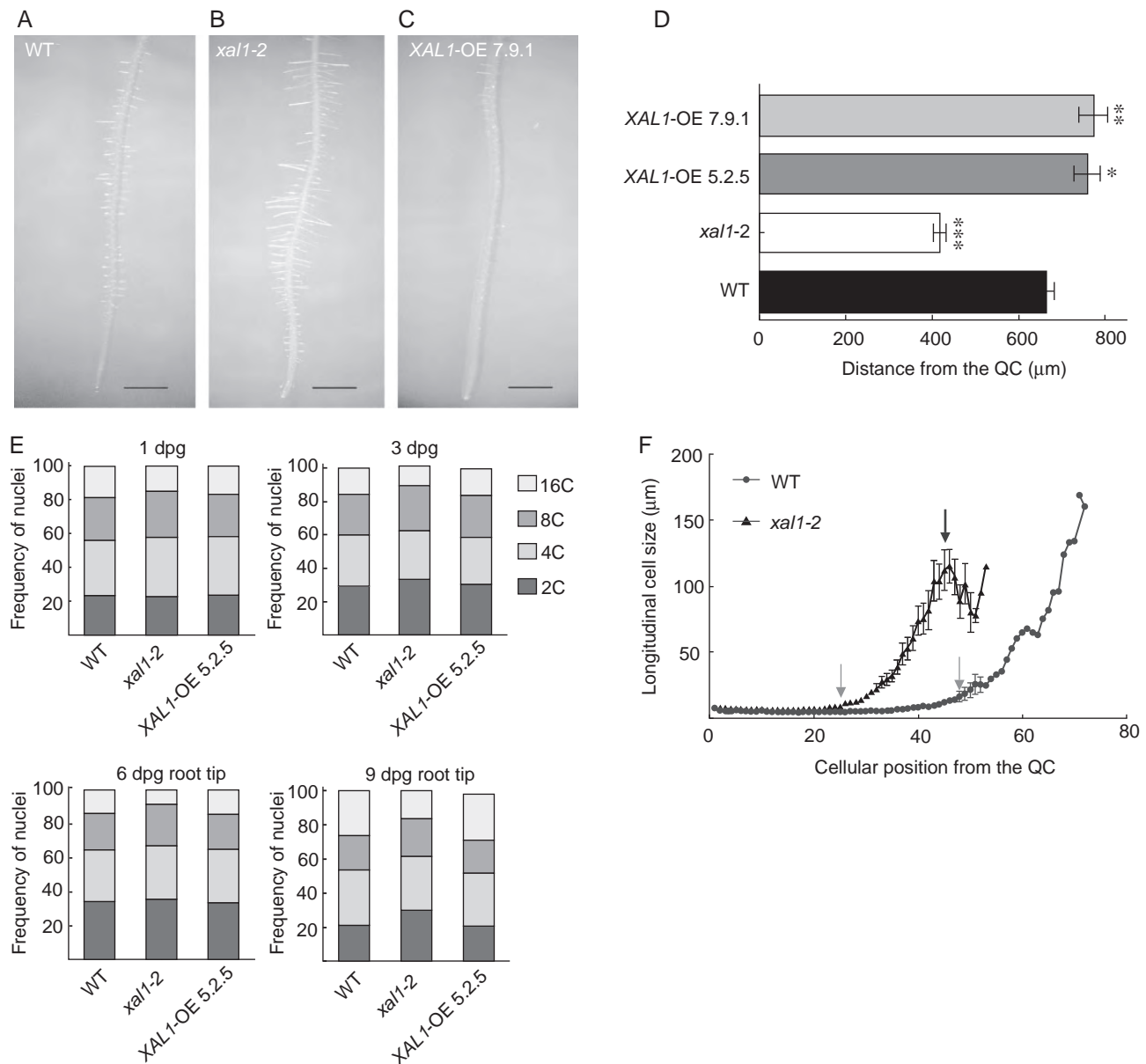


FIG. 4. XAL1 regulates cell transitions to differentiation in *Arabidopsis* root. (A–C) *xal1-2* (B) has larger root hairs and these appear at shorter distances from the root-tip, while *XAL1*-OE 7.9.1 (C) has shorter root hairs that first appear at more distant positions with respect to the QC in comparison to WT (A). Roots of 5 dpg plants. Scale bars = 1 cm. (D) Distance to the first root hair from the QC in WT, *xal1-2* and both overexpression lines, 5.2.5 and 7.9.1, in 5 dpg seedlings. Data correspond to mean \pm s.e. and statistically significant differences ($*P < 0.05$, $**P < 0.01$, $***P < 0.001$) were obtained with the Kruskal–Wallis test ($n = 15$). (E) Ploidy distribution of nuclei DNA content of WT, *xal1-2* and *XAL1*-OE 5.2.5 from 1 and 3 dpg whole roots and 6 and 9 dpg root-tips (1 cm long). (F) Cell size profiles of cortex root cells of *xal1-2* and WT roots from the QC to the first root hair in 5 dpg roots. Grey arrows show the point at which cells start to elongate, and the black arrow indicates the point at which cortex cells stop growing. The last point in the curve corresponds to the first cell that presents a root hair. Data correspond to mean \pm s.e. ($n = 20$).

such as *rhl1*, *rhl2*, *bin4* and *mid* showed very few root hairs and less developed trichomes than wild-type plants (Sugimoto-Shirasu *et al.*, 2002; Kirik *et al.*, 2007). As endoreplication and higher ploidy levels have been related to cell differentiation as in trichome cells (Walker *et al.*, 2000; Pattanaik *et al.*, 2014), it is surprising that the *xal1* mutant with low ploidy levels is able to develop root hairs that are rather longer, and not shorter, than wild-type roots. Also, it was unexpected that in the OE lines ploidy levels were not significantly different from those observed in wild-type roots, although as XAL1 is a MADS-

domain transcriptional factor it is possible that its function requires the participation of additional MADS-domain proteins. This is the case in floral organ development during which the overexpression of single MADS-domain proteins is not sufficient to cause the conversion of leaves into floral organs (Honma and Goto, 2001). Overexpression of *XAL1* is probably not sufficient to alter cell growth and endoreplication.

In conclusion, the data presented in this study suggest that XAL1 participates in the temporal pattern of cell-fate decisions, particularly during the elongation/differentiation transition,

probably by affecting endoreplication maintenance and compromising the final cell size of cortical cells (Tapia-Lopez *et al.*, 2008).

Several signals including plant hormones alter root development, particularly proliferation profiles along the root, and the rate and distance from the QC at which cells transit from the proliferation to elongation/differentiation zones are affected by auxin and cytokinin concentrations, at least (Dello Ioio *et al.*, 2007, 2008; Moubayidin *et al.*, 2010; Takahashi *et al.*, 2013). Indeed, auxins and cytokinins have been associated with all or most of these phenotypes in *Arabidopsis* root development (Dello Ioio *et al.*, 2008; Moubayidin *et al.*, 2010; Su *et al.*, 2011). The *xal1* mutant and *XAL1*-OE lines have similar phenotypes to those described above. We also know that *XAL1* is positively regulated by auxins (Tapia-Lopez *et al.*, 2008) and the *PLT1* gene is induced by *XAL1* (Fig. 2C). Hence, these hormone networks and the *XAL1* regulatory module are probably interconnected and together underlie proper root development.

XAL1 participates in cell division regulation at the SCN

The *XAL1* loss-of-function mutant (Tapia-Lopez *et al.*, 2008) and OE lines presented abnormal stem-cell proliferation (Fig. 3). Therefore, it is likely that *XAL1* is a component of the complex regulatory network that underlies stem-cell divisions in the *Arabidopsis* roots. Among other transcription factors, the *PLT* genes are important components of such a network (Azpeitia *et al.*, 2013; Davila-Velderrain *et al.*, 2014a, b). *PLTs* are necessary for stem-cell maintenance and cell division in the root (Aida *et al.*, 2004; Galinha *et al.*, 2007) and also their proteins accumulation level define the location of developmental zones (proliferation, elongation and differentiation) (Mahonen *et al.*, 2014). Interestingly, here we have shown that *XAL1* is a positive regulator of *PLT1* (Fig. 2C). *PLT1* is an AP2 transcription factor family member that regulates *CYCB1;1* transcription during root development (Aida *et al.*, 2004). *PLT1* presents nine CArG boxes in its regulatory region that suggest that *XAL1* could directly bind the *PLT1* promoter [plant *cis*-acting regulatory DNA elements (PLACE), <http://www.dna.affrc.go.jp/PLACE/>]. Interestingly, the *plt1 plt2* double mutant has reduced cell division rate in the root meristem and also shows diminished levels of *CYCB1;1::GUS* expression (Galinha *et al.*, 2007), as was found for *xal1-2*. Furthermore, in a recent genomic study that inferred regulatory networks for *Arabidopsis* root from available microarray data, we found interactions between *XAL1* and *PLT* genes (Chavez Montes *et al.*, 2014).

In conclusion, our study further documents that *XAL1* is an important component of the network underlying cell proliferation and elongation/differentiation transitions and overall cell proliferation at the root stem-cell niche. Moreover, *XAL1* participates in the maintenance of cell endoreplication. The results presented here for this MADS-box factor together with previous studies (Tapia-Lopez *et al.*, 2008; Chavez Montes *et al.*, 2014) suggest that the regulatory networks in which this, and probably other MADS-domain proteins participate, underlie all such dynamics. The role of *XAL1* in cell proliferation, cell-cycle duration, cell transition to elongation/differentiation and endocycle performance may be explained, at least in part, by its regulatory role of some relevant cell-cycle components.

SUPPLEMENTARY DATA

Supplementary information is available online at www.aob.oxfordjournal.org and consist of the following. Fig. S1: *pCYCB1;1::GUS* mitosis marker in WT, *xal1-2* and *XAL1*-OE 5.2.5 line at 1, 3 and 7 dpg. Fig. S2: *XAL1* mRNA accumulation in *XAL1*-overexpression lines. Fig. S3: Cell production rate and mature cortical cell length in *XAL1* mutant and overexpression lines. Table S1: Primer sequences used for quantitative and semi-quantitative RT-PCR.

ACKNOWLEDGEMENTS

This work constitutes a partial fulfilment of the Graduate Program ‘Doctorado en Ciencias Biomédicas’ of the Universidad Nacional Autónoma de México in which Karla V. García-Cruz developed this project. We acknowledge the Consejo Nacional de Ciencia y Tecnología (CONACYT, México) that provided her scholarship. This work was supported by CONACYT: 240180 and 180380; PAPIIT, UNAM: IN203214-3; IN203113-3; IN203814-3; IN211516 and BFU2012-34821 from MINECO (Spain) to C.G., and an institutional grant from Fundación Ramón Areces to Centro de Biología Molecular Severo Ochoa. We thank David Cruz Sánchez and Diana Romo for technical and logistical support, respectively.

LITERATURE CITED

- Abel S, Nguyen MD, Theologis A. 1995. The PS-IAA4/5-like family of early auxin-inducible mRNAs in *Arabidopsis thaliana*. *Journal of Molecular Biology* **251**: 533–549.
- Aida M, Beis D, Heidstra R, *et al.* 2004. The PLETHORA genes mediate patterning of the *Arabidopsis* root stem cell niche. *Cell* **119**: 109–120.
- Alvarez-Buylla ER, Liljeblad SJ, Pelaz S, *et al.* 2000a. MADS-box gene evolution beyond flowers: expression in pollen, endosperm, guard cells, roots and trichomes. *The Plant Journal* **24**: 457–66.
- Alvarez-Buylla ER, Pelaz S, Liljeblad SJ, *et al.* 2000b. An ancestral MADS-box gene duplication occurred before the divergence of plants and animals. *Proceedings of the National Academy of Sciences USA* **97**: 5328–33.
- Azpeitia E, Weinstein N, Benítez M, Mendoza L, Alvarez-Buylla ER. 2013. Finding missing interactions of the *Arabidopsis thaliana* root stem cell niche gene regulatory network. *Frontiers in Plant Science* **4**: 110.
- Boudolf V, Vlieghe K, Beemster GT, *et al.* 2004. The plant-specific cyclin-dependent kinase CDKB1;1 and transcription factor E2Fa-DPa control the balance of mitotically dividing and endoreduplicating cells in *Arabidopsis*. *The Plant Cell* **16**: 2683–2692.
- Boudolf V, Lammens T, Boruc J, *et al.* 2009. CDKB1;1 forms a functional complex with CYCA2;3 to suppress endocycle onset. *Plant Physiology* **150**: 1482–1493.
- Boye E, Nordstrom K. 2003. Coupling the cell cycle to cell growth. *EMBO Reports* **4**: 757–760.
- Breuer C, Stacey NJ, West CE, *et al.* 2007. BIN4, a novel component of the plant DNA topoisomerase VI complex, is required for endoreduplication in *Arabidopsis*. *Plant Cell* **19**: 3655–3668.
- Castellano MM, Boniotti MB, Caro E, Schnittger A, Gutierrez C. 2004. DNA replication licensing affects cell proliferation or endoreplication in a cell type-specific manner. *The Plant Cell* **16**: 2380–2393.
- Chavez Montes RA, Coello G, Gonzalez-Aguilera KL, Marsch-Martinez N, de Folter S, Alvarez-Buylla ER. 2014. ARACNe-based inference, using curated microarray data, of *Arabidopsis thaliana* root transcriptional regulatory networks. *BMC Plant Biology* **14**: 97.
- Colon-Carmona A, You R, Haimovich-Gal T, Doerner P. 1999. Technical advance: spatio-temporal analysis of mitotic activity with a labile cyclin-GUS fusion protein. *Plant Journal* **20**: 503–508.

- Czechowski T, Stitt M, Altmann T, Udvardi MK, Scheible WR. 2005. Genome-wide identification and testing of superior reference genes for transcript normalization in *Arabidopsis*. *Plant Physiology* 139: 5–17.
- Davila-Velderrain J, Martínez-García JC, Alvarez-Buylla ER. 2014a. Epigenetic landscape models: the post genomic era. bioRxiv 004192; doi: <http://dx.doi.org/10.1101/004192>.
- Davila-Velderrain J, Servin-Marquez A, Alvarez-Buylla ER. 2014b. Molecular evolution constraints in the floral organ specification gene regulatory network module across 18 angiosperm genomes. *Molecular Biology and Evolution* 31: 560–573.
- De Veylder L, Larkin JC, Schnittger A. 2011. Molecular control and function of endoreplication in development and physiology. *Trends in Plant Science* 16: 624–634.
- Dello Ioio R, Linhares FS, Scacchi E, et al. 2007. Cytokinins determine *Arabidopsis* root-meristem size by controlling cell differentiation. *Current Biology* 17: 678–682.
- Dello Ioio R, Nakamura K, Moubayidin L, et al. 2008. A genetic framework for the control of cell division and differentiation in the root meristem. *Science* 322: 1380–1384.
- Dewitte W, Scofield S, Alcasabas AA, et al. 2007. *Arabidopsis CYCD3 D-type cyclins link cell proliferation and endocycles and are rate-limiting for cytokinin responses*. *Proceedings of the National Academy of Sciences USA* 104: 14537–42.
- Dick FA, Rubin SM. 2013. Molecular mechanisms underlying RB protein function. *Nature Reviews Molecular Cell Biology* 14: 297–306.
- Dittmer TA, Stacey NJ, Sugimoto-Shirasu K, Richards EJ. 2007. LITTLE NUCLEI genes affecting nuclear morphology in *Arabidopsis thaliana*. *The Plant Cell* 19: 2793–2803.
- Doerner P, Jorgensen JE, You R, Steppuhn J, Lamb C. 1996. Control of root growth and development by cyclin expression. *Nature* 380: 520–523.
- Dolan L, Janmaat K, Willemse V, et al. 1993. Cellular organisation of the *Arabidopsis thaliana* root. *Development* 119: 71–84.
- Edgar BA, Zielke N, Gutierrez C. 2014. Endocycles: a recurrent evolutionary innovation for post-mitotic cell growth. *Nature Reviews Molecular Cell Biology* 15: 197–210.
- Eloy NB, de Freitas Lima M, Van Damme D, et al. 2011. The APC/C subunit 10 plays an essential role in cell proliferation during leaf development. *The Plant Journal* 68: 351–363.
- Farkas IJ, Wu C, Chennubhotla C, Bahar I, Oltvai ZN. 2006. Topological basis of signal integration in the transcriptional-regulatory network of the yeast, *Saccharomyces cerevisiae*. *BMC Bioinformatics* 7: 478.
- Foreman J, Dolan L. 2001. Root hairs as a model system for studying plant cell growth. *Annals of Botany* 88: 1–7.
- Fox DT, Duronio RJ. 2013. Endoreplication and polyploidy: insights into development and disease. *Development* 140: 3–12.
- Galbraith DW, Harkins KR, Maddox JM, Ayres NM, Sharma DP, Firoozabady E. 1983. Rapid flow cytometric analysis of the cell cycle in intact plant tissues. *Science* 3: 1049–1051.
- Galinha C, Hofhuis H, Luijten M, et al. 2007. PLETHORA proteins as dose-dependent master regulators of *Arabidopsis* root development. *Nature* 449: 1053–1057.
- Garay-Arroyo A, Ortiz-Moreno E, de la Paz Sanchez M, et al. 2013. The MADS transcription factor XAL2/AGL14 modulates auxin transport during *Arabidopsis* root development by regulating PIN expression. *EMBO Journal* 32: 2884–2895.
- Guimil S, Dunand C. 2007. Cell growth and differentiation in *Arabidopsis* epidermal cells. *Journal of Experimental Botany* 58: 3829–3840.
- Hacham Y, Holland N, Butterfield C, et al. 2011. Brassinosteroid perception in the epidermis controls root meristem size. *Development* 138: 839–848.
- Herr JM. 1971. A new clearing-squash technique for the study of ovule development in angiosperms. *American Journal of Botany* 58: 785–790.
- Honma T, Goto K. 2001. Complexes of MADS-box proteins are sufficient to convert leaves into floral organs. *Nature* 409: 525–529.
- Inze D, De Veylder L. 2006. Cell cycle regulation in plant development. *Annual Review of Genetics* 40: 77–105.
- Ishida T, Fujiwara S, Miura K, et al. 2009. SUMO E3 ligase HIGH PLOIDY2 regulates endocycle onset and meristem maintenance in *Arabidopsis*. *Plant Cell* 21: 2284–2297.
- Ivanov V, Dubrovsky J. 1997. Estimation of the cell cycle duration in the root apical meristem: model of linkage between cell-cycle, rate of cell production and rate of root growth. *International Journal of Plant Sciences* 158: 757–763.
- Ivanov VB, Dubrovsky JG. 2013. Longitudinal zonation pattern in plant roots: conflicts and solutions. *Trends in Plant Science* 18: 237–243.
- Kirik V, Schrader A, Uhrig JF, Hulskamp M. 2007. MIDGET unravels functions of the *Arabidopsis* topoisomerase VI complex in DNA endoreduplication, chromatin condensation, and transcriptional silencing. *The Plant Cell* 19: 3100–3110.
- Kondorosi E, Roudier F, Gendreau E. 2000. Plant cell-size control: growing by ploidy? *Current Opinions in Plant Biology* 3: 488–492.
- Lempe J, Lachowiec J, Sullivan AM, Queitsch C. 2013. Molecular mechanisms of robustness in plants. *Current Opinions in Plant Biology* 16: 62–69.
- Li C, Potuschak T, Colon-Carmona A, Gutierrez RA, Doerner P. 2005. *Arabidopsis TCP20 links regulation of growth and cell division control pathways*. *Proceedings of the National Academy of Sciences USA* 102: 12978–12983.
- Lim S, Kaldus P. 2013. Cdks, cyclins and CKIs: roles beyond cell cycle regulation. *Development* 140: 3079–3093.
- Magyar Z, Horvath B, Khan S, et al. 2012. *Arabidopsis E2FA stimulates proliferation and endocycle separately through RBR-bound and RBR-free complexes*. *EMBO Journal* 31: 1480–1493.
- Mahonen AP, ten Tusscher K, Siligato R, et al. 2014. PLETHORA gradient formation mechanism separates auxin responses. *Nature* 515: 125–129.
- Menges M, Hennig L, Gruissem W, Murray JA. 2003. Genome-wide gene expression in an *Arabidopsis* cell suspension. *Plant Molecular Biology* 53: 423–442.
- Menges M, de Jager SM, Gruissem W, Murray JA. 2005. Global analysis of the core cell cycle regulators of *Arabidopsis* identifies novel genes, reveals multiple and highly specific profiles of expression and provides a coherent model for plant cell cycle control. *The Plant Journal* 41: 546–566.
- Menges M, Samland AK, Planchais S, Murray JA. 2006. The D-type cyclin CYCD3;1 is limiting for the G1-to-S-phase transition in *Arabidopsis*. *The Plant Cell* 18: 893–906.
- Messenguy F, Dubois E. 2003. Role of MADS box proteins and their cofactors in combinatorial control of gene expression and cell development. *Gene* 316: 1–21.
- Morgan DO. 1997. Cyclin-dependent kinases: engines, clocks, and microprocessors. *Annual Review of Cell Development Biology* 13: 261–91.
- Moubayidin L, Perilli S, Dello Ioio R, Di Mambro R, Costantino P, Sabatini S. 2010. The rate of cell differentiation controls the *Arabidopsis* root meristem growth phase. *Current Biology* 20: 1138–1143.
- Murashige T, Skoog F. 1962. A revised medium for rapid growth and bio assays with tobacco tissue cultures. *Physiologia Plantarum* 15: 473–497.
- Nakagami H, Sekine M, Murakami H, Shinmyo A. 1999. Tobacco retinoblastoma-related protein phosphorylated by a distinct cyclin-dependent kinase complex with Cdc2/cyclin D in vitro. *The Plant Journal* 18: 243–252.
- Nakagami H, Kawamura K, Sugisaka K, Sekine M, Shinmyo A. 2002. Phosphorylation of retinoblastoma-related protein by the cyclin D/cyclin-dependent kinase complex is activated at the G1/S-phase transition in tobacco. *The Plant Cell* 14: 1847–1857.
- Napsucialy-Mendivil S, Alvarez-Venegas R, Shishkova S, Dubrovsky JG. 2014. *Arabidopsis homolog of trithorax1 (ATX1) is required for cell production, patterning, and morphogenesis in root development*. *Journal of Experimental Botany* 65: 6373–6384.
- Naya FJ, Olson E. 1999. MEF2: a transcriptional target for signaling pathways controlling skeletal muscle growth and differentiation. *Current Opinion in Cell Biology* 11: 683–688.
- Pattanaik S, Patra B, Singh SK, Yuan L. 2014. An overview of the gene regulatory network controlling trichome development in the model plant, *Arabidopsis*. *Frontiers in Plant Science* 5: 259.
- Perez-Ruiz RV, Garcia-Ponce B, Marsch-Martinez N, et al. 2015. XAANTAL2 (AGL14) is an important component of the complex gene regulatory network that underlies *Arabidopsis* shoot apical meristem transitions. *Molecular Plant* 8: 796–813.
- Perilli S, Di Mambro R, Sabatini S. 2012. Growth and development of the root apical meristem. *Current Opinions in Plant Biology* 15: 17–23.
- Rounseley SD, Ditta GS, Yanofsky MF. 1995. Diverse roles for MADS box genes in *Arabidopsis* development. *The Plant Cell* 7: 1259–1269.
- Sablowski R. 2011. Plant stem cell niches: from signalling to execution. *Current Opinions in Plant Biology* 14: 4–9.
- Sablowski R, Carnier Dornelas M. 2014. Interplay between cell growth and cell cycle in plants. *Journal of Experimental Botany* 65: 2703–2714.

- Sanchez ML, Costas C, Sequeira-Mendes J, Gutierrez C.** 2012. Regulating DNA replication in plants. *Cold Spring Harbor Perspectives in Biology* **4**: a010140.
- Sarkar AK, Luijten M, Miyashima S, et al.** 2007. Conserved factors regulate signalling in *Arabidopsis thaliana* shoot and root stem cell organizers. *Nature* **446**: 811–814.
- Schnittger A, Schobinger U, Stierhof YD, Hulskamp M.** 2002. Ectopic B-type cyclin expression induces mitotic cycles in endoreduplicating *Arabidopsis* trichomes. *Current Biology* **12**: 415–420.
- Slavov N, Botstein D.** 2011. Coupling among growth rate response, metabolic cycle, and cell division cycle in yeast. *Molecular Biology of the Cell* **22**: 1997–2009.
- Smaczniak C, Immink RG, Angenent GC, Kaufmann K.** 2012. Developmental and evolutionary diversity of plant MADS-domain factors: insights from recent studies. *Development* **139**: 3081–3098.
- Su YH, Liu YB, Zhang XS.** 2011. Auxin-cytokinin interaction regulates meristem development. *Molecular Plant* **4**: 616–625.
- Sugimoto-Shirasu K, Roberts K.** 2003. “Big it up”: endoreduplication and cell-size control in plants. *Current Opinions in Plant Biology* **6**: 544–553.
- Sugimoto-Shirasu K, Stacey NJ, Corsar J, Roberts K, McCann MC.** 2002. DNA topoisomerase VI is essential for endoreduplication in *Arabidopsis*. *Current Biology* **12**: 1782–1786.
- Takahashi N, Kajihara T, Okamura C, et al.** 2013. Cytokinins control endo-cycle onset by promoting the expression of an APC/C activator in *Arabidopsis* roots. *Current Biology* **23**: 1812–1817.
- Tapia-Lopez R, Garcia-Ponce B, Dubrovsky JG, et al.** 2008. An AGAMOUS-related MADS-box gene, XAL1 (AGL12), regulates root meristem cell proliferation and flowering transition in *Arabidopsis*. *Plant Physiology* **146**: 1182–92.
- Uemukai K, Iwakawa H, Kosugi S, et al.** 2005. Transcriptional activation of tobacco E2F is repressed by co-transfection with the retinoblastoma-related protein: cyclin D expression overcomes this repressor activity. *Plant Molecular Biology* **57**: 83–100.
- van den Berg C, Willemsen V, Hendriks G, Weisbeek P, Scheres B.** 1997. Short-range control of cell differentiation in the *Arabidopsis* root meristem. *Nature* **390**: 287–289.
- Vandesompele J, De Preter K, Pattyn F, et al.** 2002. Accurate normalization of real-time quantitative RT-PCR data by geometric averaging of multiple internal control genes. *Genome Biol* **3**: RESEARCH0034.
- Vanstraelen M, Baloban M, Da Ines O, et al.** 2009. APC/C-CCS52A complexes control meristem maintenance in the *Arabidopsis* root. *Proceedings of the National Academy of Sciences USA* **106**: 11806–11811.
- Verkest A, Manes CL, Vercruyse S, et al.** 2005. The cyclin-dependent kinase inhibitor KRP2 controls the onset of the endoreduplication cycle during *Arabidopsis* leaf development through inhibition of mitotic CDKA;1 kinase complexes. *The Plant Cell* **17**: 1723–1736.
- Walker JD, Oppenheimer DG, Concienne J, Larkin JC.** 2000. SIAMESE, a gene controlling the endoreduplication cell cycle in *Arabidopsis thaliana* trichomes. *Development* **127**: 3931–3940.
- Weingartner M, Criqui MC, Meszaros T, et al.** 2004. Expression of a nondegradable cyclin B1 affects plant development and leads to endomitosis by inhibiting the formation of a phragmoplast. *Plant Cell* **16**: 643–657.
- Zhao S, Fernald RD.** 2005. Comprehensive algorithm for quantitative real-time polymerase chain reaction. *Journal of Computational Biology* **12**: 1047–1064.
- Zhou X, Li Q, Chen X, et al.** 2011. The *Arabidopsis* RETARDED ROOT GROWTH gene encodes a mitochondria-localized protein that is required for cell division in the root meristem. *Plant Physiology* **157**: 1793–1804.

Apéndice 3. Análisis de perfiles de longitudes celulares en lenguaje R

Instrucciones para analizar un perfil de longitudes celulares a través del paquete 'strucchange' con un ejemplo. Es necesario instalar el paquete desde el repositorio de R la primera vez que se usa. Los comentarios dentro del código están precedidos por el signo #.

```
1 install.packages("strucchange")
2 # Una vez instalado se carga y está listo para usarse
3 library(strucchange)
4 # A continuación muestro un ejemplos de cómo calcular el número
5 # óptimo de transiciones , su respectiva posición y sendos intervalos
6 # del 95 % de confianza . Se muestra también cómo calcular los tamaños críticos
7
8 # Se declara un perfil de longitudes celulares
9
10 wt.9DAS.4<-c(7.32,8.87,9.36,8.34,5.18,5.45,5.60,4.44,6.71,6.71,6.84,6.88,4.28,4.55,
11 3.93,4.41,3.80,4.07,3.93,4.07,7.87,6.71,7.82,5.81,4.34,3.95,5.98,7.02,6.35,4.87,4.36,
12 4.14,4.60,5.05,3.93,3.71,4.36,7.19,7.84,7.84,8.28,6.97,7.41,7.20,6.76,6.97,8.71,8.93,
13 9.15,7.84,6.54,6.75,6.75,8.28,8.06,13.29,16.12,16.77,17.00,14.16,15.90,18.98,17.87,
14 23.97,28.57,27.94,25.82,37.29,40.03,44.55,45.76,52.88,64.97,130.16,99.90,106.07,
15 103.62,99.61,114.69,91.06)
16
17 # Se declara un vector con las posiciones de las células del perfil analizado
18 # La posición cero corresponde al CQ
```

```
19  
20 x1 <- seq(0,length(wt.9DAS.4)-1)  
21  
22 # Con la función 'breakpoints' se crea el modelo de múltiple cambio estructural  
23 # usando como parámetros el perfil de longitudes y el vector de posiciones  
24 # Se guarda en el objeto 'modelo' y se llama a éste para ver los resultados  
25  
26 modelo<-breakpoints(wt.9DAS.4~x1)  
27 modelo  
28  
29 # Para observar cómo se determinó el número óptimo de transiciones a partir del  
30 # criterio de información Bayesiana  
31  
32 plot(modelo)  
33  
34 # Para el caso de este perfil el número óptimo de transiciones es uno  
35 # El intervalo de confianza de la posición se puede calcular con 'confint'  
36  
37 confint(modelo)  
38  
39 # En caso de que se desee calcular dos transiciones para este perfil  
40 # creamos y llamamos un nuevo modelo a partir del ya creado  
41  
42 modelo_2<-breakpoints(modelo, breaks=2)  
43 modelo_2  
44  
45 # Para calcular los tamaños críticos simplemente usamos la función 'breakpoints'  
46 # pero ordenando de menor a mayor el perfil de longitudes celulares  
47 # guardamos este perfil ordenado en un nuevo objeto llamado 's1'  
48  
49 s1 <-sort(wt.9DAS.4)  
50
```

```
51 # Creamos un modelo MCE para el perfil ordenado
52 # Dado que es el mismo número de células , se puede usar el mismo
53 # vector de posiciones 'x1'
54
55 model_s1 <- breakpoints(s1~x1)
56 model_s1
57
58 # Este modelo del perfil ordenado tiene dos transiciones en las posiciones 54 y 68
59 # Se usa la primera transición para calcular el tamaño crítico de división
60 # Se calcula un modelo lineal para las longitudes ordenadas de las células del
61 # dominio de proliferación
62
63 lmd1 <- lm(s1[1:55]~x1[1:55])
64 lmd1
65
66 # Usamos los coeficientes calculados (intercept = 3.41, x1 = 0.1)
67 # para interpolar en la posición 54 el tamaño crítico de división
68
69 lcritD1 <- 0.1*54 + 3.4
70 lcritD1
71
72 # Ahora usamos la segunda transición del modelo MCE para calcular
73 # el tamaño crítico de inicio del alargamiento rápido
74
75 # Se calcula el modelo lineal para las longitudes ordenadas del dominio
76 # de transición
77
78 lme1 <- lm(s1[56:69]~x1[56:69])
79 lme1
80
81 # Usamos los coeficientes calculados (intercept = -94.7, x1=1.9)
82 # para calcular el tamaño crítico de inicio del alargamiento rápido
```

```
83 # interpolamos en la posición 68  
84  
85 lcritE1 <- 1.9*68 - 94.7  
86 lcritE1
```

Apéndice 4. Análisis de perfiles de longitudes celulares en lenguaje PHP

A continuación presento el código de un sitio web público disponible en www.ibiologia.com.mx/MSA_analysis que obtiene modelos MCE para perfiles de longitudes celulares. Primero un documento básico HTML que sirve para que el usuario introduzca sus datos e indique si desea analizar el perfil calculando uno o dos límites.

```
1  <!DOCTYPE HTML PUBLIC> <html lang= "en">
2  <head>
3  <meta charset="utf-8">
4  <title> MSC analysis for roots</title>
5  </head>
6  <body>
7  Cell lengths: <br>
8  <textarea rows="10" cols="120" name="double" value= "<?php echo $double;?>">
9  </textarea>
10 <br>
11 <input type="submit" value= "One breakpoint analysis" name="one">
12 <input type="submit" value= "Two breakpoints analysis" name="two">
13 </body>
14
15 </html>
```

Una vez que se introducen los datos y se indica que tipo de análisis se desea hacer, el siguiente código PHP realiza los cálculos para determinar la posición de las transiciones entre las diferentes regiones del perfil de longitudes celulares introducido. Además, se calculan los parámetros de las ecuaciones lineales correspondientes

a cada región del perfil, el tamaño crítico de inicio de la división celular (LCritD) y el tamaño crítico de inicio del alargamiento rápido (LCritE). Este código no calcula los intervalos de confianza para las posiciones de las transiciones ni el número óptimo de transiciones por el criterio de información Bayesiana, para calcular estos es necesario recurrir al paquete *strucchange* de R (Zeileis *et al.*, 2002).

```
1 <?php
2
3 function independent ( $cells ){
4 $independent = range(0, count($cells) -1);
5 return $independent; }
6
7
8 function LSM( $cells , $positions ){
9 $numero = count($cells);
10 $mediay = array_sum($cells) / $numero;
11 $mediax = array_sum($positions) / $numero;
12 $dify = array();
13 $difx = array();
14 for($i = 0; $i <= $numero; $i++){
15 $ly = $cells[$i] - $mediay;
16 $lx = $positions[$i] - $mediax;
17 array_push($dify , $ly );
18 array_push($difx , $lx ); }
19 $mult = array();
20 $cuad = array();
21 for($i = 0; $i <= $numero ; $i++){
22 $difmul = $difx[$i] * $dify[$i];
23 $difpow = pow($difx[$i], 2);
24 array_push($mult , $difmul);
25 array_push($cuad , $difpow); }
26
27 $numerador = array_sum($mult);
28 $denominador = array_sum($cuad);
```

```
29 $pendiente = $numerador / $denominador;
30 $intersection = $mediay - ($pendiente * $mediamx);
31
32
33 $predicts = array();
34 for($i = 0; $i <= $numero ; $i++){
35 $teorico = $intersection + ($pendiente * $positions[$i]);
36 array_push($predicts , $teorico );
37 }
38 $residuals = array();
39 for($i = 0; $i <= $numero ;
40 $i++){ $residuo = $predicts[$i] - $cells[$i];
41 $resquar = pow($residuo , 2);
42 array_push($residuals , $resquar );
43 }
44 return array_sum($residuals );
45 }
46
47
48 function lsmO ($cells , $positions){
49 $numero = count($cells); $mediay = array_sum($cells) / $numero;
50 $mediamx = array_sum($positions) / $numero;
51 $dify = array(); $difx = array();
52 for($i = 0; $i <= $numero; $i++){
53 $difcells = $cells[$i] - $mediay;
54 $difpos = $positions[$i] - $mediamx;
55 array_push($dify , $difcells );
56 array_push($difx , $difpos ); }
57
58 $mult = array();
59 $cuad = array();
60 for($i = 0; $i <= $numero-2 ; $i++){
```

```
61 $prod = $difx[$i] * $dify[$i];
62 $potencia = pow($difx[$i], 2);
63 array_push($mult, $prod);
64 array_push($cuad, $potencia); }

65

66 $numerador = array_sum($mult);
67 $denominador = array_sum($cuad);
68 $pendiente = $numerador /$denominador;
69 $intersection = $mediay - ($pendiente * $mediamx);
70 $resultado = array($pendiente, $intersection);
71 return $resultado;
72 }

73 function leftResiduals ($cells, $positions){
74 $residualsLeft = array();
75 for($i = 2; $i <= count($cells) - 2; $i++){
76 $hResidual = LSM(array_slice($cells, 0, $i), array_slice($positions, 0, $i));
77 array_push($residualsLeft, $hResidual);
78 }
79 return $residualsLeft;
80 }

81 function rightResiduals($cells, $positions){
82 $residualsRight = array();
83 for($i = 2; $i <= count($cells) - 2; $i++){
84 $hresidual= LSM(array_slice($cells, $i, count($cells) - $i),
85 array_slice($positions, $i, count($positions) - $i));
86 array_push($residualsRight, $hresidual);
87 }
88 return $residualsRight;
89 }

90

91 function sumaDobleResiduales($cells, $positions){
92 $izquierda = leftResiduals($cells, $positions);
```

```
93 $derecha = rightResiduals($cells, $positions);
94 $sumaDobleR = array();
95 for($i = 0; $i <= count($izquierda) - 1; $i++){
96 $resi = array($izquierda[$i] + $derecha[$i]);
97 array_push($sumaDobleR, array_sum($resi));
98 }
99 return $sumaDobleR;
100 }
101
102 function limite($cells){
103 $positions = independent($cells);
104 $suma = sumaDobleResiduales($cells, $positions);
105 $minimum = min($suma);
106 $i = 0; $fin = count($cells);
107
108 while ($i < $fin) {
109 if($suma[$i] == $minimum){
110 $i = $i + 2; break;
111 } else{ $i++; }
112 }
113 $reslimite = array($minimum, $i-1); return $reslimite;
114 }
115
116 function tres_residuales($cells){
117 $postotal = independent($cells);
118 $residualGlobal= array();
119 $EZresidual = array();
120 for($l = 8; $l <= count($cells) -2; $l++){
121 $residuales_derecha = LSM(array_slice($cells, $l, count($cells)-$l),
122 array_slice($postotal, $l, count($postotal)-$l));
123 array_push($EZresidual, $residuales_derecha);
124 }
```

```
125 $tdpositions = array(); $RAMresiduales = array();  
126 for($l = 8; $l <=count($cells)-2; $l++){  
127 $resLimites = limite(array_slice($cells, 0, $l));  
128 array_push($RAMresiduales, $resLimites[0]);  
129 array_push($tdpositions, $resLimites[1]); }  
130  
131 for($m = 0; $m <=count($EZresidual) -1; $m++){  
132 $sumaTriple = array($RAMresiduales[$m] + $EZresidual[$m]);  
133 array_push($residualGlobal, array_sum($sumaTriple)); }  
134  
135 $minimoTotal = min($residualGlobal);  
136 $n = 0; $fin = count($residualGlobal);  
137  
138 while ($n < $fin) {  
139 if($residualGlobal[$n] == $minimoTotal){  
140 break; }  
141 else{ $n++; }  
142 }  
143  
144 $tzGlobal = $n + 8;  
145 $tdGlobal = $tdpositions[$n];  
146 $posicionLimites = array($tdGlobal-1, $tzGlobal-1);  
147 return $posicionLimites;  
148 }  
149  
150 function td($cells){  
151 $tz = limite($cells);  
152 $ram = array_slice($cells, 0, $tz);  
153 $td = limite($ram)+1;  
154 $limites = array($td, $tz);  
155 return $limites;  
156 }
```

```
157
158 function limiteO ($cells){
159 $ordenado = $cells;
160 sort($ordenado);
161 return limite($ordenado);
162 }
163
164 function tdOrdenado($cells){
165 $ordenado = $cells;
166 sort($ordenado);
167 return td($ordenado);
168 }
169
170 function MSC ($cells){
171 $ordenado = $cells;
172 sort($ordenado);
173 $MSC_simple = tres_residuales($cells);
174 $MSC_ordenado = tres_residuales($ordenado);
175 $pdSize = array_sum(array_slice($cells, 0, $MSC_simple[0]));
176 $ramSize = array_sum(array_slice($cells, 0, $MSC_simple[1]));
177 $tdSize = $ramSize - $pdSize;
178 $ezSize = array_sum($cells) - $ramSize;
179 $PD = lsmO(array_slice($cells, 0, $MSC_simple[0]),
180 array_slice(independent($cells), 0, $MSC_simple[0]));
181 $TD = lsmO(array_slice($cells, $MSC_simple[0],
182 $MSC_simple[1] - $MSC_simple[0]), array_slice(independent($cells),
183 $MSC_simple[0], $MSC_simple[1] - $MSC_simple[0]));
184 $EZ = lsmO(array_slice($cells, $MSC_simple[1],
185 count($cells) - $MSC_simple[1]),
186 array_slice(independent($cells), $MSC_simple[1],
187 count($cells) - $MSC_simple[1]));
188
```

```
189 $PDo = lsm0(array_slice($ordenado, 0, $MSC_ordenado[0]),  
190 array_slice(independent($ordenado), 0, $MSC_ordenado[0]));  
191 $TDo = lsm0(array_slice($ordenado, $MSC_ordenado[0],  
192 $MSC_ordenado[1] - $MSC_ordenado[0]), array_slice(independent($ordenado),  
193 $MSC_ordenado[0], $MSC_ordenado[1] - $MSC_ordenado[0]));  
194 $criticalSize = $PDo[1] +($PDo[0]*($MSC_ordenado[0]-1));  
195 $elongationSize = $TDo[1] +($TDo[0]*($MSC_ordenado[1]-1));  
196  
197  
198 echo "Number of Proliferation Domain cells = ". $MSC_simple[0];  
199 echo "<br/>";  
200 echo "<br/>"; echo "Number of RAM cells = ". $MSC_simple[1] ;  
201 echo "<br/>";  
202 echo "<br/>"; echo "Proliferation Domain size = ". round($pdSize,0) ;  
203 echo "<br/>";  
204 echo "<br/>"; echo "Transition Domain size = ". round($tdSize,0) ;  
205 echo "<br/>";  
206 echo "<br/>"; echo "RAM size = ".round($ramSize,0); echo "<br/>";  
207 echo "<br/>"; echo "Elongation zone size = ".round($ezSize,0) ;  
208 echo "<br/>";  
209 echo "<br/>"; echo "Proliferation Domain y-intercept = ". round($PD[1],0) ;  
210 echo "<br/>";  
211 echo "<br/>"; echo "Proliferation Domain slope = ". round($PD[0],0);  
212 echo "<br/>";  
213 echo "<br/>"; echo "Transition Domain slope = ". round($TD[0],0);  
214 echo "<br/>";  
215 echo "<br/>"; echo "Elongation zone slope = ". round($EZ[0],0);  
216 echo "<br/>";  
217 echo "<br/>"; echo "Critical size of dividing cells = ". round($criticalSize,0) ;  
218 echo "<br/>";  
219 echo "<br/>"; echo "Critical size of transition  
to elongation = ". round($elongationSize,0) ;
```

```
221 echo "<br />";  
222 echo "<br />"; echo "Rank of Critical size  
223 of dividing cells = ".$MSC_ordenado[0];  
224 echo "<br />";  
225 echo "<br />"; echo "Rank of critical size of  
226 transition to elongation = ".$MSC_ordenado[1];  
227 echo "<br />";  
228 }  
229  
230 if(isset($_POST['one'])) { $cambio = $_POST['double'];  
231 $celulas = explode(',', $cambio);  
232 echo "<h2>Results for one breakpoint:</h2>"; echo "<br />";  
233 $Numpd = limite($celulas);  
234 echo "Number of Proliferation domain cells = ". $Numpd[1]; echo "<br />";  
235 echo "<br />";  
236 $RamS = array_slice($celulas, 0, $Numpd[1]); $sizeRamS = array_sum($RamS);  
237 echo "Proliferation domain size = ".round($sizeRamS,0); echo "<br />";  
238 echo "<br />";  
239 $Numtd = count($celulas) - $Numpd[1];  
240 echo "Number of transition domain cells = ". $Numtd; echo "<br />";  
241 echo "<br />";  
242 $sizeTD = array_sum($celulas)-$sizeRamS;  
243 echo "Transition domain size: ". round($sizeTD,0); echo "<br />";  
244 echo "<br />";  
245 echo "RAM size: ". round($sizeRamS + $sizeTD,0); echo "<br />";  
246 echo "<br />";  
247 $num = independent($celulas);  
248 $posRam = array_slice($num, 0, $Numpd[1]);  
249 $PDmodel= lsrn($RamS, $posRam);  
250 echo "Proliferation domain y-intercept = ". round($PDmodel[1],0); echo "<br />";  
251 echo "<br />";  
252 echo "Proliferation domain slope = ". round($PDmodel[0],0); echo "<br />";
```

```
253 echo "<br />";  
254 $tdcells = array_slice($celulas, $Numpd[1], count($celulas) - $Numpd[1]);  
255 $tdpositions = array_slice($num, $Numpd[1], count($num) - $Numpd[1]);  
256 $tdmodel = IsMO($tdcells, $tdpositions);  
257 echo "Transition domain slope = ". round($tdmodel[0], 0); echo "<br />";  
258 echo "<br />";  
259 $ramOrdenado = $celulas; sort($ramOrdenado);  
260 $rankCritDiv = limite($ramOrdenado);  
261 echo "Rank of critical size of dividing cells = ". $rankCritDiv[1]; echo "<br />";  
262 echo "<br />";  
263 $prolifLengths = array_slice($ramOrdenado, 0, $rankCritDiv[1]);  
264 $posProlifLengths = array_slice($num, 0, $rankCritDiv[1]);  
265 $modelCritDiv = IsMO($prolifLengths, $posProlifLengths);  
266 $criticalSize = $modelCritDiv[1] +($modelCritDiv[0]*($rankCritDiv[1]-1));  
267 echo "Critical size of dividing cells = ". round($criticalSize, 0); echo "<br />";  
268 echo "<br />";  
269 }  
270  
271  
272 if(isset($_POST['two'])) {  
273 $cambio = $_POST['double'];  
274 echo "<br />"; echo "<h2>Results for two breakpoints:</h2>"; echo "<br />";  
275 $celulas = explode(',', $cambio);  
276 MSC($celulas);  
277 }  
278 ?>
```

Apéndice 5. Análisis cuantitativo de raíces *Arabidopsis*, ecotipo C24

Cuadro A3: Análisis cuantitativo de raíces de *Arabidopsis* C24 tipo silvestre a los 15 días después de la germinación por modelos MCE, ($n = 12$).

	Media (d.t)	I.C 95 %
Número de células DP	42 (10)	[35, 48]
Número de células RAM	53 (12)	[46, 60]
Longitud DP (μm)	280 (61)	[241, 319]
Longitud DT (μm)	215 (55)	[180, 250]
Longitud RAM (μm)	495 (102)	[430, 560]
Pendiente DP ($\mu\text{m}/\text{posición celular}$)	0	0
Pendiente DT ($\mu\text{m}/\text{posición celular}$)	2.0 (1.2)	[1.2, 2.8]
Pendiente ZA ($\mu\text{m}/\text{posición celular}$)	11 (5)	[8, 14]
LCritD (μm)	9.4 (1.2)	[8.6, 10.2]
LCritA (μm)	29 (7)	[24, 33]

Bibliografía

- ALVAREZ-BUYLLA, E.R., LILJEGREN, S.J., PELAZ, S., GOLD, S.E., BURGEFF, C., DITTA, G.S., VERGARA-SILVA, F., Y YANOFSKY, M.F. MADS-box gene evolution beyond flowers: expression in pollen, endosperm, guard cells, roots and trichomes. *Plant J.* **24**(4):457–66 (2000)
- ALVAREZ-BUYLLA, E.R., BENÍTEZ, M., CORVERA-POIRÉ, A., CHAOS CADOR, A., DE FOLTER, S., GAMBOA DE BUEN, A., GARAY-ARROYO, A., GARCÍA-PONCE, B., JAIMES-MIRANDA, F., PÉREZ-RUIZ, R.V., PIÑEYRO-NELSON, A., Y SÁNCHEZ-CORRALES, Y.E. Flower development. *Arabidopsis Book* **8**(1):e0127 (2010)
- BAI, J. Estimation of a Change Point in Multiple Regression Models. *Rev. Econ. Stat.* **79**(4):551–563 (1997)
- BAI, J. Y PERRON, P. Computation and analysis of multiple structural change models. *J. Appl. Econom.* **18**(1):1–22 (2003)
- BALUŠKA, F. Y MANCUSO, S. Root apex transition zone as oscillatory zone. *Front. Plant Sci.* **4**(October):354 (2013)
- BALUŠKA, F., MANCUSO, S., VOLKMANN, D., Y BARLOW, P.W. Root apex transition zone: A signalling-response nexus in the root (2010)
- BEEMSTER, G.T. Y BASKIN, T.I. Analysis of cell division and elongation underlying the developmental acceleration of root growth in *Arabidopsis thaliana*. *Plant Physiol.* **116**(4):1515–26 (1998)
- BELLMAN, R. Y ROTH, R. Curve Fitting by Segmented Straight Lines. *J. Am. Stat. Assoc.* **64**(327):1079–1084 (1969)
- BERG, C.V.D., WILLEMSSEN, V., HENDRICKS, G., WEISBEECK, P., Y SCHERES, B. Short-range control of cell differentiation in the *Arabidopsis* root meristem. *Nature* págs. 287–289 (1997)
- BOWMAN, J.L., SMYTH, D.R., Y MEYEROWITZ, E.M. Genes directing flower development in *Arabidopsis*. *Plant Cell* **1**(1):37–52 (1989)

- BOWMAN, J.L., SMYTH, D.R., Y MEYEROWITZ, E.M. Genetic interactions among floral homeotic genes of *Arabidopsis*. *Development* **112**(1):1–20 (1991)
- BURGEFF, C., LILJEGREN, S.J., TAPIA-LÓPEZ, R., YANOFSKY, M.F., Y ALVAREZ-BUYLLA, E.R. MADS-box gene expression in lateral primordia, meristems and differentiated tissues of *Arabidopsis thaliana* roots. *Planta* **214**(3):365–72 (2002)
- CASAMITJANA-MARTÍNEZ, E., HOFHUIS, H.F., XU, J., LIU, C.M., HEIDSTRA, R., Y SCHERES, B. Root-specific CLE19 overexpression and the *sotl/2* suppressors implicate a CLV-like pathway in the control of *Arabidopsis* root meristem maintenance. *Curr. Biol.* **13**(16):1435–1441 (2003)
- CLOWES, F.A.L. NUCLEIC ACIDS IN ROOT APICAL MERISTEMS OF *ZEA*. *New Phytol.* **55**(1):29–34 (1956)
- COEN, E.S. Y MEYEROWITZ, E.M. The war of the whorls: genetic interactions controlling flower development. *Nature* **353**(6339):31–37 (1991)
- DE FOLTER, S., IMMINK, R.G.H., KIEFFER, M., PARENICOVÁ, L., HENZ, S.R., WEIGEL, D., BUSSCHER, M., KOOIKER, M., COLOMBO, L., KATER, M.M., DAVIES, B., Y ANGENENT, G.C. Comprehensive interaction map of the *Arabidopsis* MADS Box transcription factors. *Plant Cell* **17**(5):1424–33 (2005)
- DELLO IOIO, R., LINHARES, F.S., SCACCHI, E., CASAMITJANA-MARTINEZ, E., HEIDSTRA, R., COSTANTINO, P., Y SABATINI, S. Cytokinins determine *Arabidopsis* root-meristem size by controlling cell differentiation. *Curr. Biol.* **17**(8):678–82 (2007)
- DOBROCHAEV, A.E. Y IVANOV, V.B. Variations in the size of mitotic cells in the root meristem. *Ontogenet.* **32**(4):252–62 (2001)
- DOLAN, L., JANMAAT, K., WILLEMSSEN, V., LINSTEAD, P., POETHIG, S., ROBERTS, K., Y SCHERES, B. Cellular organisation of the *Arabidopsis thaliana* root. *Development* **119**:71–84 (1993)
- DOLZNIG, H., GREBIEN, F., SAUER, T., BEUG, H., Y MÜLLNER, E.W. Evidence for a size-sensing mechanism in animal cells. *Nat. Cell Biol.* **6**(9):899–905 (2004)
- DUBROVSKY, J., CONTRERAS-BURCIAGA, L., Y IVANOV, V.B. Cell cycle duration in the root meristem of Sonoran Desert Cactaceae as estimated by cell-flow and rate-of-cell-production methods. *Ann. Bot.* **81**:619–624 (1998a)
- DUBROVSKY, J.G., NORTH, G.B., Y NOBEL, P.S. Root growth, developmental changes in the apex, and hydraulic conductivity for *Opuntia ficus-indica* during drought. *New Phytol.* **138**(1):75–82 (1998b)

- EGEA-CORTINES, M., SAEDLER, H., Y SOMMER, H. Ternary complex formation between the MADS-box proteins SQUAMOSA, DEFICIENS and GLOBOSA is involved in the control of floral architecture in *Antirrhinum majus*. *EMBO J.* **18**(19):5370–5379 (1999)
- FRENCH, A.P., WILSON, M.H., KENOBI, K., DIETRICH, D., VOSS, U., UBEDA-TOMÁS, S., PRIDMORE, T.P., Y WELLS, D.M. Identifying biological landmarks using a novel cell measuring image analysis tool: Cell-o-Tape. *Plant Methods* **8**(1):7 (2012)
- GALINHA, C., HOFHUIS, H., LUIJTEN, M., WILLEMSSEN, V., BLILOU, I., HEIDSTRA, R., Y SCHERES, B. PLETHORA proteins as dose-dependent master regulators of *Arabidopsis* root development. *Nature* **449**(7165):1053–7 (2007)
- GALINHA, C., BILSBOROUGH, G., Y TSANTIS, M. Hormonal input in plant meristems: A balancing act. *Semin. Cell Dev. Biol.* **20**(9):1149–56 (2009)
- GAN, Y., FILLEUR, S., RAHMAN, A., GOTENSPARRE, S., Y FORDE, B.G. Nutritional regulation of ANR1 and other root-expressed MADS-box genes in *Arabidopsis thaliana*. *Planta* **222**(4):730–42 (2005)
- GARAY-ARROYO, A., DE LA PAZ SÁNCHEZ, M., GARCÍA-PONCE, B., AZPEITIA, E., Y ÁLVAREZ-BUYLLA, E.R. Hormone symphony during root growth and development. *Dev. Dyn.* **241**(12):1867–1885 (2012)
- GARAY-ARROYO, A., ORTIZ-MORENO, E., DE LA PAZ SÁNCHEZ, M., MURPHY, A.S., GARCÍA-PONCE, B., MARSCH-MARTÍNEZ, N., DE FOLTER, S., CORVERA-POIRÉ, A., JAIMES-MIRANDA, F., PACHECO-ESCOBEDO, M.A., DUBROVSKY, J.G., PELAZ, S., Y ALVAREZ-BUYLLA, E.R. The MADS transcription factor XAL2/AGL14 modulates auxin transport during *Arabidopsis* root development by regulating PIN expression. *EMBO J.* **32**:2884–95 (2013)
- GARCÍA-CRUZ, K.V., GARCÍA-PONCE, B., GARAY-ARROYO, A., SÁNCHEZ, M.D.L.P., UGARTECHEA-CHIRINO, Y., DESVOYES, B., PACHECO-ESCOBEDO, M.A., TAPIA-LÓPEZ, R., RANSOM-RODRÍGUEZ, I., GUTIERREZ, C., Y ALVAREZ-BUYLLA, E.R. The MADS-box XAANTAL1 increases proliferation at the *Arabidopsis* root stem-cell niche and participates in transition to differentiation by regulating cell-cycle components. *Ann. Bot.* **118**:787–796 (2016)
- GONZÁLEZ-GARCÍA, M.P., VILARRASA-BLASI, J., ZHIPONOVÁ, M., DIVOL, F., MORA-GARCÍA, S., RUSSINOVÁ, E., Y CAÑO-DELGADO, A.I. Brassinosteroids control meristem size by promoting cell cycle progression in *Arabidopsis* roots. *Development* **138**(5):849–59 (2011)
- GREEN, P.B. Growth and cell pattern formation on an axis: critique of concepts, terminology, and modes of study. *Bot. Gaz.* **137**(3):187–202 (1976)

- GRIENEISEN, V.A., XU, J., MARÉE, A.F.M., HOGEWEG, P., Y SCHERES, B. Auxin transport is sufficient to generate a maximum and gradient guiding root growth. *Nature* **449**(7165):1008–1013 (2007)
- HAYASHI, K., HASEGAWA, J., Y MATSUNAGA, S. The boundary of the meristematic and elongation zones in roots: endoreduplication precedes rapid cell expansion. *Sci. Rep.* **3**:2723 (2013)
- HILL, K., WANG, H., Y PERRY, S.E. A transcriptional repression motif in the MADS factor AGL15 is involved in recruitment of histone deacetylase complex components. *Plant J.* **53**(1):172–85 (2008)
- HONMA, T. Y GOTO, K. Complexes of MADS-box proteins are sufficient to convert leaves into floral organs. *Nature* **409**:525–529 (2001)
- IVANOV, V. Critical Size and Transition of cell to Division. Successive Transition of Sister Cells to Mitosis and Obligatory Transition of Cell to Mitosis in the Root Tip of Maize Germling. *Ontogenet* **2**:524–535 (1971)
- IVANOV, V.B. Cellular Basis of Root Growth. *Sov. Sci. Rev. D. Physicochem. Biol.* **2**:365–392 (1981)
- IVANOV, V.B. Y DUBROVSKY, J.G. Longitudinal zonation pattern in plant roots: conflicts and solutions. *Trends Plant Sci.* **18**(5):237–243 (2013)
- IVANOV, V.B. Root Growth Responses to Chemicals. *Sov. Sci. Rev. D. Physicochem. Biol.* **13**:1–70 (1994)
- IVANOV, V.B., DOBROCHAEV, A.E., Y BASKIN, T.I. What the Distribution of Cell Lengths in the Root Meristem Does and Does Not Reveal About Cell Division. *J. Plant Growth Regul.* **21**(1):60–67 (2002)
- IWAMOTO, A., SATOH, D., FURUTANI, M., MARUYAMA, S., OHBA, H., Y SUGIYAMA, M. Insight into the basis of root growth in *Arabidopsis thaliana* provided by a simple mathematical model. *J. Plant Res.* **119**(2):85–93 (2006)
- JAMES, G., WITTEN, D., HASTIE, T., Y TIBSHIRANI, R. *An Introduction to statistical Learning with Applications to R*. Springer (2013)
- KIM, H.J., FAY, M.P., FEUER, E.J., Y MIDTHUNE, D.N. Permutation tests for joinpoint regression with applications to cancer rates. *Stat. Med.* **19**(3):335–351 (2000)
- KIM, H.J., YU, B., Y FEUER, E.J. Selecting the Number of Change-Points in Segmented Line Regression. *Stat. Sin.* **19**:597–609 (2009). NIHMS150003
- LIU, C., XI, W., SHEN, L., TAN, C., Y YU, H. Regulation of floral patterning by flowering time genes. *Dev. Cell* **16**(5):711–22 (2009)

- LIU, J., WU, S., Y ZIDEK, J.V. On Segmented Multivariate Regression. *Stat. Sin.* **7**:497–525 (1997)
- MOUBAYIDIN, L., PERILLI, S., DELLO IOIO, R., DI MAMBRO, R., COSTANTINO, P., Y SABATINI, S. The rate of cell differentiation controls the *Arabidopsis* root meristem growth phase. *Curr. Biol.* **20**(12):1138–43 (2010)
- MUGGEO, V.M.R. Estimating regression models with unknown break-points. *Stat. Med.* **22**(19):3055–3071 (2003)
- NAWY, T., LEE, J.Y., COLINAS, J., WANG, J.Y., THONGROD, S.C., MALAMY, J.E., BIRNBAUM, K., Y BENFEY, P.N. Transcriptional Profile of the *Arabidopsis* Root Quiescent Center. *Plant Cell* **17**(July):1908–1925 (2005)
- PACHECO-ESCOBEDO, M.A., IVANOV, V.B., RANSOM-RODRÍGUEZ, I., ARRIAGA-MEJÍA, G., ÁVILA, H., BAKLANOV, I.A., PIMENTEL, A., CORKIDI, G., DOERNER, P., DUBROVSKY, J.G., ÁLVAREZ-BUYLLA, E.R., Y GARAY-ARROYO, A. Longitudinal zonation pattern in *Arabidopsis* root tip defined by a multiple structural change algorithm. *Ann. Bot.* **118**:763–776 (2016)
- PELAZ, S., TAPIA-LÓPEZ, R., ALVAREZ-BUYLLA, E.R., Y YANOFSKY, M.F. Conversion of leaves into petals in *Arabidopsis*. *Curr. Biol.* **11**(3):182–4 (2001)
- ROBERT, L., HOFFMANN, M., KRELL, N., AYMERICH, S., ROBERT, J., Y DOUMIC, M. Division in *Escherichia coli* is triggered by a size-sensing rather than a timing mechanism. *BMC Biol.* **12**:17 (2014)
- ROST, T. Y BAUM, S. On the correlation of primary root length, meristem size and protoxylem tracheary element position in pea seedlings. *Am. J. Bot.* **75**(3):414–424 (1988)
- SABATINI, S., HEIDSTRA, R., WILDWATER, M., Y SCHERES, B. SCARECROW is involved in positioning the stem cell niche in the *Arabidopsis* root meristem. *Genes Dev.* **17**(3):354–8 (2003)
- SABLICKI, R.W.M. Y MEYEROWITZ, E.M. A homolog of NO APICAL MERISTEM is an immediate target of the floral homeotic genes APETALA3/PISTILLATA. *Cell* **92**(1):93–103 (1998)
- SINNOTT, E.W. Growth and Differentiation in Living Plant Meristems. *Proc. Natl. Acad. Sci. U. S. A.* **25**(2):55–58 (1939)
- SRIDHAR, V.V., SURENDRARAO, A., Y LIU, Z. APETALA1 and SEPALLATA3 interact with SEUSS to mediate transcription repression during flower development. *Development* **133**(17):3496–3496 (2006)

- TAKAHASHI, N., KAJIHARA, T., OKAMURA, C., KIM, Y., KATAGIRI, Y., OKUSHIMA, Y., MATSUNAGA, S., HWANG, I., Y UMEDA, M. Cytokinins control endocycle onset by promoting the expression of an APC/C activator in *Arabidopsis* roots. *Curr. Biol.* **23**(18):1812–7 (2013)
- TAPIA-LÓPEZ, R., GARCÍA-PONCE, B., DUBROVSKY, J.G., GARAY-ARROYO, A., PÉREZ-RUÍZ, R.V., KIM, S.H., ACEVEDO, F., PELAZ, S., Y ALVAREZ-BUYLLA, E.R. An AGAMOUS-related MADS-box gene, XAL1 (AGL12), regulates root meristem cell proliferation and flowering transition in *Arabidopsis*. *Plant Physiol.* **146**(3):1182–92 (2008)
- THEISSEN, G. Development of floral organ identity: stories from the MADS house. *Curr. Opin. Plant Biol.* **4**(1):75–85 (2001)
- THEISSEN, G. Y SAEDLER, H. Plant biology. Floral quartets. *Nature* **409**(6819):469–71 (2001)
- TSUKAGOSHI, H., BUSCH, W., Y BENFEY, P.N. Transcriptional regulation of ROS controls transition from proliferation to differentiation in the root. *Cell* **143**(4):606–16 (2010)
- TURNER, J., EWALD, J., Y SKOTHEIM, J. Cell Size Control in Yeast. *Curr. Biol.* **22**(9):R350–R359 (2012)
- UBEDA-TOMÁS, S., FEDERICI, F., CASIMIRO, I., BEEMSTER, G.T.S., BHALLERAO, R., SWARUP, R., DOERNER, P., HASELOFF, J., Y BENNETT, M.J. Gibberellin signaling in the endodermis controls *Arabidopsis* root meristem size. *Curr. Biol.* **19**(14):1194–9 (2009)
- VAN DER WEELE, C., JIANG, H., PALANIAPPAN, K., IVANOV, V., PALANIAPPAN, K., Y BASKIN, T. A New Algorithm for Computational Image Analysis of Deformable Motion at High Spatial and Temporal Resolution Applied to Root Growth. Roughly Uniform Elongation in the Meristem and Also, after an Abrupt Acceleration, in the Elongation Zone. *Plant Physiol.* **132**:1138–1148 (2003)
- VANSTRAELEN, M., BALOBAN, M., DA INES, O., CULTRONE, A., LAMMENS, T., BOUDOLF, V., BROWN, S.C., DE VEYLDER, L., MERGAERT, P., Y KONDOROSI, E. APC/C-CCS52A complexes control meristem maintenance in the *Arabidopsis* root. *Proc. Natl. Acad. Sci. U. S. A.* **106**(28):11806–11 (2009)
- WEBSTER, P. Y MACLEOD, R.D. Characteristics of root apical meristem cell population kinetics: a review of analyses and concepts. *Environ. Exp. Bot.* **20** (1980)
- WEIZBAUER, R., PETERS, W.S., Y SCHULZ, B. Geometric Constraints and the Anatomical Interpretation of Twisted Plant Organ Phenotypes. *Front. Plant Sci.* **2**:1–8 (2011)
- YANG, L., HAN, Z., MACLELLAN, W.R., WEISS, J.N., Y QU, Z. Linking cell division to cell growth in a spatiotemporal model of the cell cycle. *J. Theor. Biol.* **241**(1):120–133 (2006)

- YAO, Y.C. Estimating the number of change-points via Schwarz' criterion. *Stat. Probab. Lett.* **6**(3):181–189 (1988)
- ZEILEIS, A., LEISCH, F., HORNICK, K., Y KLEIBER, C. strucchange: an R package for testing for structural change in linear regression models. *J. Stat. Softw.* **7**(2):1–38 (2002)
- ZEILEIS, A., KLEIBER, C., WALTER, K., Y HORNICK, K. Testing and dating of structural changes in practice. *Comput. Stat. Data Anal.* **44**(1-2):109–123 (2003)
- ZHANG, H. Y FORDE, B.G. An *Arabidopsis* MADS box gene that controls nutrient-induced changes in root architecture. *Science (80-)* **279**(5349):407–9 (1998)
- ZHOU, X., LI, Q., CHEN, X., LIU, J., ZHANG, Q., LIU, Y., LIU, K., Y XU, J. The *Arabidopsis* RETARDED ROOT GROWTH gene encodes a mitochondria-localized protein that is required for cell division in the root meristem. *Plant Physiol.* **157**(4):1793–804 (2011)